Bedford Institute of Oceanography
l'institut oceanographiqué de Bedford
Dartmouth/Nova Scotia/Canada

Physical Oceanographic Study of St. George's Bay, Newfoundland

G. H. Seibert

Report Series/BI-R-72-2/March 1972

The Bedford Institute of Oceanography is a Government of Canada establishment whose staff undertake scientific research and surveys in the marine environment. It consists of three main units, (1) the Atlantic Oceanographic Laboratory, which is part of the Marine Sciences Branch of the Department of the Environment, (2) the Marine Ecology Laboratory of the Fisheries Research Board of Canada, also of the Department of the Environment, and (3) the Atlantic Geoscience Centre of the Department of Energy, Mines and Resources.

Cover Design/Keith Clarridge

BEDFORD INSTITUTE

Dartmouth, Nova Scotia,
Canada

PHYSICAL OCEANOGRAPHIC STUDY
OF
ST. GEORGE'S BAY, NEWFOUNDLAND

by

G.H. Seibert

Atlantic Oceanographic Laboratory
Marine Sciences Branch
Department of the Environment

MARCH 1972 REPORT SERIES BI-R-72-2

SUMMARY

An intensive oceanographic study of St. George's Bay was carried out during November 1970 and May 1971. Results indicate that wind is the dominant factor in water movement, with tide and fresh water influence being secondary. A weak counterclockwise circulation is easily masked. This report is limited by the observations not covering all the seasons.

TABLE OF CONTENTS

LIST OF FIGURES

I. INTRODUCTION

1.1 Background and Objectives

Canadian Javelin Limited under its subsidiary Melville Pulp and Paper Limited is presently constructing a linerboard mill complex at Stephenville, Newfoundland (Fig. 1). When operational, the plant is expected to produce 1000 to 1200 tons of linerboard daily.

The Stephenville Mill will be using an unbleached Kraft pulping process. Estimates of the effluent volume released daily range from 5.9×10^4 to 8.3×10^4 m^3. At present, no provisions for effluent treatment have been made; the wastes are to be discharged into the waters of St. George's Bay via an underwater diffuser pipe.

In order to assess the effects of the mill's effluent discharge method on the waters and marine life of St. George's Bay, the Federal Department of Fisheries requested that the Bedford Institute carry out an oceanographic survey in the Stephenville Pond - St. George's Bay area. This report presents analysis of data obtained from a preliminary survey in November, 1970 and from a more intensive survey in May, 1971.

1.2 Description of the St. Georges Bay Area

1.2.1 Geography

St. George's Bay forms the largest embayment along the west coast of Newfoundland (Fig. 1). It is somewhat triangular in shape - narrowing uniformly from 62 Km at the mouth to 6 Km at the head of the Bay. It has a surface area of 1.8×10^9 m^2, is about 76 Km long, and has a volume content of 1.2×10^{11} m^3.

The southeastern shore is dominated by the steep escarpment of the Cape Anguille mountains which rise to over 600 m, and the St. George's Lowlands. The northshore is formed by the Port aux Port Penninsula; this region, although mountainous, has less relief than the Anguille mountains (Fig. 1). The sediments of the coastal plain consist of sedimentary rocks of the Carboniferous period whereas those of the mountainous regions are mainly sedimentary and volcanic of Ordovician, Silurian and Devonian Age (Murray and Harmon, 1969).

1.2.2 Bathymetry

St. George's Bay may be divided into two parts: a large outer bay comprising 83% of the surface area and a small inner bay defined by an area east of a line drawn from Isthmus Bay on the northern shore to Bank Head on the southern shore. This line also serves to separate the two areas morphologically by a broad sill having a maximum continuous depth of 24 m (Fig. 2). The inner bay, with a volume of 7.3×10^9 m^3, consists of a large depression having a maximum depth of 101 m. Shallow regions, with depths less than 1 m, border the southeastern shore with tidal flats predominant near Flat Island. The depths in the outer bay are dominated by a troughlike feature which runs parallel and close to the southeastern shore. The northern portions of the outer bay possess

uniform depths varying between 50 m to 75 m. Some of the physical dimensions are given in Table 1.

TABLE 1

Physical Dimensions for St. George's Bay

Depth Interval(m)	Area Between Depth Interval ($\times 10^8 m^2$)	Volume Between Depth Interval ($\times 10^9 m^3$)
0-18	1.80	1.6_2
18-37	2.30	6.3_3
37-55	2.70	12.4_2
55-73	1.50	9.6_0
73-91	3.80	30.1_6
91-110	3.40	34.1_7
110-128	1.60	19.0_4
128-146	0.70	9.5_9
TOTAL	17.8	123.9

1.2.3. Climatology

The island of Newfoundland, being situated on the east coast of a large continent has a typically continental rather than maritime climate. However, as a result of the proximity of the cold Labrador current, summer and winter temperatures are considerably modified. Winters are longer and milder with springs late and cool. Summers are short and cool.

Precipitation is distributed uniformly throughout the year (Table 2) yet the year to year quantities for particular months may vary considerably, and one would need comprehensive, long term data, to form any meaningful averages. Annual precipitation values vary regionally. The highest precipitation amounts are recorded at the coastal stations. As with most sub-arctic regions, much of the precipitation during winter is in the form of snow. Since a considerable part of the drainage area (Fig 1) lies in the mountainous regions, winter storage plays an important regulating effect on the runoff. The runoff which occurs during the winter months is mostly derived from precipitation falling on the coastal plain where temperatures are milder.

Wind speed and direction, air temperatures have been recorded at Stephenville Airport and St. Andrews for a number of years. The seasonal wind distribution for Stephenville Airport is summarized in Table 3 and 4. On the basis of these data, the prevailing winds are westerly to west-southwest in summer with equal amounts of west, west-southwest and east to east-northeast winds in winter. The inward blowing or westerly

TABLE 2

Monthly Precipitation (cm) at Stephenville, NFLD

(Equivalent snow +water has been included)

Year	Jan	Feb	Mar	Apr	May	Jun	Jul	Aug	Sep	Oct	Nov	Dec	TOTAL
1952	7.9	8.9	2.5	4.6	6.1	13.7	10.7	7.1	4.6	8.9	15.0	4.8	94.8
1953	10.2	9.9	3.6	4.6	6.1	6.9	11.7	9.1	7.6	10.9	9.9	15.2	105.7
1954	13.2	6.1	8.4	4.1	9.4	3.0	9.1	10.9	4.6	14.2	7.1	9.7	99.8
1955	4.8	3.8	10.4	2.8	6.4	6.4	9.9	17.3	16.8	8.9	9.9	12.2	109.6
1956	6.1	12.2	9.1	4.1	10.9	8.1	5.3	6.4	8.1	3.6	9.9	14.2	98.0
1957	13.9	12.2	6.9	8.6	3.3	6.6	6.4	8.4	10.7	10.7	12.2	13.7	114.6
1958	6.4	6.9	1.0	7.1	10.2	8.6	10.2	15.2	19.3	8.1	19.6	12.2	124.8
1959	19.6	14.5	16.3	1.5	6.6	4.6	6.4	10.4	10.9	10.2	13.7	9.9	124.6
1960	10.9	2.6	4.3	5.9	3.9	2.8	7.7	-	7.9	-	-	10.6	-
1967	7.8	9.1	6.8	3.8	-	9.6	5.1	12.9	15.1	11.9	11.9	9.1	-
1968	16.4	8.3	14.5	10.3	5.9	12.9	7.2	8.8	6.8	13.4	14.5	11.2	130.2
1969	7.3	8.5	7.8	8.1	13.5	9.5	5.0	10.1	7.6	7.6	12.8	13.8	111.6
1970	7.8	6.7	9.0	3.3	17.5	10.5	9.8	12.8	8.9	8.7	15.6	8.9	119.5
Average	10.2	8.4	7.7	5.3	8.3	7.9	8.0	10.8	9.9	9.8	12.7	11.2	112.1
SD*	4.4	3.4	4.4	2.6	4.2	3.4	2.3	3.3	4.6	2.8	3.3	2.8	11.8

* SD = Standard Deviation (cm)

- = No Data

TABLE 3

Percentage Distribution of Wind Directions, Stephenville, Nfld, (1955 - 1966)*

	Jan	Feb	Mar	Apr	May	Jun	Jul	Aug	Sep	Oct	Nov	Dec	Year
N	3	3	5	5	3	1	1	1	3	3	3	4	3
NNE	3	2	4	4	3	2	2	2	3	4	2	2	3
NE	7	7	9	7	7	7	6	5	7	6	6	5	7
ENE	11	10	12	10	9	11	8	8	7	7	10	8	9
E	10	10	8	8	9	8	8	7	5	7	9	8	8
ESE	2	2	3	3	3	3	3	3	1	2	3	2	3
SE	1	1	1	1	2	2	2	2	1	1	2	2	2
SSE	1	1	1	2	3	2	2	3	2	2	3	2	2
S	3	3	1	2	3	3	4	4	4	4	4	4	3
SSW	2	2	2	2	3	4	4	4	4	3	3	3	3
SW	2	3	4	7	8	8	10	9	9	6	4	4	6
WSW	7	9	7	11	14	15	15	15	12	10	8	7	11
W	14	11	9	6	6	8	8	11	11	12	13	16	10
WNW	14	10	9	5	4	3	3	4	7	9	9	12	7
NW	7	6	7	5	4	3	2	4	5	6	6	7	5
NNW	4	5	5	5	4	2	2	2	4	4	4	4	4
Calm	9	15	13	17	15	18	20	16	15	14	11	10	14

*Canadian Met. Branch

TABLE 4

Distribution of Wind Speed (m sec^{-1}), Stephenville, Nfld. (1955-1966)*

	Jan	Feb	Mar	Apr	May	Jun	Jul	Aug	Sep	Oct	Nov	Dec	Year
N	4.2	4.2	4.2	4.9	3.7	2.7	3.0	2.5	2.7	3.1	3.5	3.3	3.5
NNE	3.4	2.7	3.4	3.3	2.5	2.2	2.1	2.1	2.0	2.5	2.6	3.0	2.6
NE	3.7	3.1	3.8	3.5	2.9	2.8	2.2	2.2	2.5	2.5	3.1	3.3	3.0
ENE	4.6	4.8	4.8	4.8	3.7	3.6	2.9	3.2	3.2	3.4	3.9	4.0	3.9
E	5.4	5.7	5.5	5.1	4.0	3.7	3.4	3.4	3.5	4.2	4.4	4.8	4.4
ESE	5.8	6.5	7.5	5.7	4.6	3.9	3.3	3.5	4.1	4.1	4.0	4.5	4.8
SE	5.1	5.3	5.3	4.0	3.6	3.3	3.7	3.3	3.6	4.4	4.5	4.5	4.2
SSE	4.5	4.1	4.2	3.7	3.7	3.3	3.4	3.2	3.2	3.6	4.6	4.4	3.8
S	4.6	4.0	4.2	3.3	3.4	3.0	3.2	3.5	3.9	4.2	4.3	4.4	3.8
SSW	4.7	4.5	4.7	3.4	2.8	2.7	2.9	3.4	3.7	3.9	4.6	4.9	3.8
SW	7.2	6.1	4.8	4.1	3.5	3.4	3.5	4.0	4.5	5.1	5.4	6.7	4.9
WSW	7.3	6.6	5.8	4.2	4.0	3.7	3.6	4.3	4.5	5.1	5.7	7.2	5.2
W	6.6	5.5	5.2	3.9	3.7	3.4	3.7	4.0	4.5	4.7	5.0	6.0	4.7
WNW	5.4	4.0	5.1	4.7	4.4	3.8	4.0	3.9	4.6	4.6	4.9	5.5	4.6
NW	4.5	4.5	4.6	4.7	4.3	4.2	4.0	4.1	4.2	4.1	4.7	4.7	4.4
NNW	4.2	4.9	4.6	4.6	4.1	3.9	4.0	3.8	3.9	3.7	4.2	3.9	4.2
Mean	4.8	4.3	4.2	3.7	3.2	2.8	2.6	3.0	3.3	3.6	4.0	4.5	3.7

*Canadian Met. Branch

TABLE 5a

Monthly mean temperature (°C) at St. Andrew's, Nfld. (1951-1960)*

	Mean Daily Tem	Mean Daily Max	Mean Daily Min	Max Temp	Min Temp
Jan	-4.1	-0.9	-7.3	12.8	-23.9
Feb	-4.7	-1.2	-7.9	14.4	-23.9
Mar	-2.8	0.7	-6.4	14.4	-23.9
Apr	1.3	5.1	-2.4	18.3	-16.1
May	6.2	10.5	1.8	21.7	-6.7
Jun	11.1	15.5	6.7	35.6	-2.8
Jul	15.2	19.4	10.8	27.2	1.7
Aug	15.6	19.6	11.7	26.1	1.7
Sep	12.0	16.2	7.8	25.0	-1.1
Oct	7.2	10.9	3.5	20.6	-5.0
Nov	2.9	6.1	- .03	17.2	-8.9
Dec	-1.7	1.5	-4.8	15.0	-15.6
Year	4.9	8.7	1.1	27.2	-23.9

* Canadian Met. Branch

TABLE 5b

Monthly mean temperature (°C), Stephenville, Nfld. (1951-1960)*

	Mean Daily Tem	Mean Daily Max	Mean Daily Min	Max Temp	Min Temp
Jan	-5.0	-1.9	-8.2	12.2	-26.1
Feb	-5.7	-2.4	-9.1	11.7	-27.2
Mar	-2.8	0.7	-6.3	17.2	-22.8
Apr	1.8	5.3	-1.8	17.2	-12.2
May	7.2	11.2	3.2	27.2	-6.1
Jun	12.2	16.3	8.1	30.0	-1.1
Jul	16.4	20.0	12.7	30.6	4.4
Aug	16.6	20.0	13.1	28.3	3.9
Sep	12.7	16.4	9.1	27.8	-0.6
Oct	7.2	10.4	4.0	22.2	-3.9
Nov	2.5	5.3	-0.3	19.4	-12.2
Dec	-2.2	0.9	-5.3	15.6	-17.2
Year	5.1	8.6	1.7	30.6	-27.2

* Canadian Met. Branch

winds usually are the strongest (Table 3 and 4). Thus winds at Stephenville are predominantly onshore both summer and winter, however, significant periods of offshore winds occur in winter.

Air temperature data from Stephenville and St. Andrews (Nfld.) covering a ten-year period (1951 - 1960) indicate a yearly mean daily temperature of 5.1°C and 4.9°C, respectively. Extremes vary from a low of -27°C to a high of 30°C. The highest mean daily temperatures are observed in mid-July at Stephenville and early August in St. Andrews. The lowest mean daily temperatures are observed in late January or early February (Table 5). The average season of thaw (the period when the daily mean temperatures are greater than 0°C) lasts some 247 days at St. Andrews and 242 days at Stephenville. This season starts approximately April 3 and has an average temperature of 8.6°C (Murray and Harmon, 1969). From the above, it can be seen that the climatological conditions are fairly uniform around the bay. Stephenville, being more sheltered experiences higher temperatures and, winds which are less variable and weaker, than those at St. Andrews.

1.2.4 Fresh Water Sources

Some thirty rivers and brooks of assorted size drain a watershed of total area 4.93 x $10^9 m^2$ into St. George's Bay. This area is approximately 2.7 times the water surface area of St. George's Bay. The seven largest rivers, mostly located along the southeastern shore (Fig. 1), drain over 66% of the basin area. Some of their morphometric characteristics are given in Table 6.

TABLE 6

Morphometric Characteristics of Major River Basins*

River Name	Basin Area (km)	Mean Width (km)	Perimeter (km)	Relief (m)	Axial Length/ Mean Width
Harry's River	816.4	11.9	182.2	597	3.22
Southwest and Bott. Bk	815.1	9.7	177.2	627	5.50
Flat Bay Bk	635.6	11.1	168.5	594	4.71
Crabbes Bk	550.6	12.2	174.3	625	3.86
Robinsons Rv.	439.0	7.7	144.8	625	6.58
Fishels Bk	360.0	5.8	134.5	594	8.41
Little Barachois Bk	354.3	5.8	153.5	594	9.47

* Based on data presented in: "A preliminary consideration of the factors affecting the productivity of Newfoundland Streams" by A.R. Murray and J.J. Harmon, FRB Tech. Rept. #130, 1969.

Direct measurements of fresh water discharge at Harry's River, below the Trans Canada Highway bridge, have been carried out by the Inland Waters Branch, Water Survey of Canada, Since 1968. Stream

gauging on the rivers shown in Table 6 was carried out on a daily basis during May - June, 1971. Using our own values of discharge and precipitation measurements from Stephenville, a precipitation-discharge coefficient was evaluated for each stream. Using data supplied by the Water Survey of Canada for the coincident period, a similar coefficient was calculated for Harry's River. In order to estimate the total fresh water contributions from the major rivers it was assumed that the precipitation-discharge coefficient relationships between the various rivers determined from our data was constant over the year. As the coefficients for Harry's River based on our data and the Water Survey of Canada data did not differ significantly, it was used as a standard and the variations in the coefficients for the other rivers were adjusted accordingly. Total fresh water contributions, evaluated for each month of a mean year, are given in Table 7. The monthly coefficients are based on three year's discharge values metered at Harry's River. Precipitation amounts are mean monthly totals as measured at Stephenville over nine years. Evaporation rates are based on the work of Lauzier and Hull (1962). The water budget given in Table 7 should only be considered as a first order approximation. The assumptions leading up to choosing a constant precipitation-discharge relationship for the area based on one standard river and a comparison of just over a month (May to June 3, 1971) leave a lot to be desired. In addition, the evaporation rates derived by Lauzier are based on little data. Thus the calculated fresh water contribution (net) periods where the precipitation-evaporation rate is of the same order as the rate contributed by land drainage is particularly susceptible.

II. DATA AND SAMPLING METHODS

2.1 Sampling Program and Methods

CSS *Dawson* (Cruise BI-70-036) occupied a grid of 36 stations (Fig. 3) on November 3, 1970. Vertical profiles of temperature and salinity were obtained at each station using a STD (salinity-temperature-depth) system. Two current meter moorings, each with an in situ recording current meter at 5 m and 45 m, were set and left in position for approximately 21 days.

A second cruise with CSS *Maxwell* was carried out between November 14 and 22, 1970. Vertical profiles of temperature and salinity were obtained at 23 locations in the inner Bay using an electrodeless induction salinometer. The station pattern was planned to give uniform coverage. Instrument malfunction made the temperature and salinity data unreliable and it has not been utilized in this report. A number of parachute drogues were released (usually set at 3 or 10 metres) and tracked during daylight hours. Four spot releases of Rhodamine B dye were made. Concentrations were measured continuously using a standard Turner Model III fluorometer.

Cruise BI-71-025 was carried out by MV *Navicula* between May 8 and June 7, 1971. A regular, fixed grid of stations (Fig. 4) was occupied at approximately weekly intervals. Vertical profiles of temperature, salinity were obtained at each station; dissolved oxygen determinations were made at selected depths at several stations. Self-recording current

TABLE 7

Average Monthly Freshwater Contribution to St. George's Bay

Month	Run-off x 10^{-3} ($m^3 sec^{-1}$/ km^2 cm)	Average Precip. (cm)	Drainage* Area Run-off ($m^3 sec^{-1}$)	Evaporation from Bay (cm)	Average Prec.-Evap (cm)	Net Fresh** Water contr. to surface of Bay ($m^3 sec^{-1}$)	Total Fresh Water addition to Bay ($m^3 sec^{-1}$)
	I	II	III=IxIIxDr.Ar.	IV	V=II-IV	VI=VxBay Ar.	VII= III + VI
Jan	2.93	10.2	147.3	2.6	7.6	51.1	198.4
Feb	1.68	8.4	69.6	2.6	5.8	43.2	112.8
Mar	1.81	7.7	68.7	2.6	5.1	34.3	103.0
Apr	6.94	5.3	181.3	7.2	-1.9	-13.2	168.1
May	14.14	8.3	578.6	7.2	1.1	7.4	586.0
Jun	6.63	7.9	258.2	7.2	0.7	4.9	263.1
Jul	2.37	8.0	93.5	14.6	-6.6	-44.4	49.1
Aug	1.98	10.8	105.4	14.6	-3.8	-25.5	79.9
Sep	2.63	9.9	128.4	14.6	-4.7	-32.6	95.8
Oct	4.00	9.8	193.3	14.6	-4.8	-32.3	161.0
Nov	3.75	12.7	234.8	14.6	-1.9	-13.2	221.6
Dec	3.36	11.2	185.5	14.6	-3.4	-22.8	162.7
Weighted*** Averages	4.33	9.19	187.9	9.8	- .6	-03.9	184.0

*Dr. Ar. ≡ Drainage area = $4.93 \times 10^3 km^2$ **Bay Ar ≡ St. George's Bay Surface Area = $1.8 \times 10^3 km^2$

***Months weighted according to number of days.

meters were moored at six locations (Fig. 4). Table 8 gives some performance statistics for these current meters. Numerous parachute or tin drogues (Fig. 5) were set and tracked. Attempts to carry out dye diffusion experiments were marginal due to frequent instrument malfunctions and bad weather. Water levels at Stephenville and Robinson's were continuously recorded. Wind velocity, radiation, relative humidity, sea surface temperature were also measured at Stephenville Airport every 15 minutes.

TABLE 8

Performance Characteristics for Current Meters

Cruise BI-71-025

Statn. No.	Depth(m)	Start time(AST)*	Stop time(AST)*	Data Interval
78	7	0830(9/5/71)	0030(23/5/71)	20 min.
78	28	0830(9/5/71)	0430(2/6/71)	20 min.
79	6	1003(9/5/71)	0203(3/6/71)	20 min.
79	16	1013(9/5/71)	0213(3/6/71)	10 min.
79	47	1108(9/5/71)	0308(3/6/71)	20 min.
80	3	1107(9/5/71)	0307(3/6/71)	20 min.
80	12	1131(9/5/71)	0531(3/6/71)	10 min.
80	41	1131(9/5/71)	0331(3/6/71)	20 min.
81	16	1710(9/5/71)	0210(2/6/71)	20 min.
81	90	1239(9/5/71)	0439(2/6/71)	20 min.
82	22	1550(9/5/71)	0550(27/5/71)	10 min.
83	22	1230(11/5/71)	1230(16/5/71)	20 min.

* Transient effects due to moorings have been removed from these data.

2.1.1 Temperature, Salinity, Oxygen Data

All vertical profiles of temperature and of salinity reported herein were obtained with an inductive salinity-temperature-depth (STD) system manufactured by Guildline Instruments, Inc. The basic unit has a temperature accuracy of 0.02°C with a ±0.003°C resolution: a salinity accuracy of 0.04‰ (in the range 28‰-35‰) with a ±0.005‰ resolution and a depth accuracy of 0.2% of the full scale with a resolution ±0.05% of the full scale. The *in situ* data are transmitted via a 7-conductor armoured cable to a data logger on board ship. Eight readings each of temperature, conductivity and pressure are written in BCD (200 bpi) format on IBM compatible magnetic tape every five seconds. The magnetic tape is then processed on the Institute's CDC 3100 using program STDHP (Keyte, 1970).

On Cruise BI-70-036, the data logger did not function correctly (discovered only at a cruise post mortem). However, no data loss occurred as duplicate recordings were made using a 4K PDP-8 DEC tape unit. The data were processed on board using programs developed by Bennett (1970). Calibration of the STD data against standard bottle cast samples showed that the STD data can be considered accurate to ±0.15‰ for salinity and ±0.05°C for temperature. The pressure sensor was not checked.

Similar comparisons for temperature and salinity were made on Cruise BI-71-025, again the data logger did not function correctly and recourse was made to reading the XY analogue traces. Comparison shows that data from this cruise can be considered accurate to ±0.06‰ in salinity and ±0.03C for temperature.

Oxygen was determined by the modified Winkler Method (Strickland and Parsons, 1965). The 'pickled' samples were analyzed within 24 hours. The method gave an average difference of ±0.03 ml/litre for 35 duplicate samples. Using complementary temperature and salinity data, oxygen saturation values were determined on the basis of Green and Carritt (1967).

2.1.2 Current Meter Observations

Currents were measured by moored, self-recording meters employing a taut-wire subsurface float. These instruments were essentially of three types. Cruise BI-70-036 utilized the buoyant, shallow-water Hydrowerkstatten (HW) meter. This is a large torpedo-shaped meter which orients itself into the current. Rates are measured by impeller revolutions, direction by magnetic compass - these parameters are recorded photographically at 5-minute intervals. Because of the rather high starting speeds of these meters, many sequences of constant rotor counts were obtained from the November, 1970 moorings. These sequences may have been caused by instrument malfunctions but, more probable, are due to ambient rates being below the meters' threshold value ($\sim$ 6 cm sec^{-1}). Also, the recording interval (5 min.) was too short to resolve, with accuracy, current changes.

Cruise BI-70-036 moored two arrays at locations shown in Fig. 3. Each array consisted of a meter at 5 meters and 45 meters; depth of water was 49 meters (Stn. 58) and 50 meters (Stn. 59). Only one record has been presented for analysis (Stn. 59 at 5 meters). The meter at Stn. 58 at 45 meters was presumed moored upsidedown. Records from Stn. 58 at 5 meters and Stn. 59 at 45 meters suffered from time check errors, erratic rate and direction readings and have not been used.

Cruise BI-71-025 utilized four types of recording current meters: (i) Braincon 316 Histogram meter, (ii) Braincon 381 Histogram meter, (iii) Plessey Model M021, and (iv) Aanderaa (Bergen) meter.

The Braincon Histogram current meter (both 316 and 381) utilize a Savonious rotor as a current speed sensor. Direction is sensed by a large vane attached to the instrument case. Instrument tilt

angle and tilt direction are sensed by an inverted plumb bob. The instrument records: number of total rotor rotations, current direction relative to magnetic north, tilt and tilt direction as a photographic analogue on 16 mm film using a phosphorescent light source. A cam system driven by an electric clock controls the sampling period, here set to 20 minutes. In addition, a luminous dial Timex watch is also projected onto the film to give an independent time reference for the record. The minimum starting velocity is 0.5 cm sec^{-1}; its direction resolution is approximately 5 degrees at 2.5 cm/sec (Warner, 1970). The rate arc is read to the nearest degree, using a calibration value of 0.403° per cam sec^{-1} for a 4 minute interval averaging time, the rate resolution for a 20-minute interval should be 0.61 cm sec^{-1}.

The Plessey Model M021 and Aanderaa meters are similar, having evolved from the same design (Aanderaa, 1964). The Plessey Model M021 consists of a horizontally suspended cylinder approximately 12.7 cm in diameter and 91 cm in length. The current speed is sensed by a screw type impeller which drives a potentiometer via a magnetic drive and reduction gear box. The current value is obtained from the change in resistance ratio of the potentiometer between consecutive readings. Direction is sensed by a magnetic compass. Once in each measuring cycle, a floating contact in the compass clamps onto a potentiometer resistance element and the resistance ratio indicating the current direction is recorded. The essential difference between the Plessey M021 and Aanderaa meter is that the latter uses a Savonious type rotor mounted in a vertical plane; a large tailfin aligns the meter in the required direction. The recording of data is very similar. All channels are recorded, at intervals determined by a cam, on 1/4 magnetic tape in serial 10-digit binary format. Both Plessey and Aanderaa meters are provided with extra channels. The Plessey M021 is fitted with an externally mounted thermistor. The Aanderaa is fitted with a thermistor, pressure transducer and conductivity cell. Both instruments are fitted with an externally mounted acoustic transducer which permits *in situ* monitoring of the instrument. Table 8 gives some performance statistics of instruments used in 1971.

2.1.3 Drogue Observations

Two types of drogues were used: (i) a standard parachute drogue similar to that described by Volkman *et al.* (1956), with a parachute canopy approximately 7 meters in diameter suspended from a small surface float (Fig. 5). Positions were determined by radar range and bearing; fixes are considered accurate to ±100 metres; (ii) drogues constructed from two metal plates intersecting at right angles and suspended from a small elliptical-shaped buoy (Fig. 5). Positional fixing was by horizontal sextant angles from shore. Horizontal angles were readable to ±1 minute of arc; with the minimum fixing distance of 4 km, the positions of the drogues can be considered accurate to ±5 meters.

2.2 Data Reduction

The data have been analyzed in a number of ways usually consisting of horizontal distributions of chemical or physical parameters on various pressure surfaces, vertical section plots, time series plots, etc. Since the current meter data forms an important part of this report, an indication of the procedure followed to reduce and edit the data to a useful form is given below.

Upon retrieval of the Braincon and HW current meters the films are developed and then read manually, at this time the record is scanned for overall instrument performance. The data is then transcribed onto columnar forms and keypunched on standard 80-column cards. At this stage, the date is listed on paper tape and paper printout and in conjunction with the mooring log books checks are carried out for reading and time errors. The rate and direction data are further edited by listing distribution histograms of rate of change of direction and rate. This stage eliminates gross spikes in the data and detects double or multiple readings.

In order to compute reliable covariance functions and spectra between two simultaneous records it is important that the two time series be related to the same time base. In this sense, obtaining a record length equal to its mooring time is critical. The system of edit checks (either by linear interpolation or examination of the original film exposures) can adequately correct the current meter record if the number of data gaps are small.

The data are then transferred to magnetic tape to give an 'updated' rate and direction. The digital Plessey M021 and Aanderaa are transferred to paper tape, then to magnetic tape. At this stage, all records, whether from digital instrument or not, follow the same sequence; (i) bivariate frequency distributions of rate and direction, (ii) the current vector is resolved along any two orthogonal directions. All current records were arbitrarily resolved north (major direction) and east (minor direction).

Tide gauge data were abstracted at 15-minute intervals from the analogue traces. A frequency distribution was carried out and readings greater than two standard deviations of the mean given special scrutiny. Many of these were found to be transcription errors and corrected. Individual height readings are considered accurate to ±2 cm with a possible maximum time error of ±5 minutes.

III. OCEANOGRAPHIC CHARACTERISTICS

3.1 Distribution of Properties

3.1.1 Vertical Sections of Temperature, Salinity, Oxygen

(a) November, 1970: Longitudinal and traverse sections of temperature and salinity are shown in Fig. 6 to 9 inclusive.

The influence of the fresh water contribution from rivers at the

head of the Bay is evident, having produced a layer of low salinity water approximately 15 meters thick with salinities less than 30.5‰ As this water moves seaward, the salinity at the surface is gradually increased from less than 29‰ (data not shown) to over 30.75‰ near the sill. Seaward of the sill surface salinities increase only slightly; the vertical stratification is reduced considerably.

A distinctive feature of the longitudinal section is the pronounced downward slope of the isotherms towards the west (mouth of the bay). The reduction of vertical stability in the outer reaches of St. George's Bay (through a reduction in the vertical salinity gradients) has increased the thickness of the isothermal wind-mixed layer from 20 meters at Stn. 35 to over 40 meters at Stn. 5. It seems, however, that this decrease in vertical stability has not, as yet, enhanced any considerable surface heat losses. In the inner bay, the cooler surface waters (temperature <9°C) are more indicative of the fresh-water influx than surface cooling.

Maximum salinities of 33.2% were found at Stn. 3 at 120 meters. At this location minimum temperatures of 1.75°C were also found. In general, minimum temperatures were observed at the bottom except at deep stations in the outer bay (Stations 2, 3, 4, 12, 16)where the bottom temperatures were slightly higher than those immediately above. The accuracy of the data (see Sect. 2.1.1) precludes the determination of geostrophic currents. Also, the variability in the depths of both isotherms and isohalines makes any inferences on currents in the outer bay doubtful.

(b) May, 1971: The grid shown in Figure 4 was occupied several times, at times incompletely. The data should be indicative of spring conditions under the influence of large fresh water run-off and vernal warming. In most cases the station grid was completed within 7 hours and thus the distribution of properties can be considered quasisynoptic. Individual section lines (except the longitudinal) were completed in considerably less time. Comparison of profiles taken at different time intervals provides valuable information on the time and space variability present in the inner portions of St. Georges Bay.

On May 10 the grid was only partially completed, areas with no data are blank. The longitudinal profile (Fig. 10) shows a water column highly stratified in both temperature and salinity. The salinity stratification, a consequence of fresh water inflow from rivers, has in effect isolated the warmer surface waters (2° 6°C) from the cooler bottom water (<0°C). The lower layer, here defined by temperature <0°C and salinities greater than 31‰, corresponds to the homogeneous surface layer formed during winter in the Gulf of St. Lawrence.

Neglecting small scale inhomogeneities in Figure 10, it can be seen that the isopleths of salinity have a tendency to slope down towards the west in the upper 6 meters and to slope down towards the east between 6 and 18 meters, approximately. Figure 11 shows

the longitudinal section occupied on May 18. Temperatures in the upper 5 meters have increased by about 0.5°C, salinities by 1‰ The average fresh water influx during the 8 days separating the occupation of these two sections did not vary significantly from the preceding (prior to May 10) 8-day average. Wind conditions had, however, changed. Wind intensity increased to about 12-15 km/hr., although maintaining directions from 250° to 275°T. The thermocline and halocline east of Station 9 has deepened and intensified considerably. Again, the mass field has a pronounced downward slope to the west in the upper 10 meters with a downward slope to the east between 10 meters and 20 meters. Comparing these sections (Fig. 10 and 11) it can be seen that large changes in heat and salt content have occurred. The water column between 10 meters and 40 meters is warmer and less saline.

The longitudinal section (Fig. 12) for May 23 indicates higher over-all temperatures than on May 18. The largest changes occurred in the upper 6-meter surface; temperatures increasing by about 3°C while surface salinities decreased slightly. The intensity of both thermocline and halocline east of Station 9 has decreased.

On May 26, when the last observations were taken, unusual conditions can be noted (Fig. 13). Comparison of the situation on May 23 and 26 is interesting, as they show the effect of strong onshore winds on the density structure within the Bay. On May 25, a storm with winds greater than 28 km/hr blowing from 250-280 T passed through the area. Winds had lessened in intensity and changed direction to 110°T at approximately 5 a.m. (May 26) some four hours prior to starting the station grid. The onshore winds have piled up the light surface layer at the eastern end of the Bay. Associated with this is a lowering and intensification of both thermo and halocline and an inward flux of cooler and saltier water from west of the sill (Fig. 13).

The section including Stations 99 to 4 was occupied ten times (Fig. 14 to 24). The temperature and salinity distributions on May 10 (Fig. 14) indicates a wedge of warm (> 4°C) and low salinity (<30‰) water in the upper 8 meters extending north from Flat Island. This section does not show the cyclonic circulation pattern frequently encountered in high latidude estuaries. It may be that this section is too close to the fresh-water sources and geostrophic effects have not become fully established. The salinity and temperature distribution from May 18 (Fig. 15) shows conditions less uniform than on May 10 although the gross features are the same. As in the longitudinal section for the same day (Fig. 11) the upper 25 meters have been more thoroughly mixed - there is no substantial temperature change in the first 5 meters, but a slight increase in salinity. Between 5 meters and 25 meters waters have been uniformly warmed up by about 3°C while decreasing their salinity by about 0.5‰ The temperature inversion near Stations 7 and 5 may be indicative of active surface mixing. The May 23 profiles (Fig. 16) indicate the influence of solar heating in the upper 6 meters. In general, temperatures in this layer have increased by 4-5°C. The low salinity water, indicative of fresh water run-off, is confined as a lens, between Stations 6 and 8. The layers below 10 meters have become cooler and more saline. Figure 17 indicates the average distribution of properties, based on six transects, across the section which includes

Stations 99 to 4. These transects were made on May 24 within 5 hours. Individual sections were occupied in less than 1 hour. Due to the time and space averaging, the distributions are less complex than those for May 23 (Fig. 16) or May 18 (Fig. 15) although retaining their gross features. Salinity varies from less than 27‰ at the surface to slightly greater than 31.25‰ near the bottom. The isohaline slopes in the layer between the surface and 35 meters indicate a net westward baroclinic flow of warmer water in the central and northern parts of the section. The return flow required for continuity probably occurs in the near bottom layers.

The effects of strong westerly (onshore) winds on the temperature and salinity distribution can be seen in Figure 18. Over a two-day period (May 24 to May 26) the surface layer thickness has increased by over 15 meters (the 6°C isotherm is taken as bounding the surface layer). These winds not only increased the depth of the surface layer but were also responsible for advecting colder and more saline water into the area. The irregular temperature distribution indicates a zone of active but incomplete mixing.

Temperature and salinity profiles indicative of conditions in the central regions are presented in Figures 25 to 31. The low salinity water, indicative of the fresh water runoff, may still be traced quite easily in Section 2 (Figures 25 to 27). Seaward of this section however, conditions have become diffused and the wedge of low salinity water is absent (Figure 28 to 31). Instead, the low salinity water has spread out across the whole section. The surface salinities have increased while surface temperatures have decreased, suggesting that vertical mixing was more pronounced than lateral.

In order to study short term variability, section 1 (Stations 99 to 4) was repeated six times, each complete occupation lasting less than one hour. The results, Figures 19 to 24, show that even in this short time interval significant changes in temperature and salinity occur. A consistent feature of these diagrams (also shown in Figures 15 to 18) is the large upward slope of the isopleths of temperature and salinity between stations 6 and 4. The change in depth of temperature and salinity isopleths cannot be totally explained by geostrophic adjustment in the mass field. The intrusion of colder and more saline waters along the bottom due to the flooding tidal streams may also be seen. Preliminary computations of geostrophic currents based on these data tend to be too high relative to those observed. In addition, this section is also too close to the sources of fresh water (see Fig. 1) for the establishment of geostrophic equilibrium. The persistence of this feature, only slightly modified by changing wind directions, implies that this feature is due to mixing or vertical advection. Data based on the drift of parachute drogues indicate a substantial cross channel circulation mode probably driven by the influx of fresh water. To compensate this outflow, and due to turbulence caused by bottom friction, the isopleths must slope up towards the surface.

3.1.2 Horizontal Distributions

(a) November, 1970: The surface water of low salinity and cooler temperature derived from the head of the Bay extends, in a broad band, along the north shore (Fig. 33). Seaward of the sill, the horizontal gradients are very small. The surface temperature and salinity distribution support the view that most of the low salinity water is being transported seaward along the north shore. Vertical mixing seems to intensify near the sill. A compensating inflow of warmer and higher salinity (30.5‰) water seems to occur along the southeastern shore.

The horizontal temperature and salinity distribution in the outer bay is very uniform. A small band of warm water (9.25°C) occurs along the southeastern shore, within which is embedded a pocket of cooler water - probably caused by local wind-induced upwelling. This feature extends down to at least 20 meters (Fig. 33 (b) and (c)).

(b) May, 1971: Figures 34 to 37 show the distribution of temperature and salinity on the 5 meter and 15 meter horizon for May 10. East of Indian Head the distribution of temperature and salinity at 5 meters is complicated because of the proximity of the fresh water sources from Main Gut, Little Barachois Brook and Flat Bay Brook. During and for the two days period immediately preceding the cruise, winds were from the west and northwest quadrant with moderate but variable rates of 6 km/hr to 15 km/hr.

These winds seem to have driven the brackish, warm water into the southeastern end of the bay holding it against the shore. Escape is probably affected by along-shore currents as can be seen by the tongue of warmer water which extends northwestward from the eastern tip of Flat Island. These northwesterly and westerly winds have also caused some shallow upwelling to occur near Indian Head. Note the pocket of cooler ($T\sim$ 3.75C) and more saline ($S\sim$ 29.25‰) waters. This effect is confined to less than 15 meters as the horizontal distributions on this surface are uniform near Indian Head (Figs. 36 and 37). West of Indian Head temperatures decrease uniformly while salinities increase and lateral (north-south) gradients are small. Temperatures at 15 meters are complicated by a cold core between Flat Island and Indian Head. Salinities increase uniformly towards the west with small lateral gradients.

By May 18, temperatures at the 5-meter level had decreased slightly in the eastern portions of the bay while increasing in the outer areas. In the preceding seven days, winds were variable in rate and direction - at times being dominated by the land-sea breeze cycle. Winds would be light (< 10 km/hr) from the northeast quadrant during dark and early morning hours changing to south, southwest and increasing in intensity in the late afternoon. The variability in the wind vector is largely reflected in the temperature and salinity structure at 5 meters (Figs. 38 and 39). In the fields a number of

relative temperature and salinity maxima are embedded which seem to be arbitrarily distributed. A temperature minimum, probably caused by local wind-induced upwelling, appears north of Flat Island.

Figure 40 illustrates the surface temperatures (at the 1 meter level) for May 23. The most interesting features are: a uniformly westerly decrease of temperature, from 9°C to 7.5°C, in the outer reaches of the bay; a convoluted structure consisting of a tongue of cool (< 9°C) water extending north and northwest from Flat Island; a band of warm (> 10°C) water in the Stephenville area. Temperatures on May 23 at the 5-meter level (Fig. 41) show an over-all rise, from those of May 18, of nearly 2°C. The pattern is complicated by localized areas of cold (< 5°C) and warm (> 7°C) water in the inner portions. The central bay consists of a large pool of cooler water (< 6°C). The salinity distribution at 5 meters (Fig. 42) shows no general increase or decrease although the areas of high or low salinity have been displaced. A small tongue of saline water (> 30.25) extends northwest from Flat Island. Combined with the cooler temperatures observed here this would indicate some local upwelling. Salinities in the outer region have decreased somewhat while at the head, i.e., near the fresh water sources, salinities have increased.

Temperatures and salinities at 15 meters for May 23 are shown in Figures 43 and 44. The salinity field is more uniform than that found on May 18; however, the temperature structure is more complicated.

On each grid occupation different distribution patterns for temperature and salinity were observed making it extremely complicated to infer what the circulation was. On occasions of persistent and strong westerly or easterly winds, changes in the mass field were quite obvious. With westerly winds, the surface waters are driven into the inner portions of the bay. A compensating outflow may occur at the surface at locations where there is a dynamic relief or at subsurface depths. The increased intensity of the wind also depresses the pycnocline in the inner bay. Easterly winds tend to be weaker than those from the west and because of this, their effects are less clear. Under the easterly winds, upwelling along Flat Island shore can occur. The fresh warm surface layer is transported northward. Below the halocline, changes in temperature and salinity in the outer portions of the bay are small and mainly due to diffusive effects or to intermittent advective effects (i.e., see May 26 longitudinal profile, Fig. 13).

3.1.3 Fresh Water Budget and Flushing

A number of methods have been proposed for computing the removal rate of a pollutant introduced into an estuary (Bowden, 1967). The renewal rate of waters in an estuary depend critically upon its dynamics. Hence, in the absence of adequate measurements, one can only make an educated guess (say, by analyzing the distribution of properties) at what the circulation is. The longitudinal temperature and salinity profiles indicate that, although steady state is never reached, above the sill the circulation most closely corresponds to a two-layer flow

with vertical mixing. Because tidal currents are small, most of the energy required for mixing must be applied at the sea surface through the action of winds. An estimate of fresh water accumulation and flushing was made based on the method proposed by Tully (1949). In order to apply this method to St. Georges Bay, a modification (which allows for lateral salinity gradients and vertical mixing) as proposed by Collias, Barnes *et al.* (1966) was used. For the evaluation of fresh water accumulation, it was assumed that all the fresh water was confined to the upper 24 meters, the approximate maximum depth at the sill.

(a) Fresh Water Distribution: The upper layer depth (H*), the depth above which 90% of the fresh water was contained for any given station, was computed by determining the concentration of fresh water C in water of salinity S_r at any depth Z by:

$$C(Z) = 1 - \frac{S(Z)}{S_r} \qquad (1)$$

where S(Z) is the salinity at depth Z,

S_r is the salinity at the reference depth (24 m) (or the bottom if shallower than 24 meters).

The equivalent thickness of fresh water layers (ΔH_1) between successive depths ΔZ was computed as

$$H_{(i+\frac{1}{2})} = \frac{1}{2}\,(C(i+1) + C(i))\Delta Z \qquad (2)$$

where the depth of $(i+\frac{1}{2}) \simeq Z$

The accumulated equivalent thickness of fresh water to any depth Z is then a summation of equation (2) from the sea surface to any depth Z i.e.,

$$H(Z) = \sum_{i=0}^{i=N} \Delta H_i \qquad (3)$$

where N = number of layers summed to reach depth Z

The fractional accumulation of fresh water to any depth is given by

$$f(Z) = \frac{H(Z)}{H(Z)_r} \qquad (4)$$

and hence H* is that depth where f(Z) = 0.9

In order to determine the mean concentration of fresh water in the upper layer some auxiliary variables have been defined by Collias, Barnes *et al.* (1966) - these serve to make the computations more stable from irregularities in the reference salinity used.

$$S_u = S_r\,(1 - \frac{0.9\Delta H(Z_r)}{H^*}) \qquad (5)$$

= mean salinity in the upper layer.

Hence, the mean concentration of fresh water in the upper layer is given by

$$FWC_u = \frac{S_b - S_u}{S_b} \qquad (6)$$

where FWC_u = mean concentration of fresh water in the upper layer

S_b = base salinity of the source water.

A base salinity of 32‰ was used for the November calculations. This corresponds to an average salinity of the upper 75 meters inflowing current along the Newfoundland side of Cabot Strait (Trites, MS 1970). In May, a value of S_b = 31‰ was chosen. This represents the average salinity at the bottom of the halocline.

The bay was divided into small regions surrounding each station, volumes of water at selected depth intervals for each region were calculated taking into account tidal fluctuations in the sea surface. By multiplying the fresh water concentration in the upper layer by the volume in the upper bay for each region, the total volume of fresh water in the upper layer (VFWU) was determined. From these data and the fresh water entering the bay, the overall exchange of fresh water is summarized in Table 9.

The depth of the upper layer (H*) and mean salinity in this layer (S_u) for November, 1970 are shown in Figure 33. The upper layer depth increases uniformly from less than 10 meters at the head of the bay to over 40 meters at the mouth with no appreciable lateral gradients in the inner portions except, perhaps, along Flat Island. It is most likely that the two layer analogy breaks down in the inner portions of the Bay and the value of upper layer depth cannot be used in interpreting say, the mean flow of fresh water seaward. The average fresh water distribution for May 18 and May 23 are presented in Figures 45 and 46. The concentration of fresh water in the upper layer varied between 1% and 16%, the highest values being observed in a band stretching from the Gut along the north-shore to Stephenville.

(b) Flushing: Calculations of flushing times, defined as the time necessary to renew the water within the estuary, have been made using the fresh water distribution as a tracer. Denoting Q as the total volume of fresh water contained in the system, and R as the volume of river flow per tidal cycle, then the flushing time t is given by

$$t = Q/R$$

Calculations were carried out for the May period and results given in Table 10. River discharge quantities represent a 17 day average prior to the occupation of T,S stations.

3.2 Currents and Circulation Patterns

3.2.1 Circulation Patterns Derived from Drogue Observations

(a) November, 1970. A number of Lagrangian current measurements were made using parachute drogues as described in Section 2.

TABLE 10; Flushing time and transports for inner George's Bay

Date	Upper Layer H* Depth(m)	Volumes $(10^6)m^3$ Fresh Water (Pf)•	Upper Layer (Pu)•	River Outflow (R)	Flushing time (tidal days) (t)	Transport Mixed (Vm)•	$(10^6)m^3$ Counter (Vs)•	Non-tidal drift (cm/sec) (NTD)•
10 May 1971	8.85	54.40	795.3	20.822	2.613	304.415	283.593	2.82
18 May 1971	7.15	53.50	985.8	21.299	2.512	392.247	370.948	3.65
23 May 1971	7.89	51.24	1078.2	19.150	2.676	403.150	383.999	3.40

• for a definition of these terms see Collias, Barnes, *et al.* (1966)

Drogues were usually set at 3 meters and/or 15 meters. Duration of drogue measurements varied from a minimum of 3 hours to 30 hours with positioning usually at intervals of 30 minutes. Trajectories of released drogues are shown in Figures 47 and 48. In the surface layer (3 m) drogues moved in the prevailing wind direction at rates of about 2-3% of the wind strength. At the deeper levels (15 m) the motion seemed to be independent of the wind direction, drogues moving southward with easterly and southeasterly winds. The remarkable fact in both figures is the apparent uniformity of drogue motion and the rapid response of the surface drogues to changes in wind direction.

(b) May, 1971. More elaborate measurements were carried out in May - June, 1971, using tin drogues described in Section 2. Figure 49 shows trajectories of drogues at nominal depths of 1 meter during May 16. Drogues were positioned at arbitrary intervals (at least every 10 minutes). The flow pattern follows the trend of the bottom contours in the initial stage, except for drogue 2 released at 1312 AST which seems to follow a complicated eddy pattern. The conspicuous change in flow direction occurred with the shift in wind direction at 1630 AST from onshore or northeast to along-shore or northwest. In all cases except drogue 6, released at 1313, the drift was northwesterly with a small onshore component.

A set of five drogues, set at 1 meter; were released on May 19 in the same general area (Fig. 50) as those on May 16. The general flow pattern in the initial stages was similar to that of May 16, i.e., a northwesterly flow with small horizontal shear. With the change in wind direction at approximately 1000 AST, from south-southeast to west-southwest, currents veered cyclonically between 0930 and 1330, and reversed their direction to southeast. In general, drift rates were highest for drogues closest to shore.

Net drift velocities for drogues set at 1 and 5 meters on May 21 are shown in Figure 51. This case is interesting as it is the only one with sustained southerly or nearly along-shore winds. It seems that the rates at the surface (1 meter) increased seaward normal to the boundary. The rates at 5 meters decreased seaward. Also, particle trajectories at the 5-meter level deviated approximately 20-30° to the left of those at the surface (1 meter).

Drogue drift observations between Indian Head and Flat Island were made on May 24. Drogues were set at 1 meter and 5 meters, their trajectories are shown in Figure 52. Flow in the surface layer is to the west with a small northward component. Observed speeds were strongest close to the north shore. Northward components might be a manifestation of an Ekman drift produced by easterly winds. Flow at 5 meters is more complicated, especially in the central regions. Again, the net drift is directed to the west with speeds being about half those at the 1-meter level.

Two more cases with onshore component winds were observed on May 28 and June 3. In both cases (Figures 53 and 54) winds in the initial stages were westerly then veered cyclonically to south-southwest. In

the early stages of drift, particle trajectories were oriented nearly parallel to the coastline, with velocities to the northwest. With the change in wind direction all started to move towards shore, those at the 1-meter level with rates approximately three times those at the 5-meter level. Interestingly, with nearly direct onshore component winds (Fig. 53) there seems to be considerable shear between 1 metre and 5-meter levels those at the surface (1 m) moving onshore to the northwest while those at the 5-meter level moving onshore but to the southeast.

The above cases have shown the effect of winds on the near-shore environment. For prediction purposes it may be worthwhile to compare observations to those derived from theoretical considerations.

The influence of prevailing winds on currents in the near-shore region is amply demonstrated by the previous drogue trajectories. It is somewhat difficult to discern what all the controlling factors are because of the short sampling periods. Wind-generated currents near an in infinitely long coast were studied theoretically by Ekman (1905, 1923) by assuming steady state conditions and neglecting horizontal momentum transfer. He defined a 'depth of frictional influence', D, a measure of the thickness of the wind current as

$$D = \pi \sqrt{\frac{N_z}{\rho \Omega \sin\phi}}$$

where ρ = density of sea water

Ω = angular velocity of earth's rotation

ϕ = latitude

N_z = vertical eddy viscosity

To determine the form of the vertical structure of the horizontal velocity vectors, the form of N_z is critical. For homogeneous water Sverdrup *et al.* (1946) suggest that N_z may be approximated by:

$$N_z(cm^2 sec^{-1}) = 4.30\ V^2 (V > 6\ m\ sec^{-1})$$
$$= 1.02\ V^3 (V < 6\ m\ sec^{-1})$$

where V is the wind speed.

During May, wind speeds were usually at, or slightly greater than, 6 m sec^{-1}. Using the appropriate formula we obtain a value for N_z = 193 cm sec^{-1}, giving D = 19 meters. As homogeneous conditions did not, in fact, exist and stratification exerts a supressing effect on vertical momentum exchange, the above value of D is an upper limit. As the total water depth d was usually less than the depth of frictional influence D, Ekman's elementary current system consisting of a pure wind drift at the surface, a geostrophic regime and a bottom boundary layer, probably did not exist. The drogue trajectories conform to the above 'elementary current' system only vaguely. It can be seen (Fig. 53) that the surface trajectories do not always deviate anticyclonically from the mean wind direction. This discrepancy may be due to the superposition of a mean current along the coast driven by the fresh water

run-off or due to boundary effects.

3.2.2 Dye Tracer Experiments

The purpose of this investigation was to examine transport phenomena (both advective and diffusive) by tracing the concentration distribution, in space and time, of Rhodamine B dye. The choice of Rhodamine B as a tracer was based on various earlier studies (Pritchard and Carpenter, 1960). The dye was introduced on the surface in concentrate form as supplied by the manufacturer (40% solution by weight) usually in 4.55-litre quantities. Although slightly denser than the surface waters, visual observations showed that the dye was confined to the upper 2 meters.

The Turner Model III fluorometer was used to determine dye concentrations. Sea water was pumped to the flow door of the fluorometer via a 22.85 meter long by 1.27 cm (I.D.) hose which also acted as a support cable for a submersible pump. The pump was stabilized by a small 'V' type depressor attached directly to the bottom of the pump. Embedded within the flow hose were a number of conductor cables used to power the submersible pump, transmitting depth and temperature of the source water to a Clevite Model 260 6-pen recorder. All parameters were recorded on separate channels.

(a) Specific Dye Experiments

(i) Release #1: 17 November, 1970 (Fig. 55). Three and one-half hours after low water, 4.55 litres of dye were released approximately 800 meters southwest of the Stephenville breakwater. Simultaneously, a parachute drogue set to open just below the surface was also released. Because of the high initial concentrations, this dye could not be sampled until 1447 AST, nearly 4½ hours after release. Visual observations of the dye patch from release time until sampled with the fluorometer gave the following.

During the first three hours after release, the dye patch elongated in the prevailing wind direction. At 1200 AST it measured approximately 300 x 50 meters. The winds during this time were steady, from the east at about 3 m sec^{-1}. Hence, the elongation speed of the patch corresponds roughly to 1% of the wind speed. Commencing at about 1200 AST, there was a reduction of wind speed and a cyclonic veering. By 1400 AST, the wind was westerly at 2 m sec^{-1}.

During the fluorometer run the wind was from 285°T at 6.5 m sec^{-1}. The dye patch had now broken into two cells with maximum concentrations of 2 ppb and 0.70 ppb respectively. The splitting was probably caused by the change in wind direction. The paradrogue, set at the initial dye drop, moved with the prevailing wind at a rate of 12 cm sec^{-1}. The paradrogue was recovered at 0830 AST on 18 November, 1970.

Its net movement was approximately 3.5 km from the last fix, at an average rate of 5.8 cm sec^{-1}.

(ii) Release #2: 18 November, 1970 (Fig. 56). 4.55 litres of dye were released two hours after low water some 8 km west-northwest from Stephenville breakwater. The wind was from 240°T at 2 m sec^{-1}. Dye sampling commenced at 1340 AST. At this time, the centre of the dye patch (A) had moved some 400 meters north-northwest from the point of origin.

Between 1545 and 1630 AST the patch moved south - in line with the changing wind conditions. It should be noted that in contrast to the previous experiment (i), neither dye nor paradrogue responded as rapidly to changes in wind direction.

(iii) Release #3: 19-20 November, 1970 (Fig. 57). 4.55 litres of dye were released approximately 2 km north of Harbour Point. The wind was northeasterly at 2 m sec^{-1}. In four hours the dye patch had moved approximately 1 km to the southwest at an average rate of 6.5 cm sec^{-1} reflecting the increase in wind speed over the previous three hours. During this interval, the paradrogue set at 3 meters moved with the prevailing wind at an average rate of 95 cm sec^{-1}. Both dye patch and paradrogue were relocated on November 20. Maximum concentrations had decreased by two decades. Both patch and paradrogue had moved west at an average rate of 12 cm sec^{-1}. The wind over the same period averaged 080°T at 2 m sec^{-1}.

(iv) Release #4: 24 November, 1970 (Fig. 58). Nine litre of dye were released at HW in the channel separating Stephenville Pond from St. George's Bay. At this time winds were from the south at 3.4 m sec^{-1}.

Due to pronounced seiching in the channel and Stephenville Pond, the dye appeared at the mouth of the channel only some 3½ hours later. At this time (1134 AST) a paradrogue was set at 3 meters in the dye patch. Once clear of the breakwater, the dye elongated in the direction of its bulk movement and drifted parallel to the shoreline. The drogue also moved parallel to the prevailing wind direction at an average rate of 25 cm sec^{-1} (between 1143 AST and 1300 AST). Between 1030 and 1130, the wind direction shifted resulting in a greater onshore component. The shift in wind direction seems to have broken up the patch into three separate cells. With the increased onshore wind component, the paradrogue drifted closer to shore and accelerated to 57 cm sec^{-1} (between 1300 and 1510).

Most information on wind-induced drift has been obtained using drift cards and bottles. These studies suggest that the surface water movements are 2-3% of the wind speed. The values of surface drift

derived from the drogue and dye tracks are of the same order for drifts removed from coastal boundaries. When the effects of coastal boundaries are felt, the above relation no longer holds true.

3.2.3 Observations from Moored Current Meters

Most of the direct current measurements were made in order to verify inferences made about circulation patterns based on drogue trajectories and the distributions of temperature and salinity. These parameters have indicated that large changes in the flow field could be correlated to periods of strong winds. Unfortunately, both drogue and temperature salinity data are small samples and it is difficult to make any meaningful statistical calculations into the effects of wind, tide, etc. The current meter data, being in serial form, have been utilized in establishing the magnitude of tidal and quasi-steady components of the current field.

(a) Quasi-steady Currents: Quasi-steady currents, in the form of net drift vectors are shown in Figure 59. Because not all series were of equal length, the statistical reliability of these vectors differ. In particular, the vector for Station 83 is based on five days data; the vector at Station 78 (7 m) is based on 14 days data.

Flow at Station 78 is northwestward at both depth levels with a relatively large shear. Speeds range from 1.5 cm sec^{-1} at 7 meters to 4 cm sec^{-1} at 28 meters. The anticyclonic veering at this station is due to bottom topography. Currents at Station 79 are north-north west with surface layer (6 m) speeds of 6.6 cm sec^{-1} to 3.8 cm sec^{-1} at 47 meters.

This should be contrasted to measurements made in November in the vicinity of Station 79 which gave a mean rate (over 21 days) of 3 cm sec^{-1} towards 029°T at the 5-meter level. The mean current vector at Station 80 seems to give a slightly different current distribution. At this station the current direction rotates cyclonically with depth, the rates increasing with depth from 3.3 cm sec^{-1} at 3 meters to nearly 6 cm sec^{-1} at 41 meters. The flows at Stations 82 and 83 at the 22 meter level seem to be very weak and from continuity considerations should be much stronger. In contrast, the flow at Station 81 at the 16-meter level shows a very high northeasterly rate of 12.2 cm sec^{-1}. The quasi-steady state circulation pattern seems to consist of a cyclonic cell in the region north of Flat Island, with rates in the upper 20 m averaging 6.5 cm sec^{-1}. On the basis of this rate, a particle injected at the eastern boundary of St. George's Bay would take approximately 4 days to reach the western limits. This value is the same order as the flushing time calculated on the basis of salinity data in Section 3.1.3.

(b) Tidal and non-tidal Currents: The variability and complexity of the flow at any location is indicated in Figures 60 to 62 where the raw data have been plotted in the form of rate and direction vs. time. Both speed and direction are quite variable, with the variability in the upper 25 m being the greatest. Note particularly the large speed pulses recorded in the upper level meters

during May 14-15 and again on the 25-26 of May. Both periods are associated with high and persistent westerly winds. Superimposed on these large surges are fluctuations having peak to trough ranges of 25 cm sec^{-1} and a period of approximately 4 hours. Variations in the currents having tidal periodicities do not stand out clearly except during periods of very low meteorological activity, e.g. Fig. 60, top.

(i) Harmonic constants - finite fourier series were fitted to the above data. As all records were less than 29 days long, two overlapping 15 day analysis were carried out. The results are presented in Table 11.

As can be seen, the constants are very small and do not seem to vary in any systematic manner. Harmonic analysis carried out on the 1970 records also gave very small amplitudes - these also differ from those evaluated above.

(ii) Long-term motions - the nature of the longer term motions say with periods greater than 3 hours, may best be visualized by examining the progressive vector diagrams for each current meter time series. These plots are also useful for indicating, qualitatively, the spatial coherence of the circulation. Prior to calculating these visual displacements, all time series were low pass filtered with a triangular (Munk *et al.* 1959) filter having a cutoff at three hours. Figures 63 to 65 show progressive vectors for the 1971 data. Time marks along the trajectory paths is every 12 hours.

A striking feature of most diagrams is the strong northward component in the flow and, the persistent vertical shear at Station 80. A high degree of variability even in the low frequency components is evident. Unfortunately, wind data needed to correlate these fluctuations were not available.

IV SUMMARY AND CONCLUSION

St. George's Bay is a typical coastal estuary where, for most of the year, precipitation and runoff exceed evaporation. The freshwater, which is discharged from the numerous small rivers in the inner bay, appears to become rapidly mixed in the upper layer. This layer of moderately low salinity moves seaward along the northern boundary of the bay as a confined coastal current with rates of approximately 3-5 cm/sec. The surface circulation in the inner bay seems cyclonic.

Winds were found to exert a large influence on the short term circulation pattern leading to advection of denser water over the sill into the Basin and also intensifying vertical exchange between low salinity surface layers and oceanic subsurface layers.

TABLE 11 (a): Harmonic constants evaluated from two 15 day analyses

Amplitude in cm sec^{-1}; Phase (in degrees) based on AST time
MAJOR (NORTH) COMPONENT

Stn Depth(m)	Zo	M_2 A/θ°	S_2 A/θ°	K_2 A/θ°	N_2 A/θ°	K_1 A/θ°	O_1 A/θ°	P_1 A/θ°	M_4 A/θ°	MS_4 A/θ°
79(47)	3.4	1.5/ 285.9	.73 67.8	-	-	-	-	-	-	-
78(28)	3.6	1.7 225.0	1.09 147.9	-	-	-	.80 182.2	-	-	-
79(6)	5.4	.8 159.0	-	-	-	-	-	-	-	-
80(3)	2.9	.8 120.2	.8 121.2	-	-	1.0 126.4	1.0 30.2	-	-	-
81(16)	11.3	7.3 307.3	7.7 243.4	-	-	1.1 23.1	-	-	-	-
80(4)	-3.5	2.2 259.0	-	-	-	.6 242.4	1.8 113.1	-	-	-
80(12)	5.0	-	1.3 233.5	-	-	0.7 94.9	.8 30.6	-	-	-

TABLE 11 (b): Harmonic constants evaluated from two 15 day analyses

Amplitude in cm sec^{-1}; Phase (degrees) based on AST time
MINOR (EAST) COMPONENT

Stn Depth(m)	Zo	M_2 A/θ°	S_2 A/θ°	K_2 A/θ°	N_2 A/θ°	K_1 A/θ°	O_1 A/θ°	P_1 A/θ°	MS_4 A/θ°
79(47)	-1.7	-	.7 176.5	-	-	-	.8 26.1	-	-
78(28)	-1.7	1.9 209.2	1.0 214.9	-	-	1.1 196.1	1.4 136.5	-	-
79(6)	-3.7	1.0 277.9	.7 173.2	-	-	.6 210.5	.7 88.4	-	-
80(3)	1.6	.8 10.5	.6 100.7	-	-	.9 140.4	1.3 100.7	-	.6 233.8
81(16)	4.6	.7 274.1	2.2 342.8	.6 342.8	-	.7 170.1	1.0 138.3	-	-
80(41)	-4.8	1.1 162.5	.9 220.4	-	-	-	-	-	-
80(12)	-1.5	1.4 201.9	1.3 330.0	-	-	.5 150.9	.9 168.4	-	-

For the purposes of effluent removal, the factors contributing to a net transport out of the Bay are most important. Under these, we consider the estuarine sequence set up by the influx of freshwater as the most important. The effects of sustained westerly or easterly winds could not be discussed. However, from theoretical considerations (Hansen and Rattray, 1965) it can be shown that the typical two layer flow can be changed into a three layered flow with transports in these layers depending on the wind direction.

When the estuarine sequence is absent, as might occur during summer conditions when the amount of precipitation and runoff barely exceeds evaporation, the factors contributing to exchange will probably be tidal currents and transient winds.

If the behaviour of the effluent is similar to that of the freshwater distribution, it is most likely that the effluent cloud will be confined to the nearshore areas. At times with winds from the northwest to southeast quadrants this cloud will most likely be pushed on shore, similar to the trajectories of the drogues. With the above comments in mind, an effluent system which seeks to maximize initial dilution will be the most desirable.

V ACKNOWLEDGEMENTS

This report could not have been completed without the considerable help of others. I particularly wish to thank J. Pritchard and T. Foote, who helped plan and carry out the field work in 1971 and 1970 respectively. A. Hartling, R. Lively, G. Taylor and D. Wilson were instrumental in reducing and plotting the large amount of data. For other aid in the field I wish to thank J.G. Clark, R. David, D. Doucette, F. Ewing and B. Swyers. The cooperation of the captains and crew of CSS *DAWSON* and M/V *NAVICULA* is also appreciated.

VI REFERENCES

1. AANDERAA, I., (1964): A recording and telemetering instrument; NATO Sub-committee on Oceanographic Research, Tech. Report No. 16.

2. BENNET, A.S., (1970): Focal language programs for salinity - temperature - depth data aquisition and processing; AOL Computer Note 1970 - 13 - C.

3. BOWDEN, K.F., (1967): Circulation and diffusion; Estuaries, AAAS Pub. 83, Lauf, ed.

4. COLLIAS, E.E., C.A. BARNES, C.B. MURTY and D.V. HANSEN, (1966): An oceanographic survey of the Bellingham - Samish Bay system, Vol. II. Analysis of Data, University of Washington Dept. of Oceanography Special Report No. 32.

5. EKMAN, V.W., (1905): On the influence of the earth's rotation on ocean currents; Ark fur Mat., Astr., och Fysik; Vol. II No. 11.

(1923): Uber Horizentalizirkulation bei winderzeugten Meeres stromungen; Ark. fur Mat., Ast., och Fysik Vol. 17 No. 26.

6. GREEN, E.G., and D.E. CARRIT, (1967): New tables for oxygen saturatien of sea water; J. Mar. Res. Vol. 24 No. 2.

7. HANSEN, D.V. and M. RATTRAY, Jr., (1965): Gravitahenil Circulation in straits and estuaries; J. Mar. Res. Vol. 23, No. 2.

8. KEYTE, F.K., (1970): Processing STD magnetic tapes; AOL Computer Notes 1970-9.

9. LAUZIER, L.M. and J.H. HULL, (1962): Sea temperatures along the Canadian Atlantic Coast 1958 - 1960, F.R.B. Progress Reports of the Atlantic Coast Stations No. 73.

10. MUNK, W.H., F.E. SNODGRASS, and M.J. TUCKER, (1959): Spectra of low frequency ocean waves; Bull. of Scnipps Inst. of Oceanography, Vol. 7 No. 4.

11. MURRAY, A.R. and T.J. HARMON, (1969): A preliminary consideration of the factors affecting the productivity of Newfoundland Streams, F.R.B. Technical Reports No. 130.

12. PRICHARD, D.W., and J.H. CARPENTER, (1960): Measurement of turbulent diffusion in estuarine and inshore waters; Assoc. Internationale d'Hydrologie Scientifique, Bull. No. 20.

13. STRICKLAND, J.D.H., and T.R. PARSONS, (1965): A manual of sea water analysis; Bull. of F.R.B. No. 125, 2nd ed.

14. SVERDRUP, H.U., M.W. JOHNSON and R.H. FLEMING, (1946): The oceans, their physics, chemistry and general biology, Prentice Hall.

15. TRITES, R.W., (1970): The Gulf as a physical oceanographic system; 2nd Gulf of St. Lawrence Workshop held at Bedford Inst.

16. TULLY, J.P., (1949): Oceanography and prediction of pulp mill pollutien in Alberni Inlet, F.R.B. Bull. No. 83.

17. VOLKMAN, B., J. KNAUSS and A. VINE, (1956): The use of parachute drogues in the measurement of subsurface ocean currents Trans. Amer. Geophys. Union, Vol. 37, No. 5.

18. WARNER, J.A., (1970): Water movement on the Scotian Shelf Ph.D. Thesis to Inst. of Ocean., Dalhousie University.

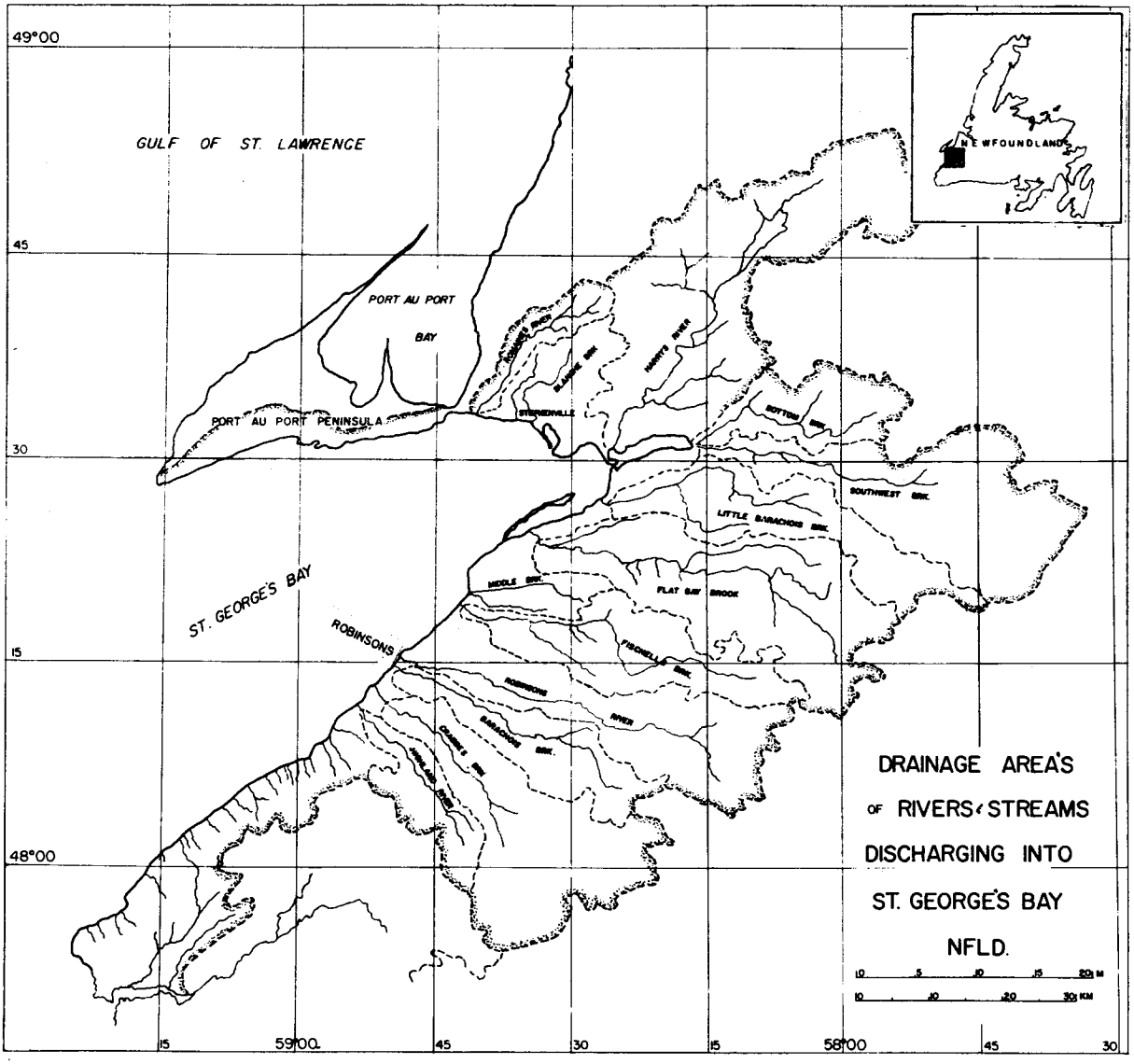

Fig. 1 Watershed of the St. George's Bay area and relevant place names

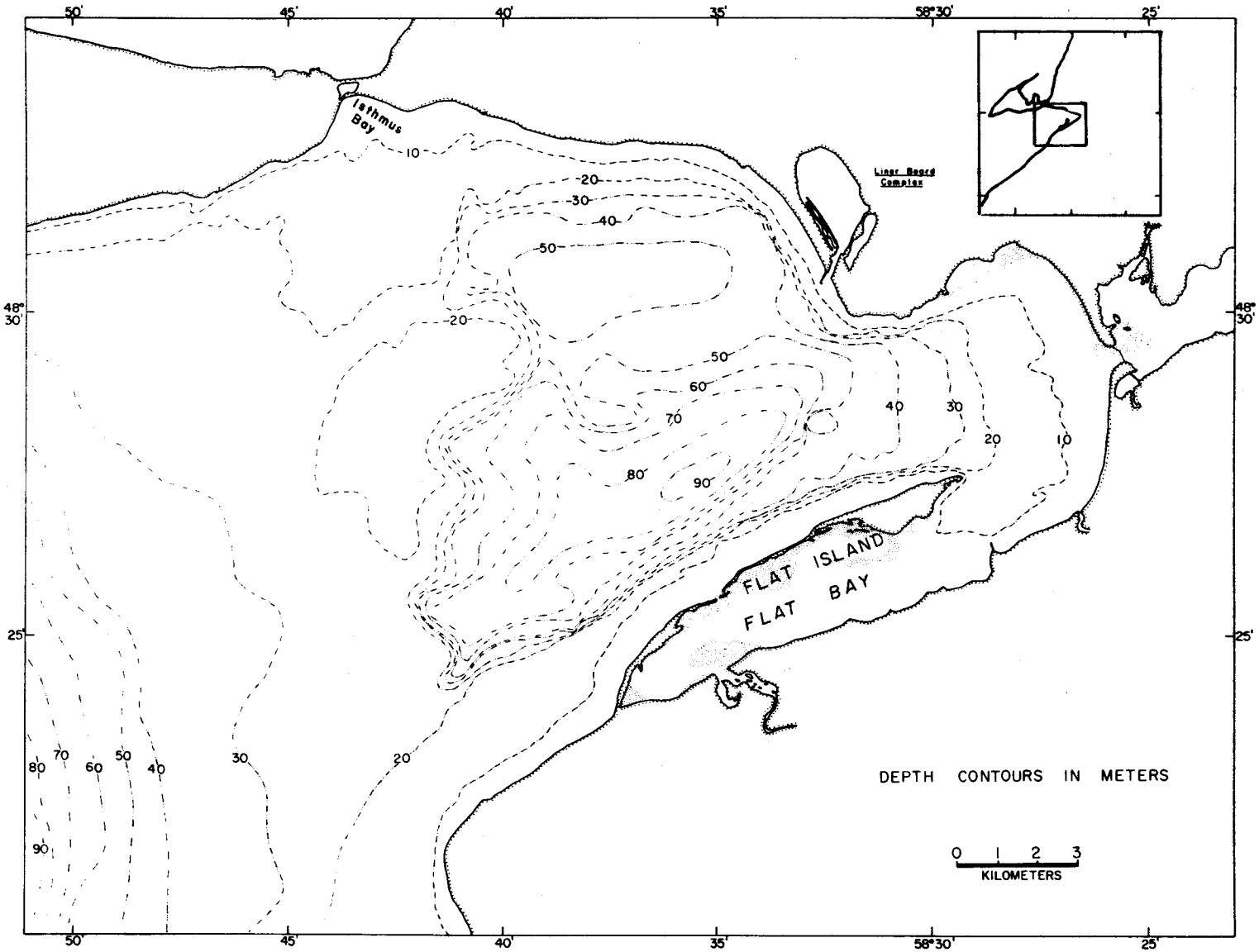

Fig. 2 Bottom topography - St. George's Bay

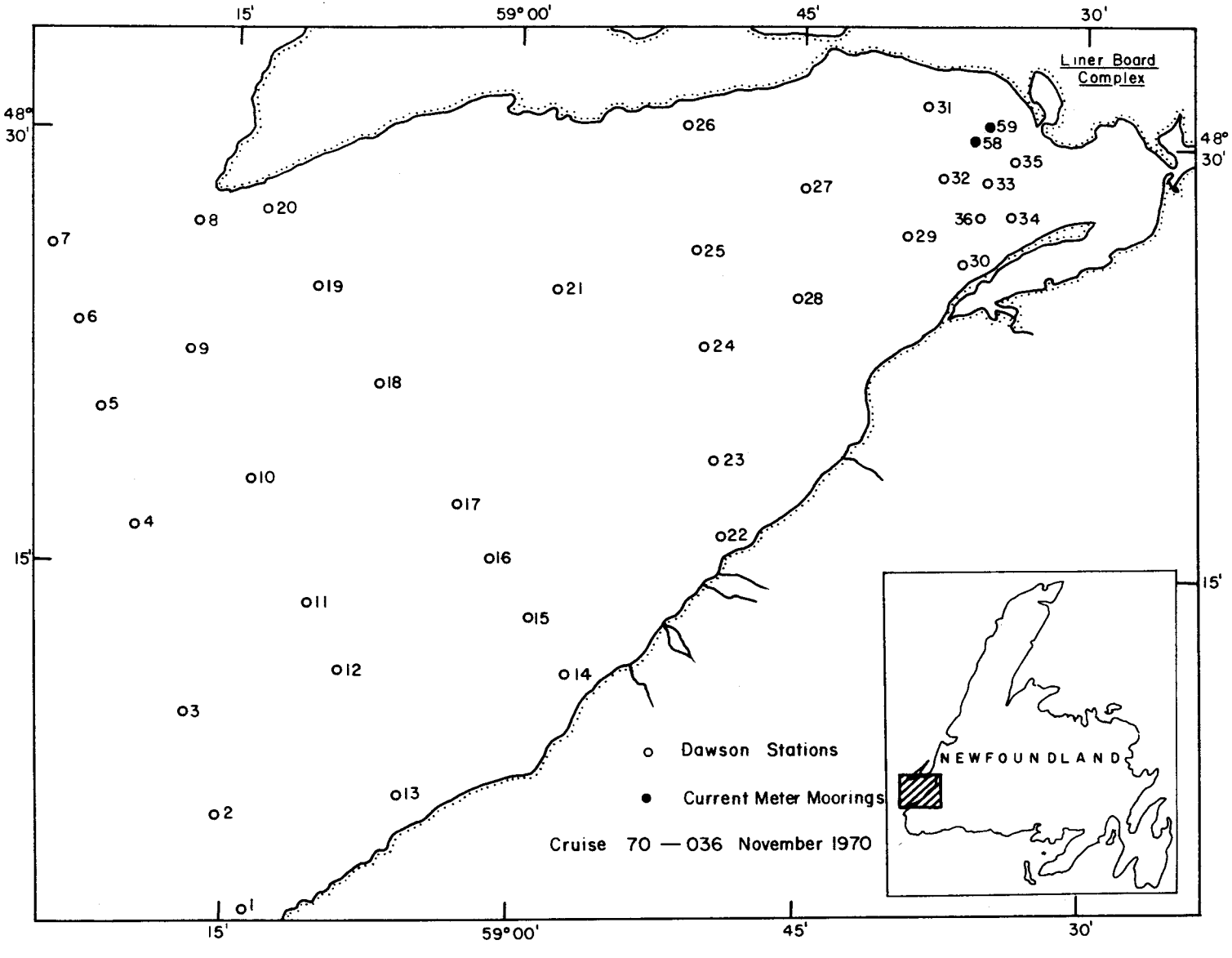

Fig. 3 Cruise 70-036 station grid (November, 1970)

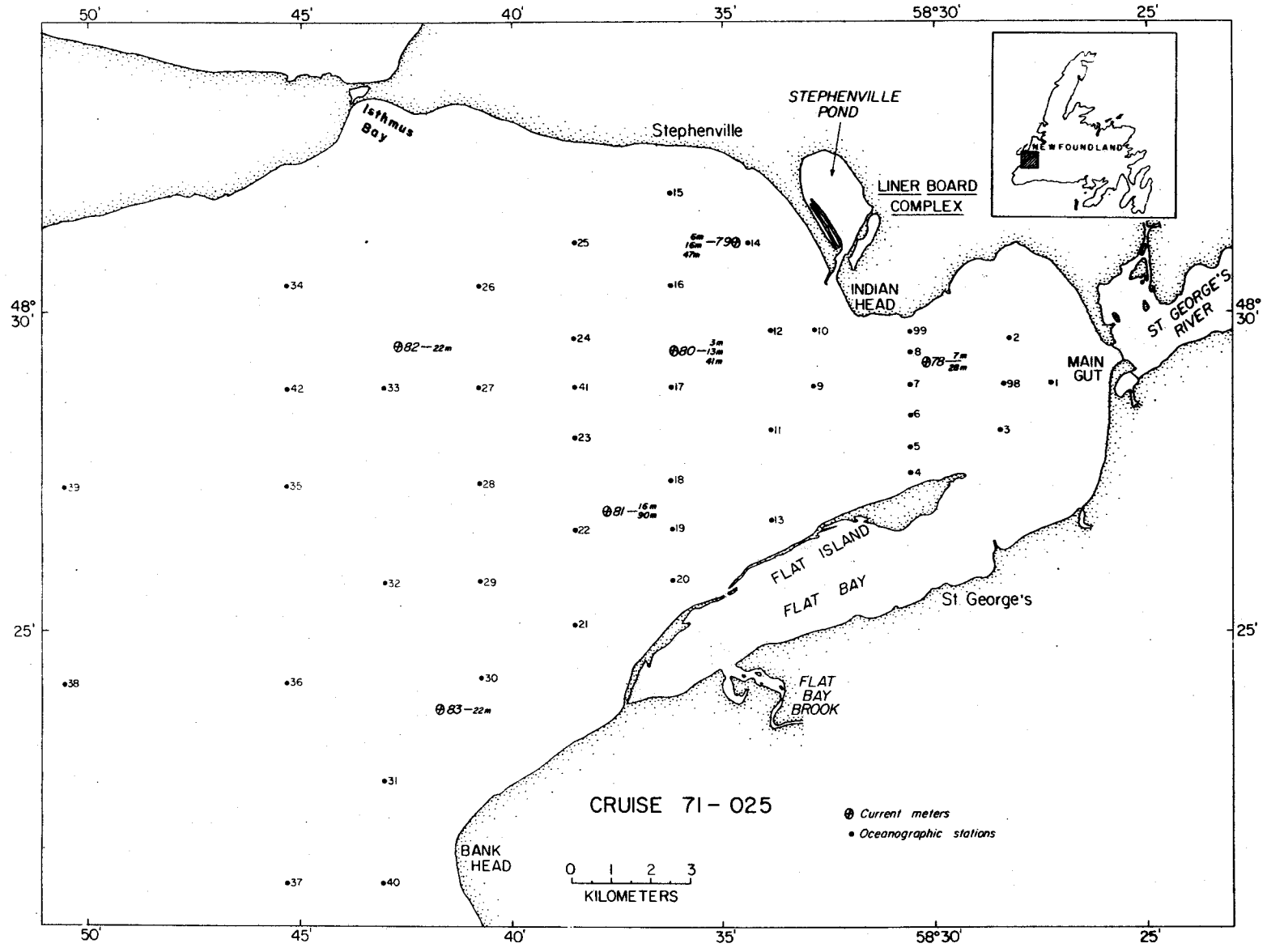

Fig. 4. Cruise 71-025 station grid and current meter locations (May, 1971).

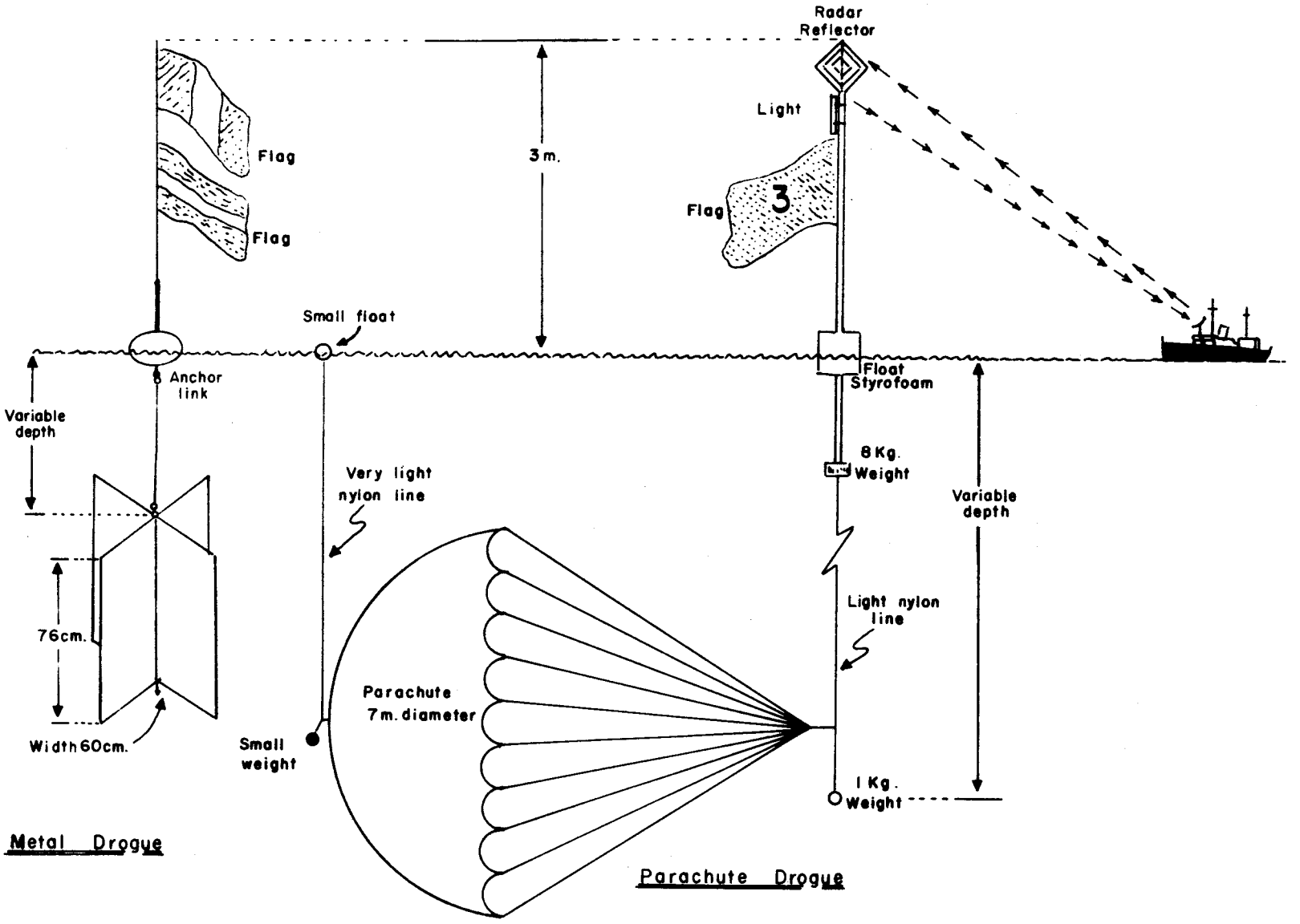

Fig. 5. Construction details of parachute or tin drifters.

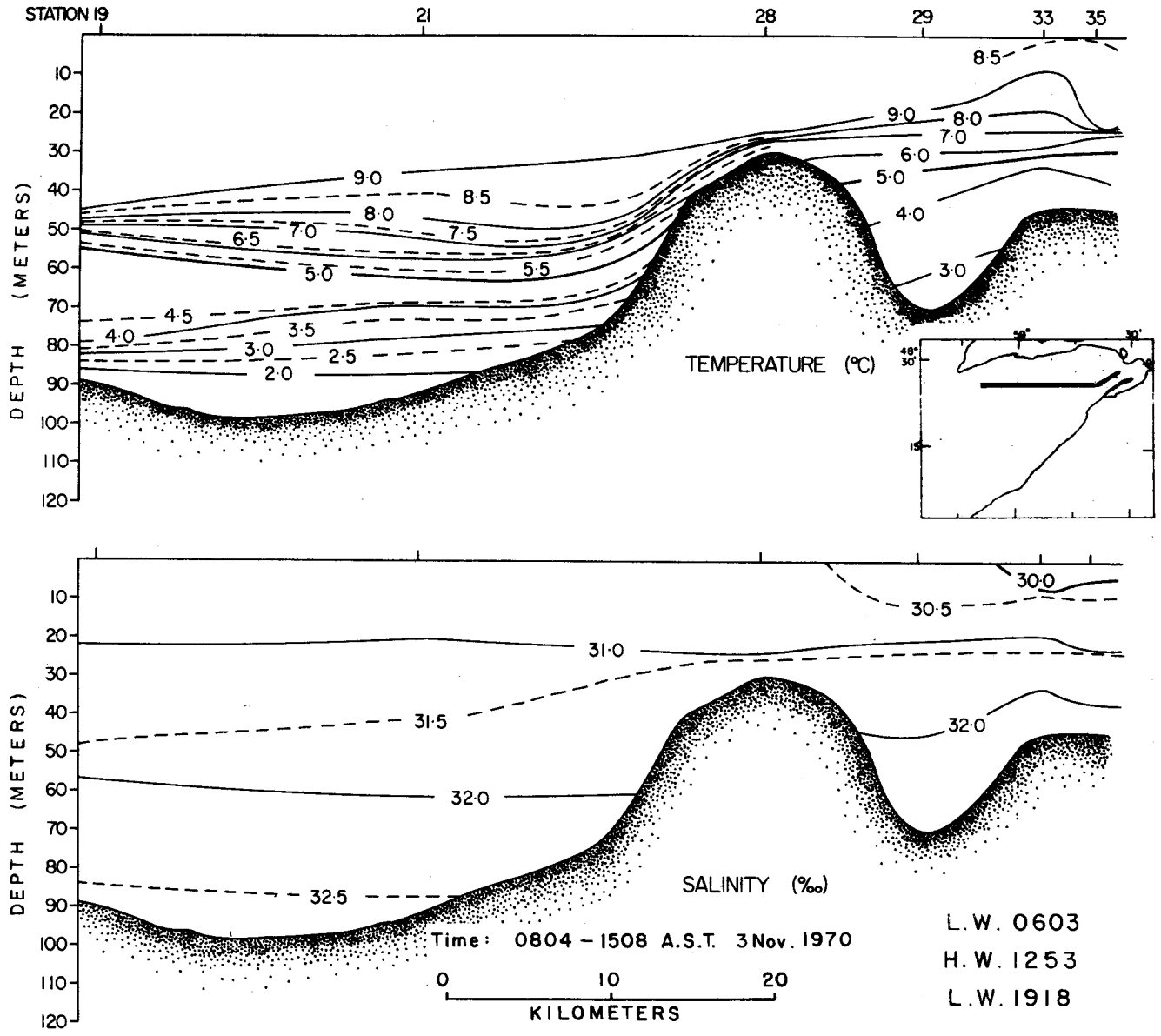

Fig. 6. Longitudinal temperature, salinity section, November 1970.

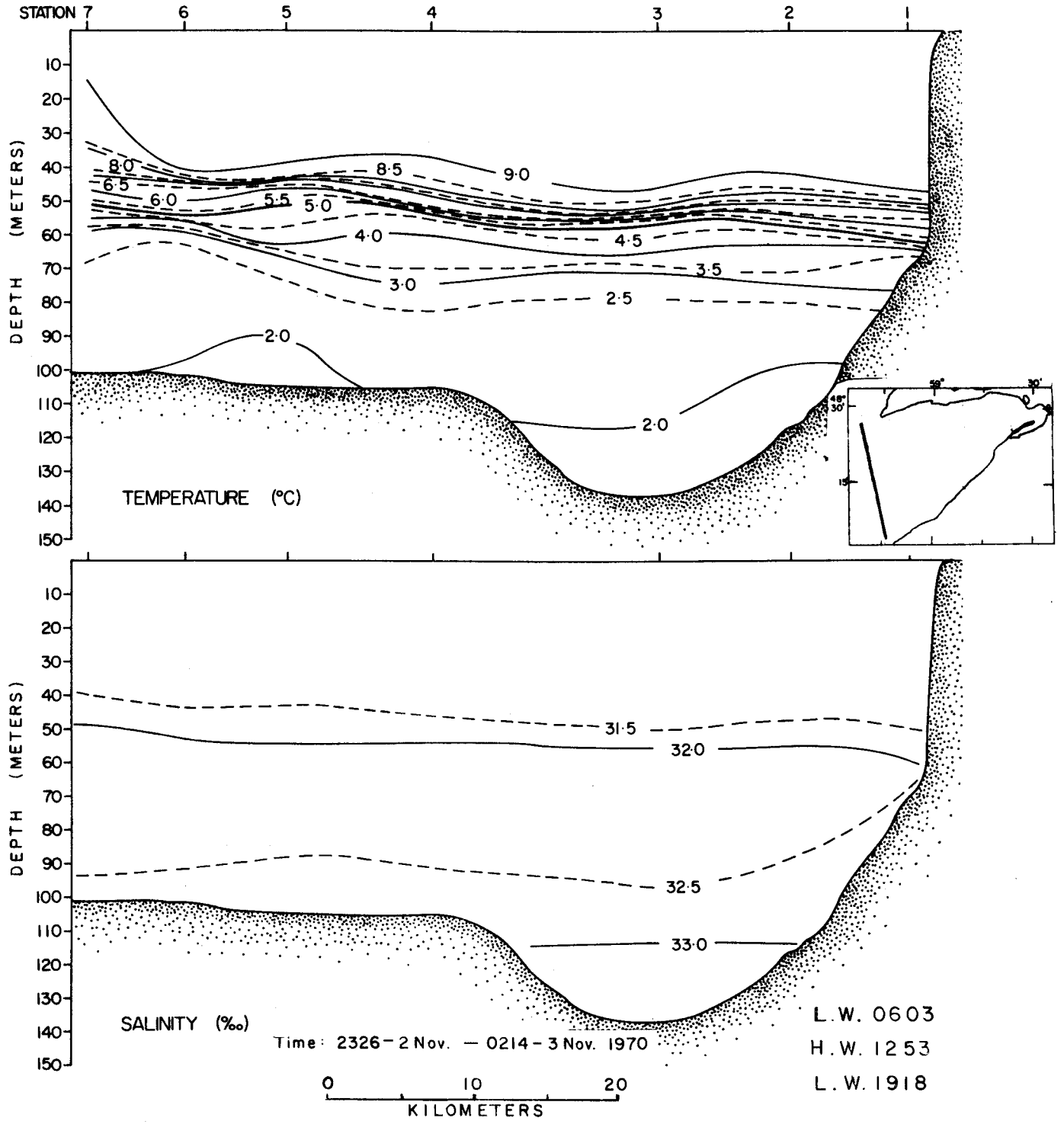

Fig. 7. Transverse temperature, salinity section, November 1970.

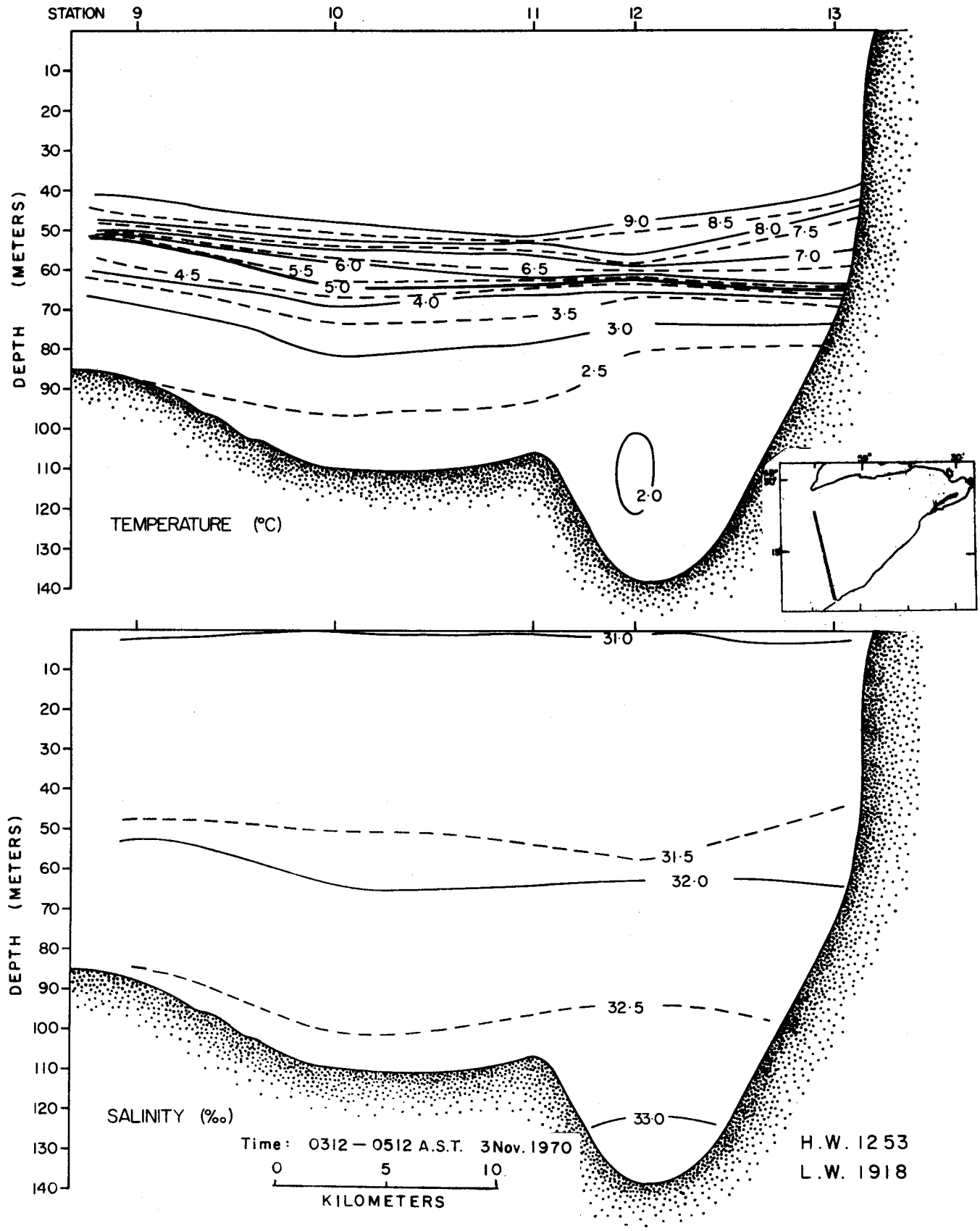

Fig. 8. Transverse temperature, salinity section, November 1970.

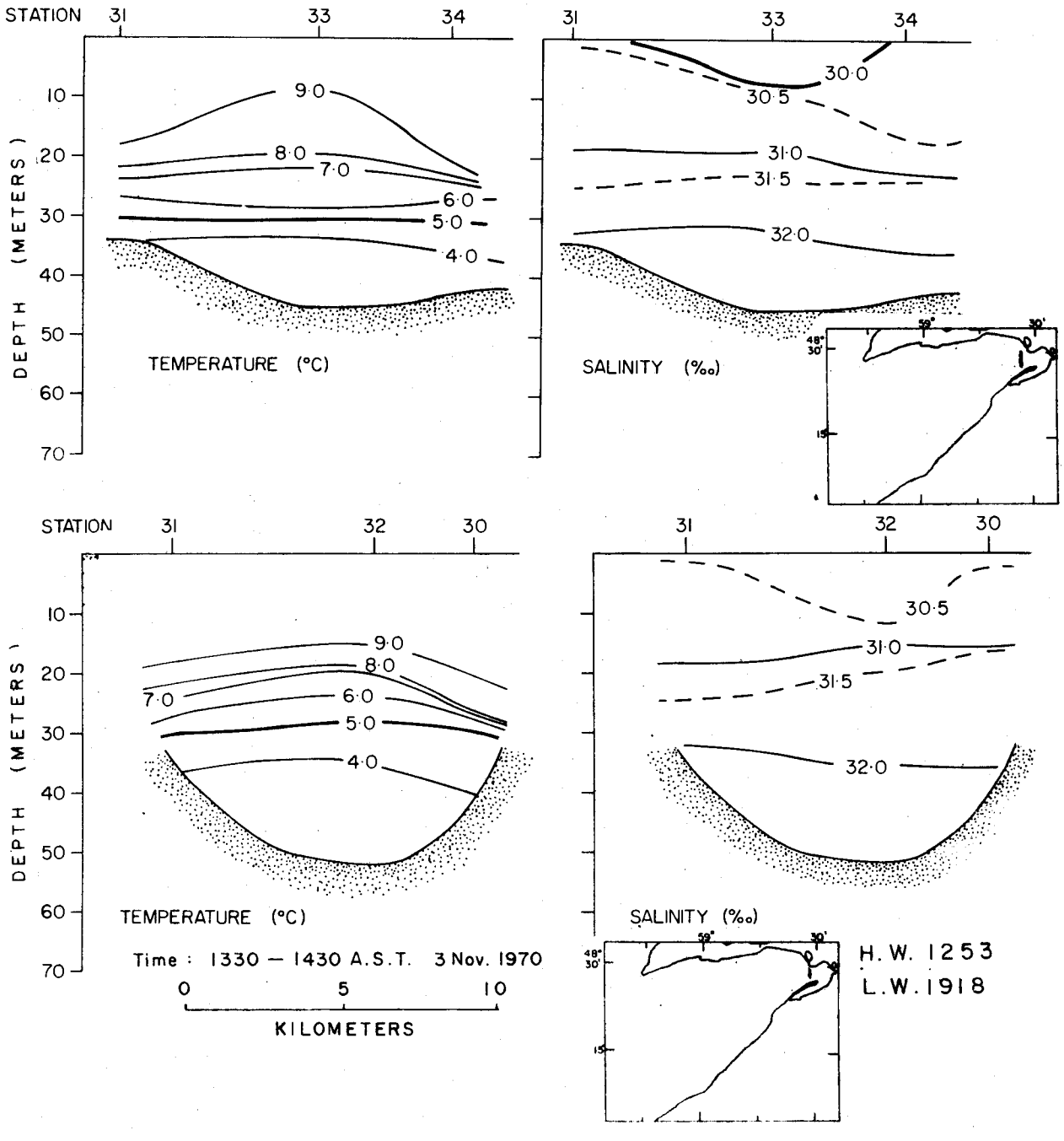

Fig. 9. Transverse temperature, salinity section, November 1970.

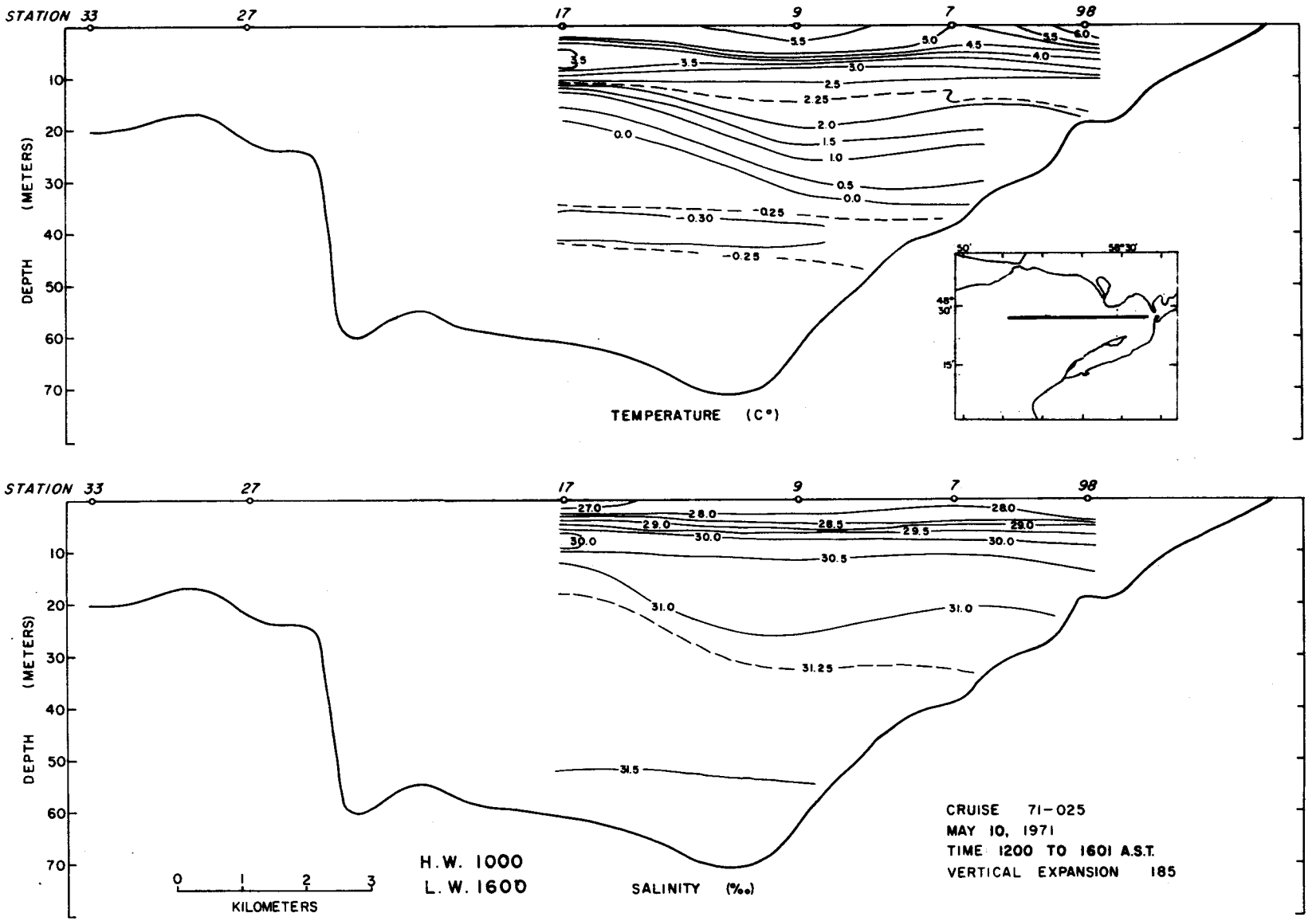

Fig. 10. Longitudinal temperature, salinity section, May 10, 1971.

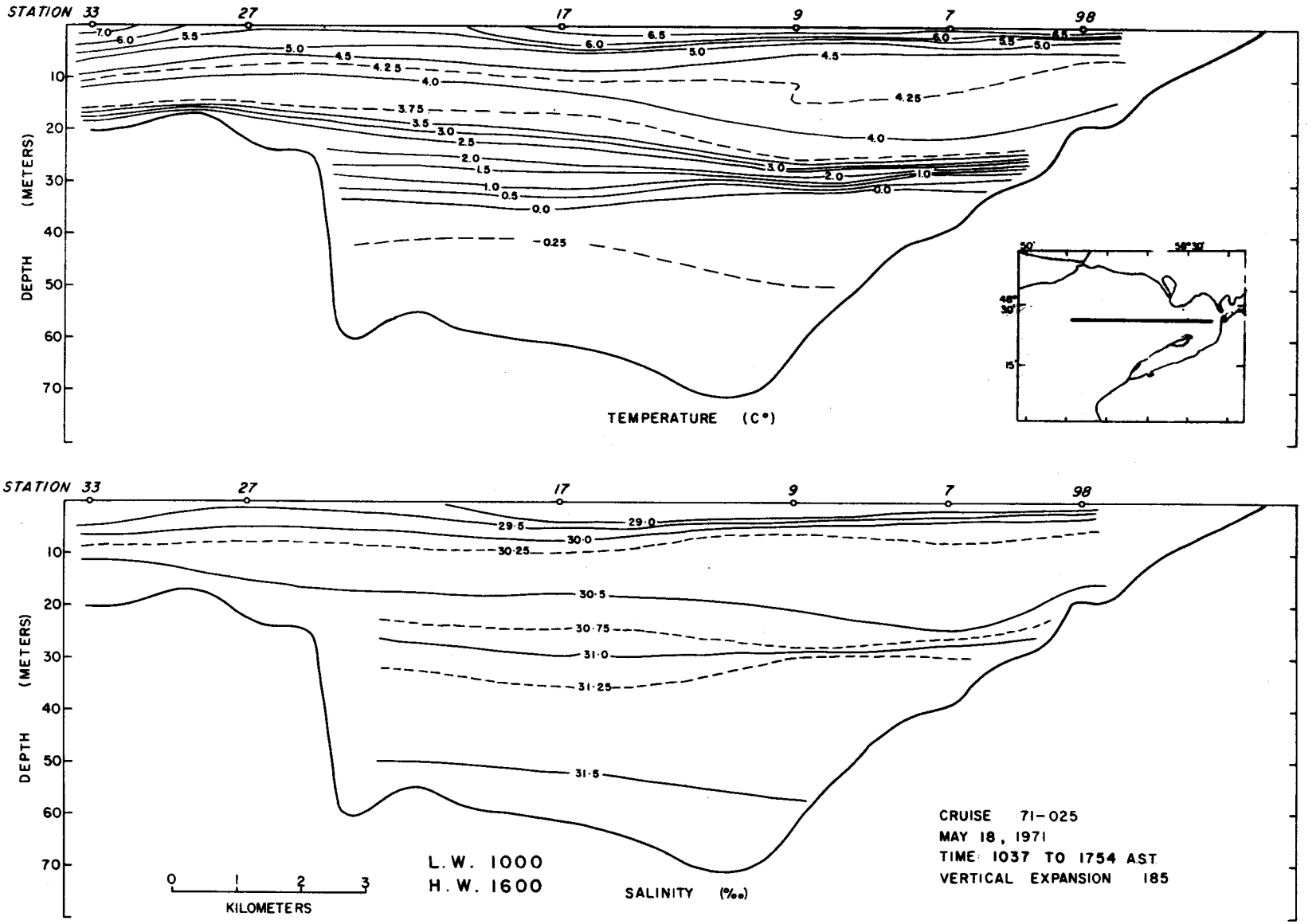

Fig. 11. Longitudinal temperature, salinity section, May 18, 1971.

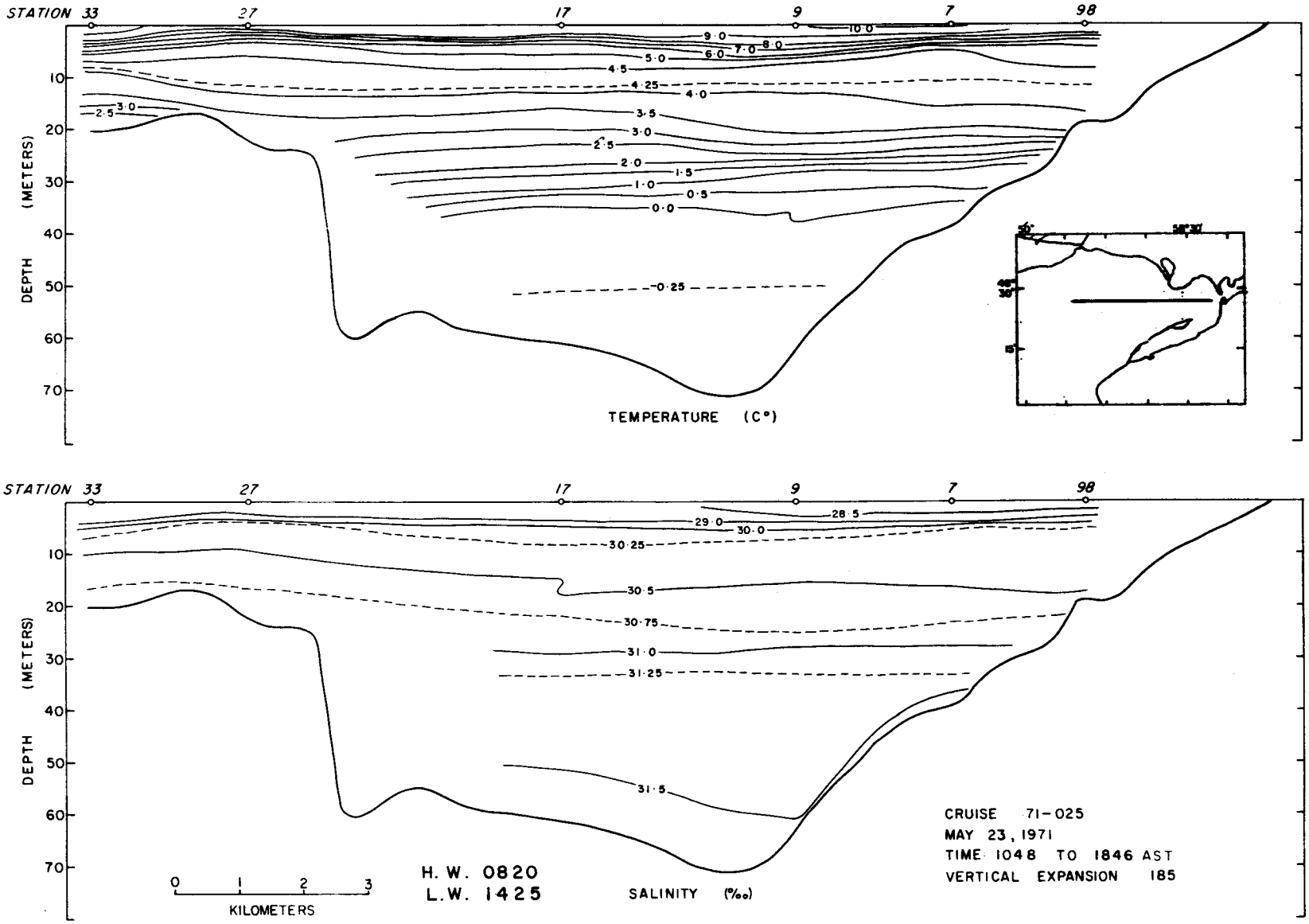

Fig. 12. Longitudinal temperature, salinity section, May 23, 1971.

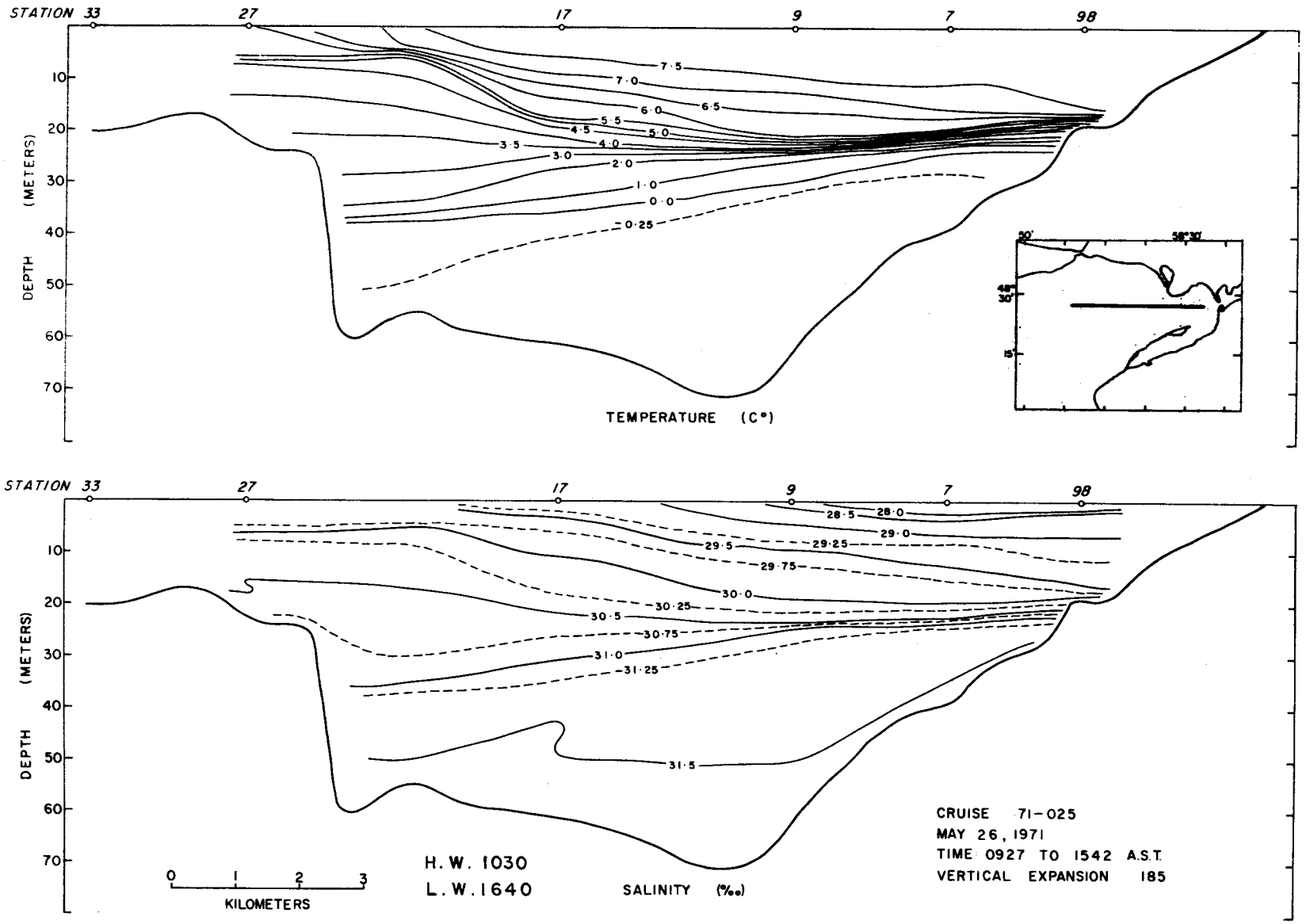

Fig. 13. Longitudinal temperature, salinity section, May 26, 1971.

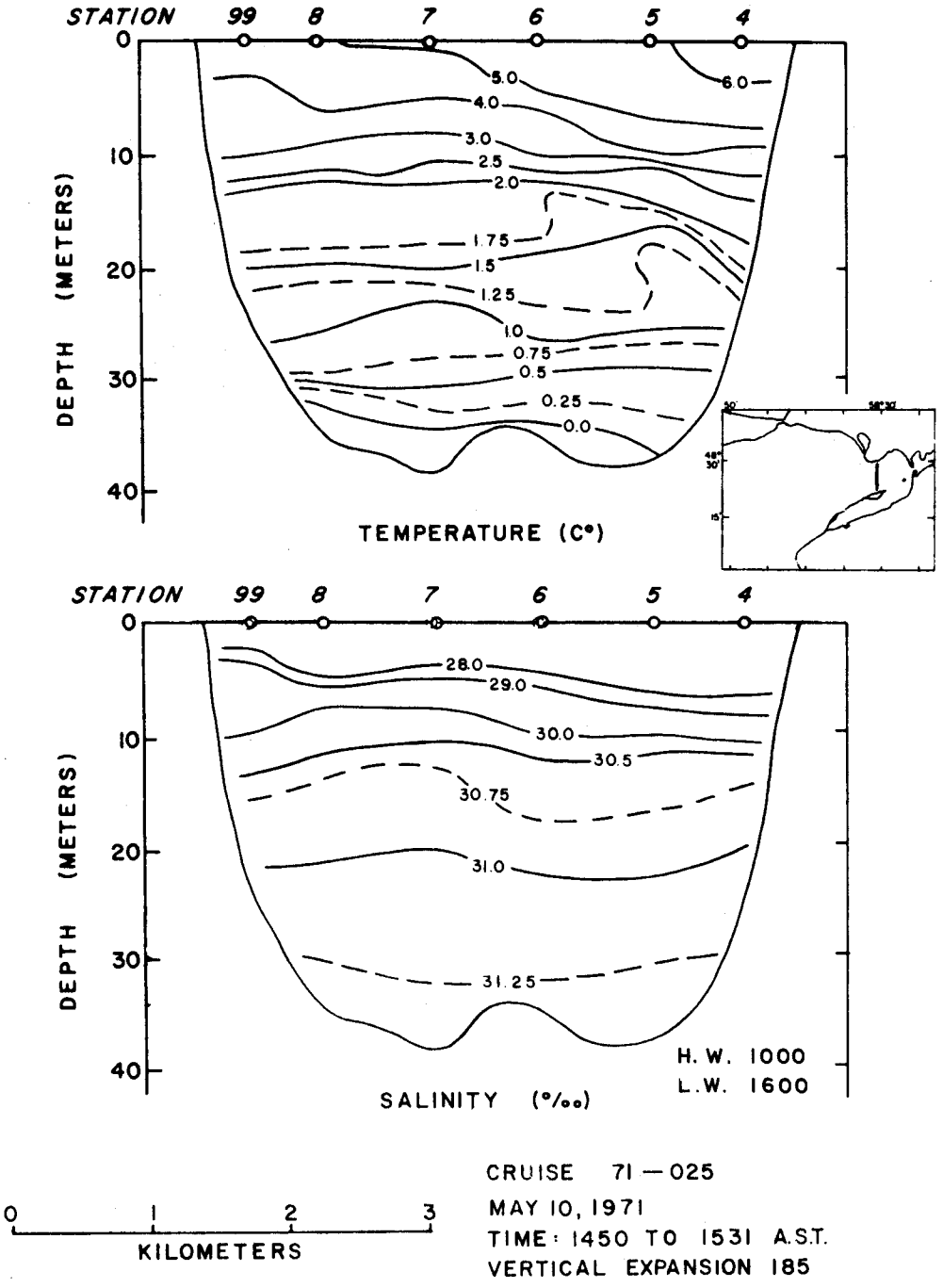

Fig. 14. Transverse temperature, salinity section (1) May 10, 1971.

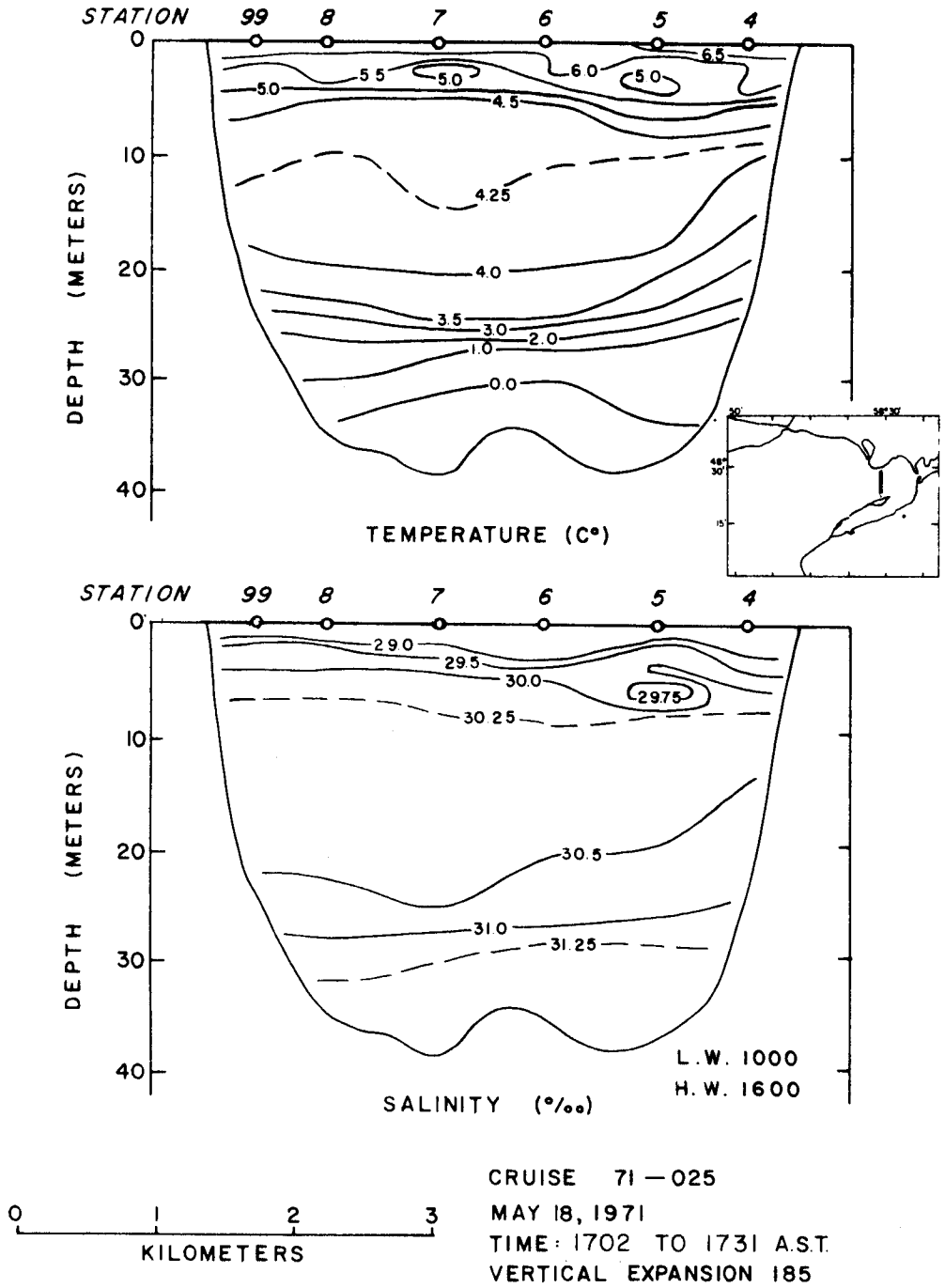

Fig. 15. Transverse temperature, salinity section (1) May 18, 1971.

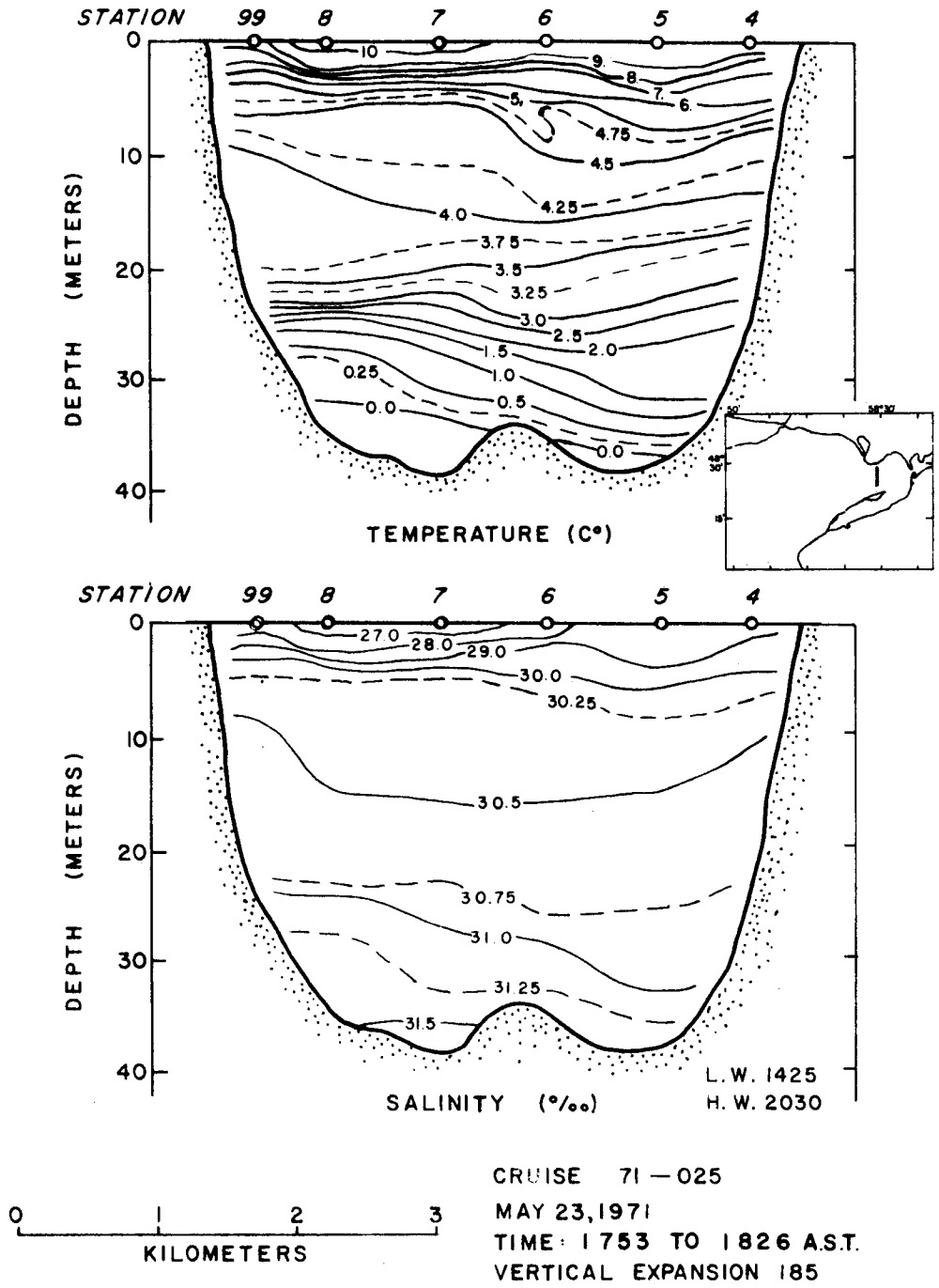

Fig. 16. Transverse temperature, salinity section (1) May 23, 1971.

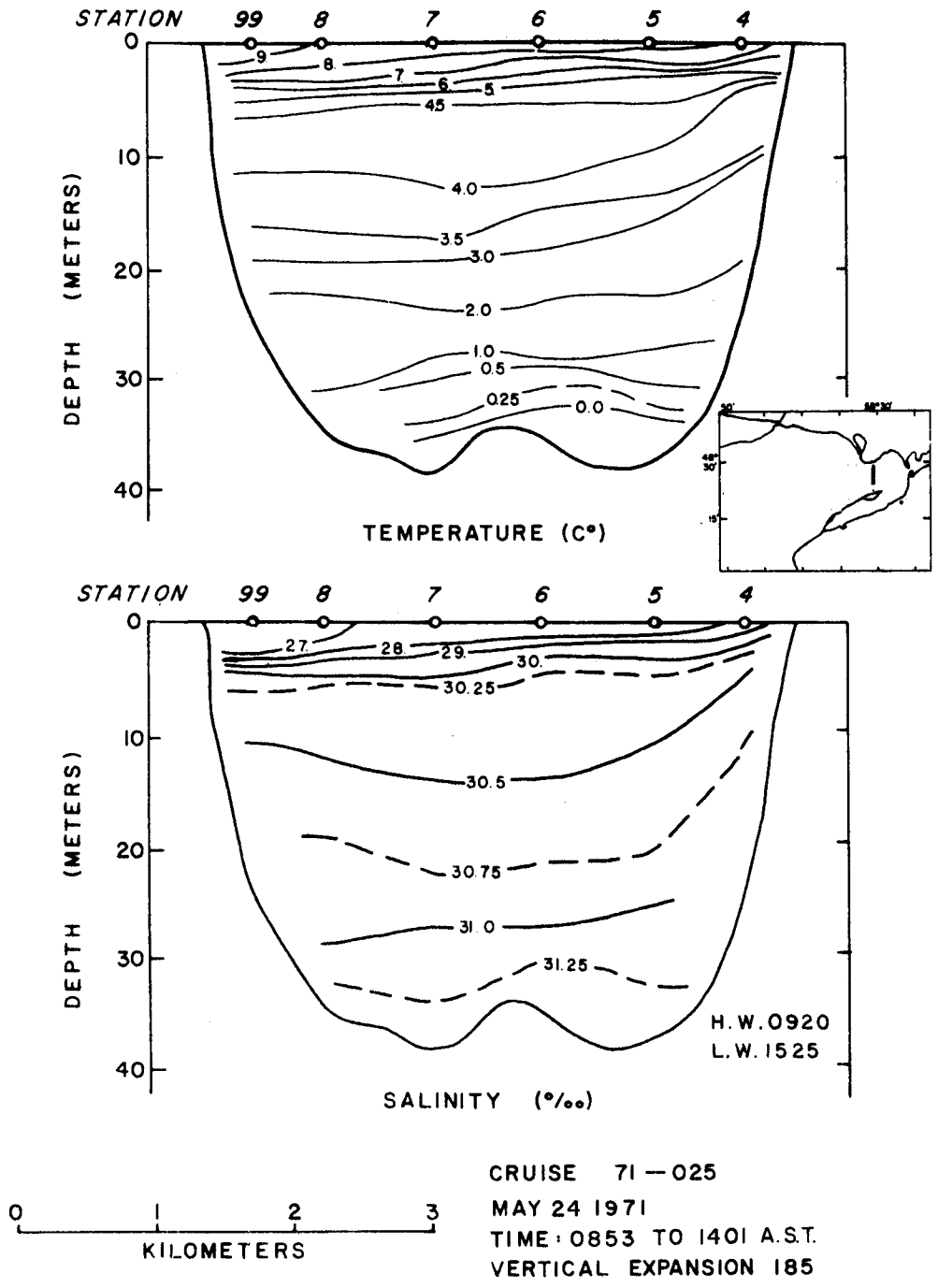

Fig. 17. Transverse temperature, salinity section (1) May 24, 1971.

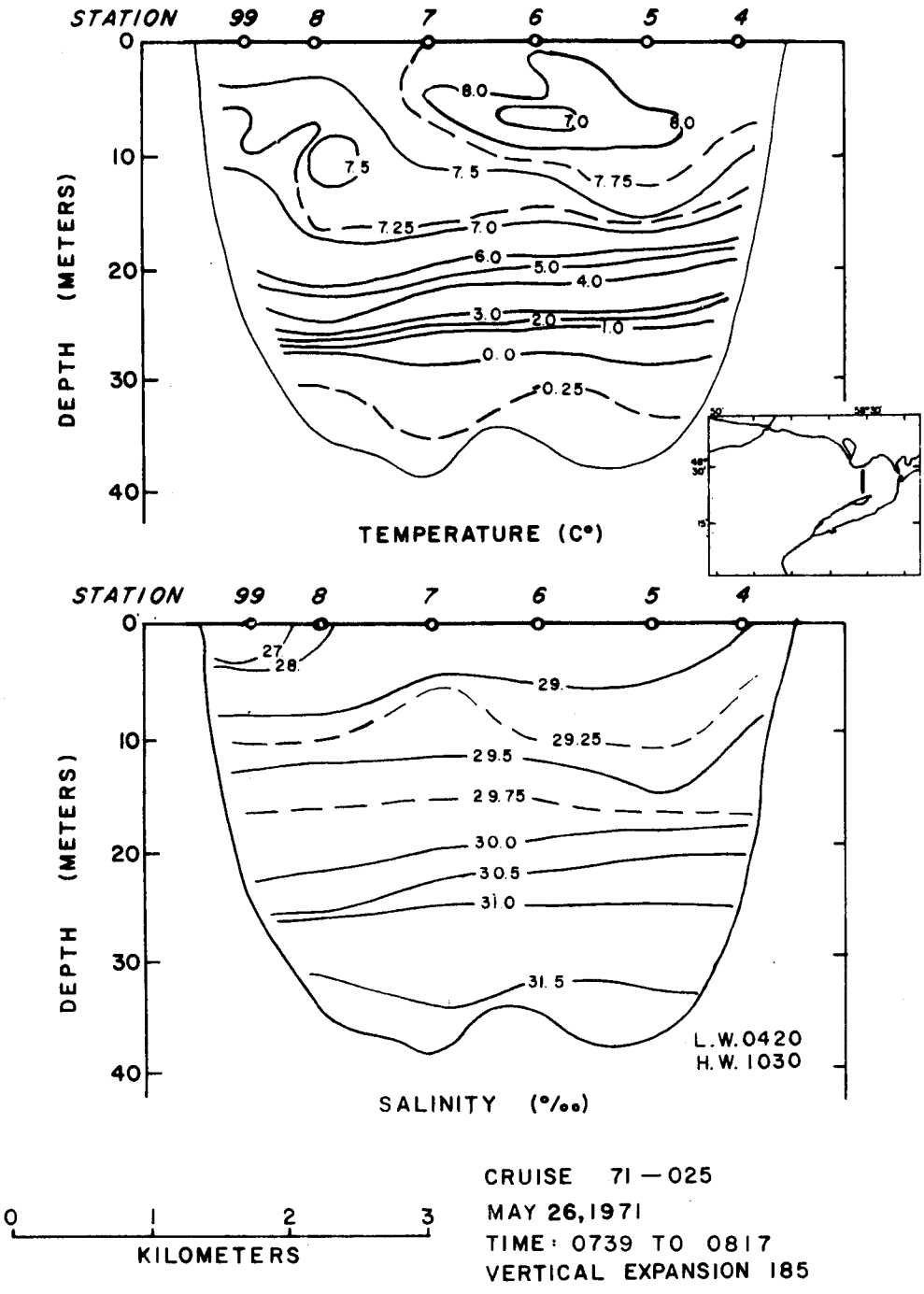

Fig. 18. Transverse temperature, salinity section (1) May 26, 1971.

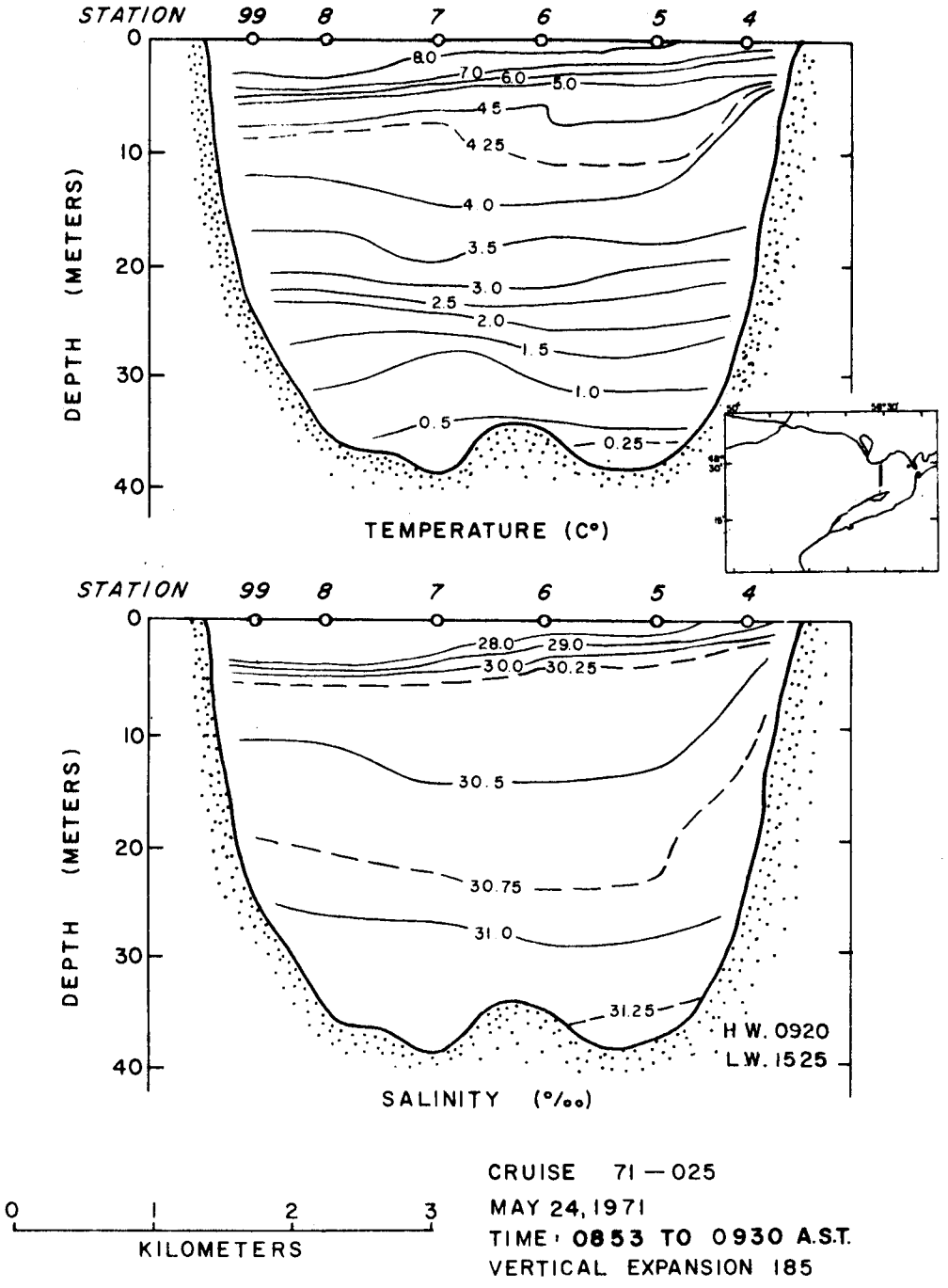

Fig. 19. Multiple occupations of section (1) May 24, 1971.

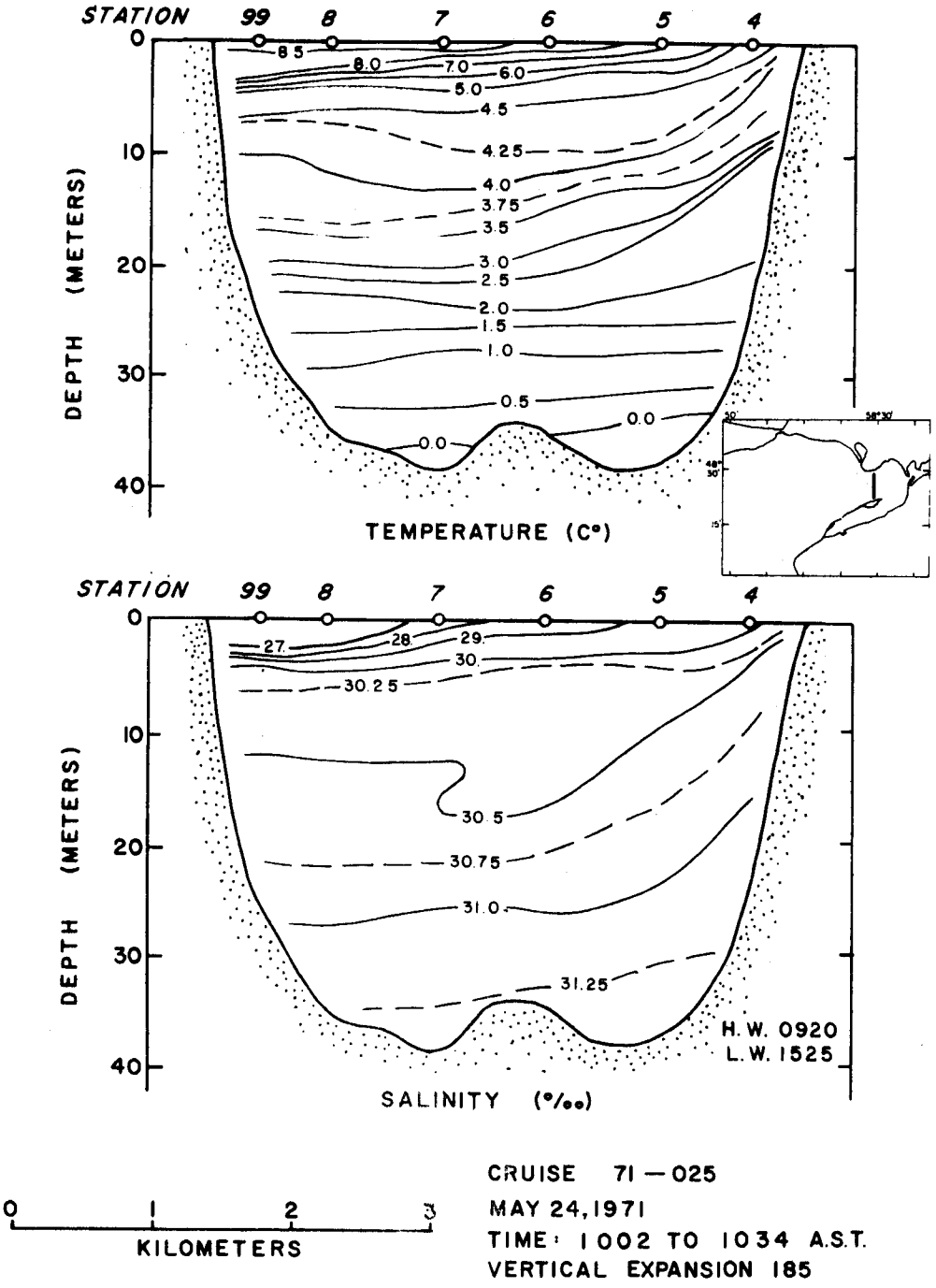

Fig. 20. Multiple occupations of section (1) May 24, 1971.

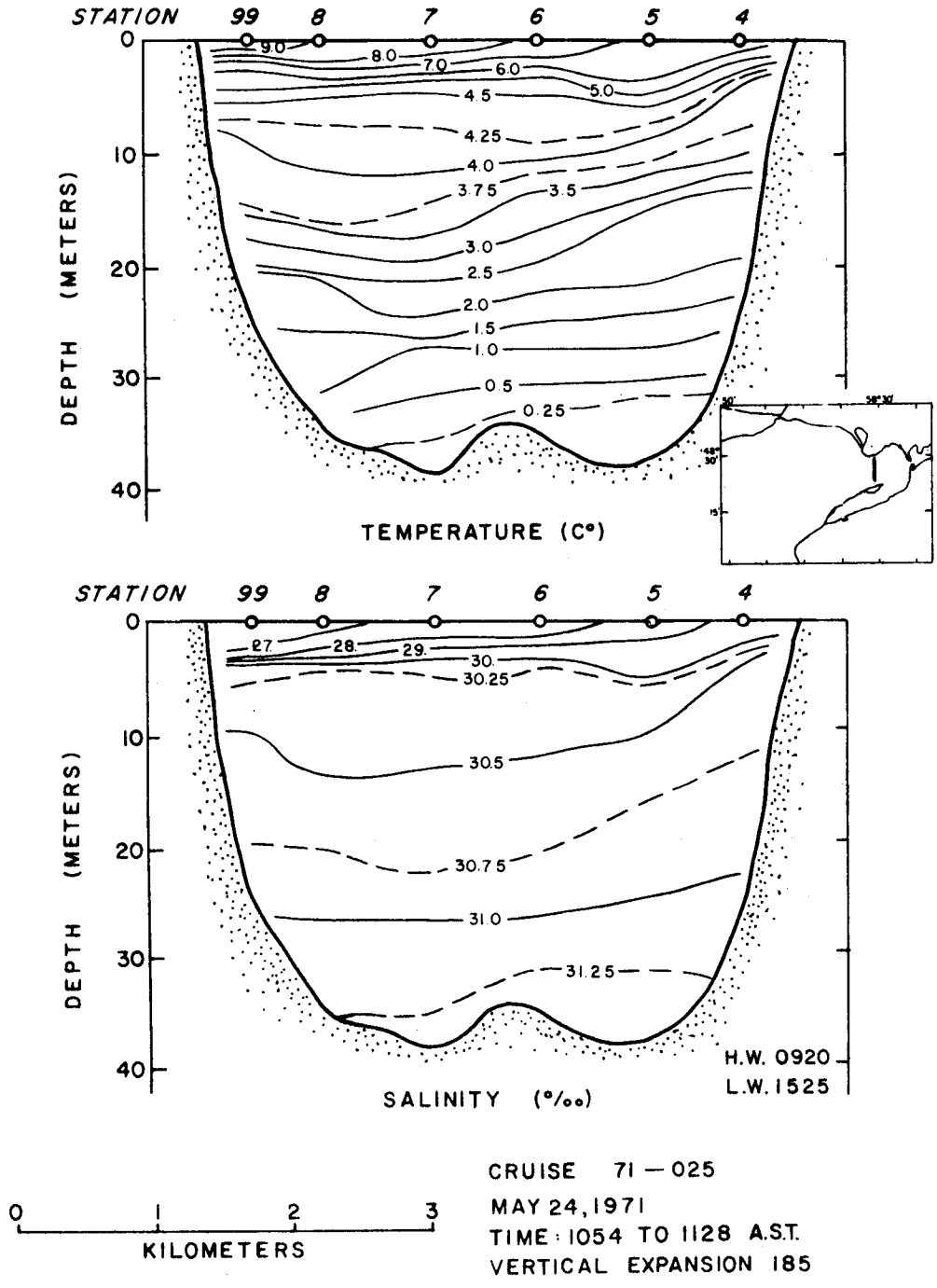

Fig. 21. Multiple occupations of section (1) May 24, 1971.

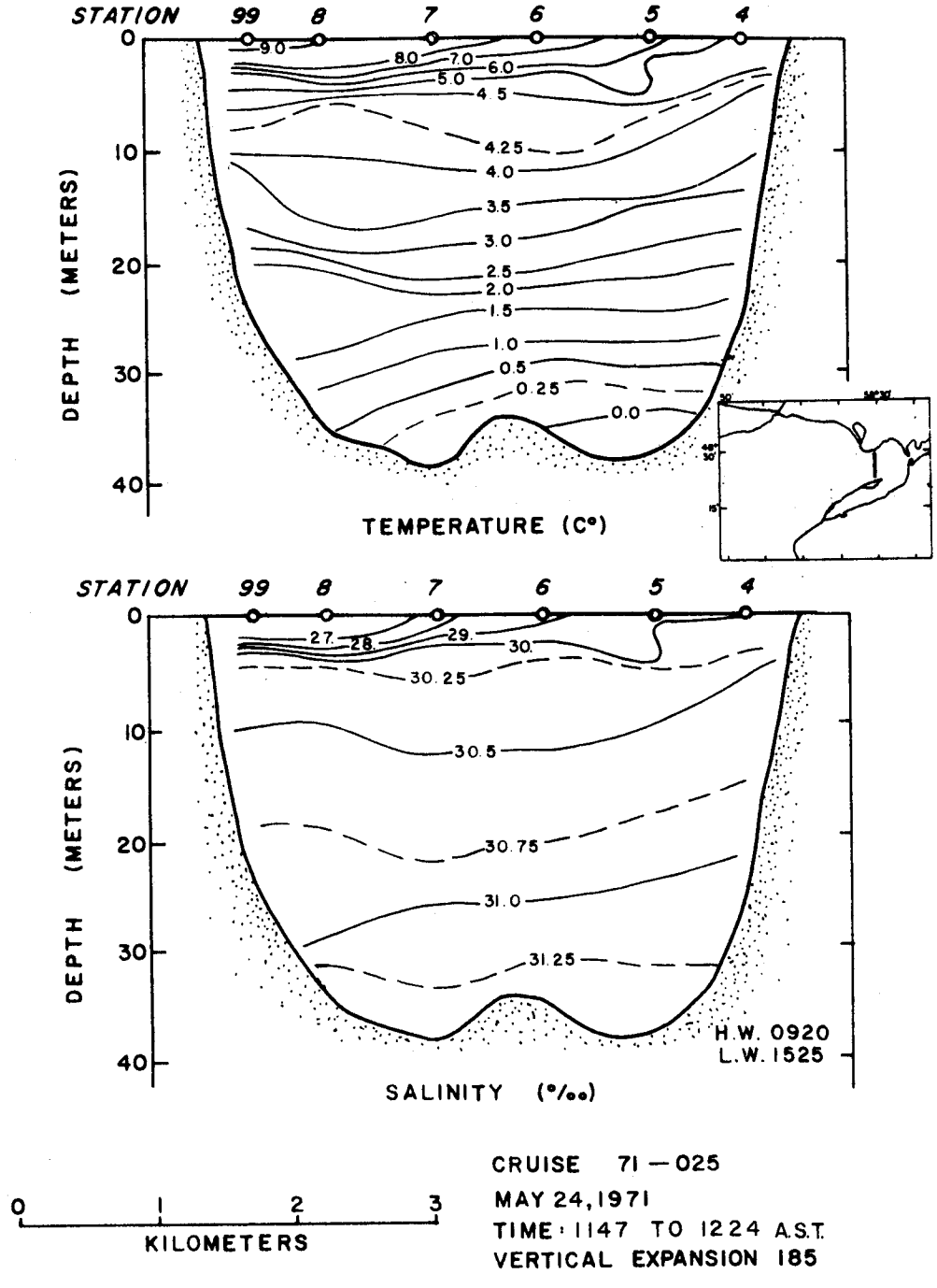

Fig. 22. Multiple occupations of section (1) May 24, 1971.

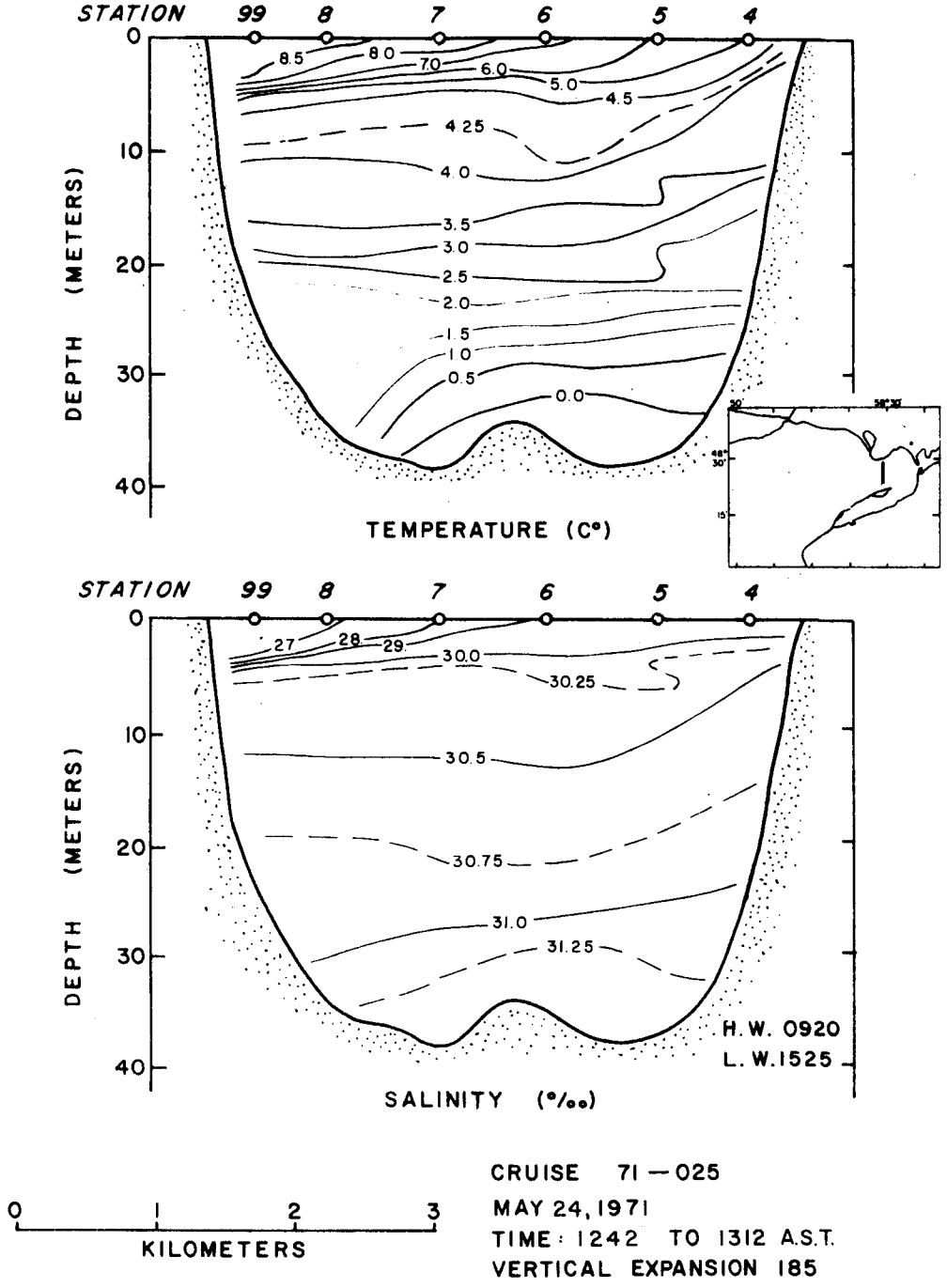

Fig. 23. Multiple occupations of section (1) May 24, 1971.

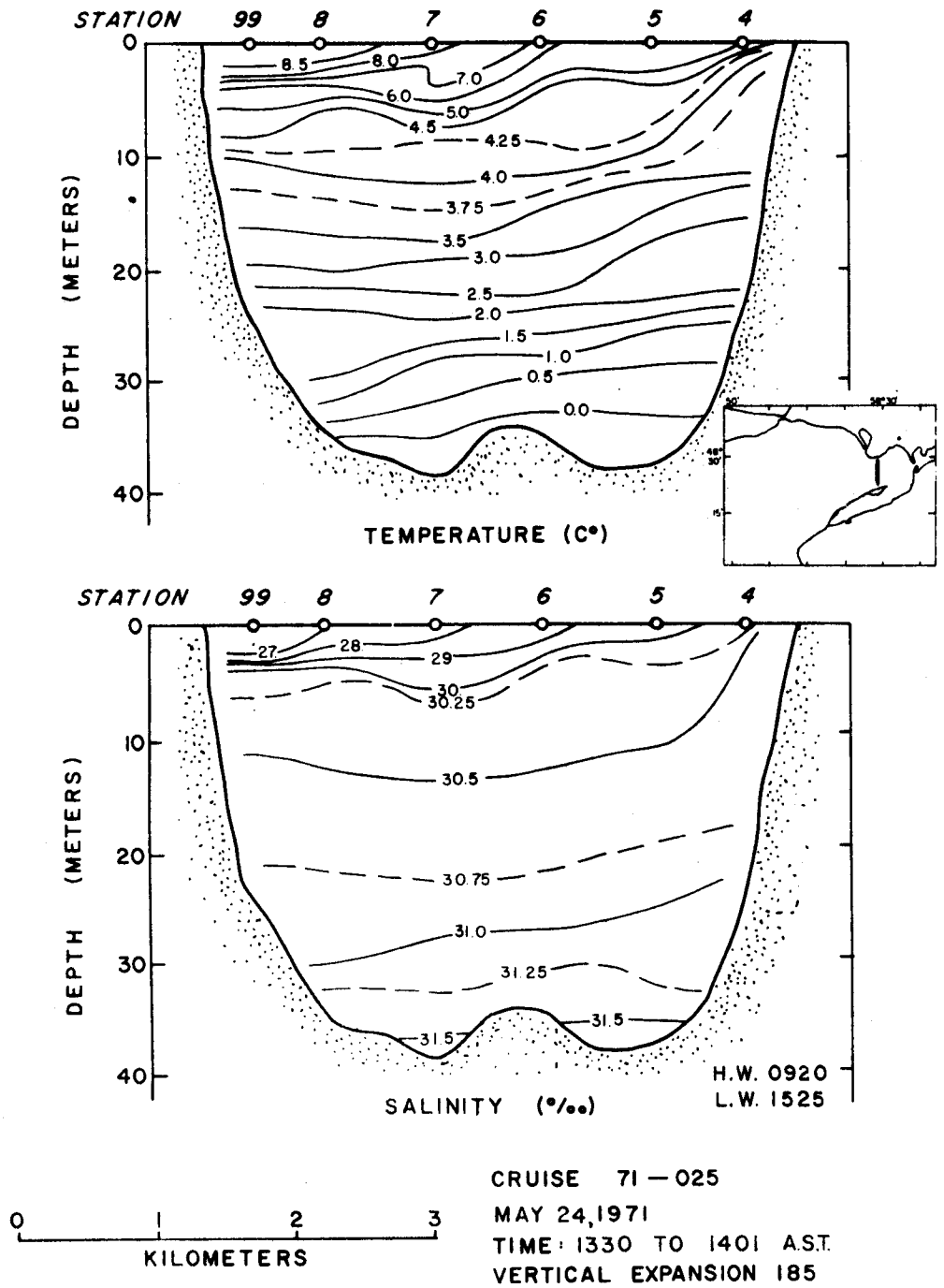

Fig. 24. Multiple occupations of section (1) May 24, 1971.

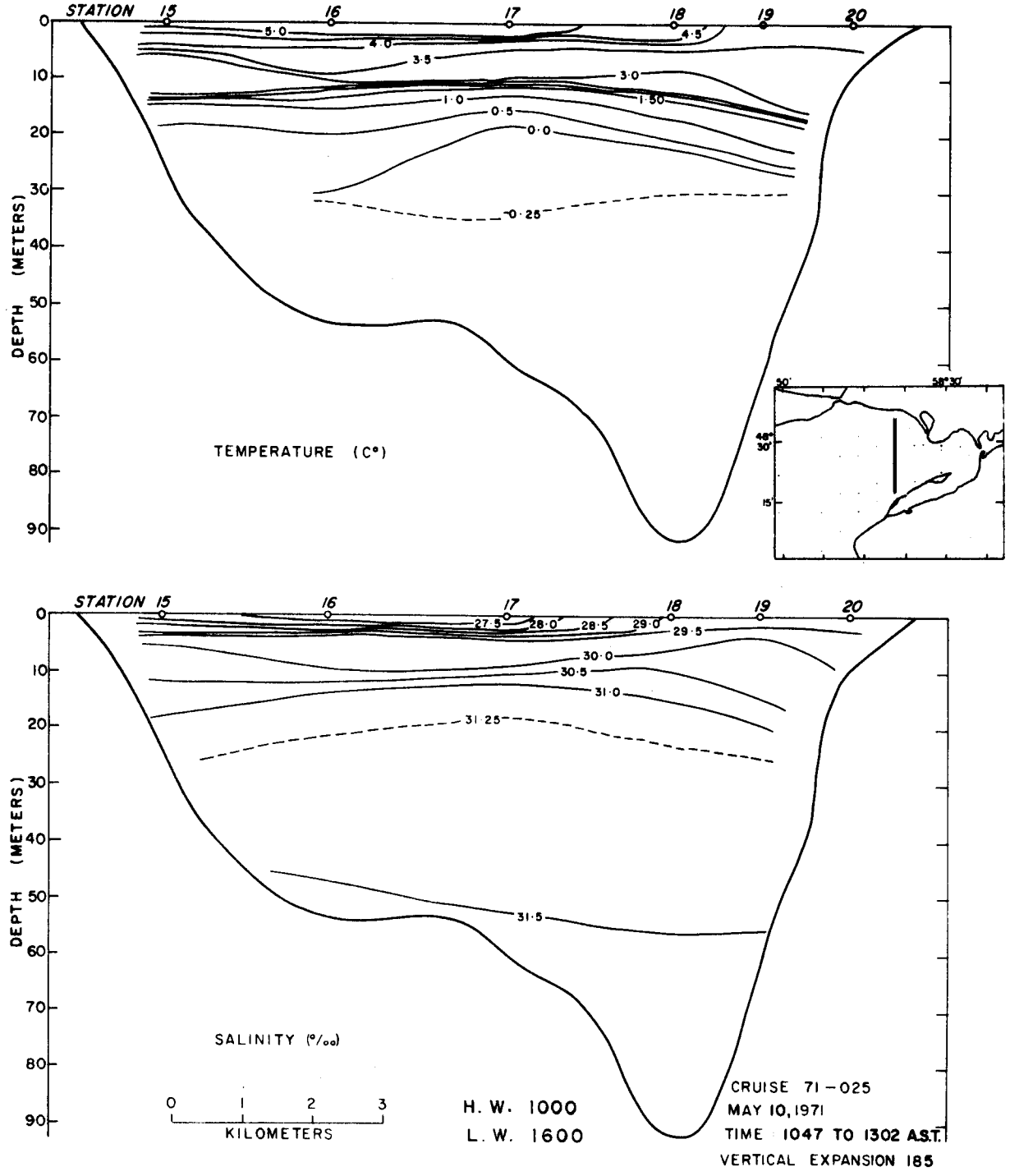

Fig. 25. Transverse temperature, salinity section (2) May 10, 1971.

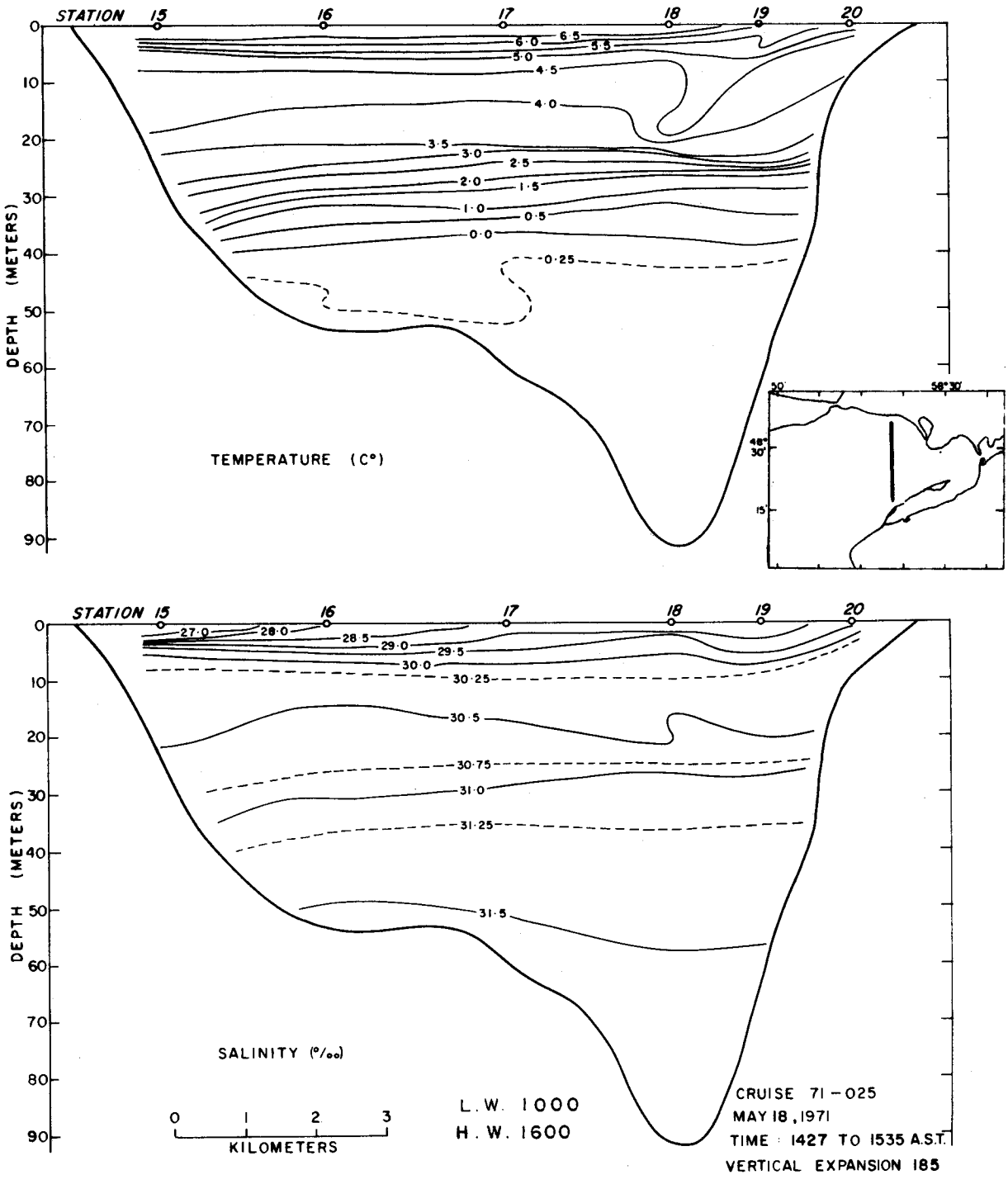

Fig. 26. Transverse temperature, salinity section (2) May 18, 1971.

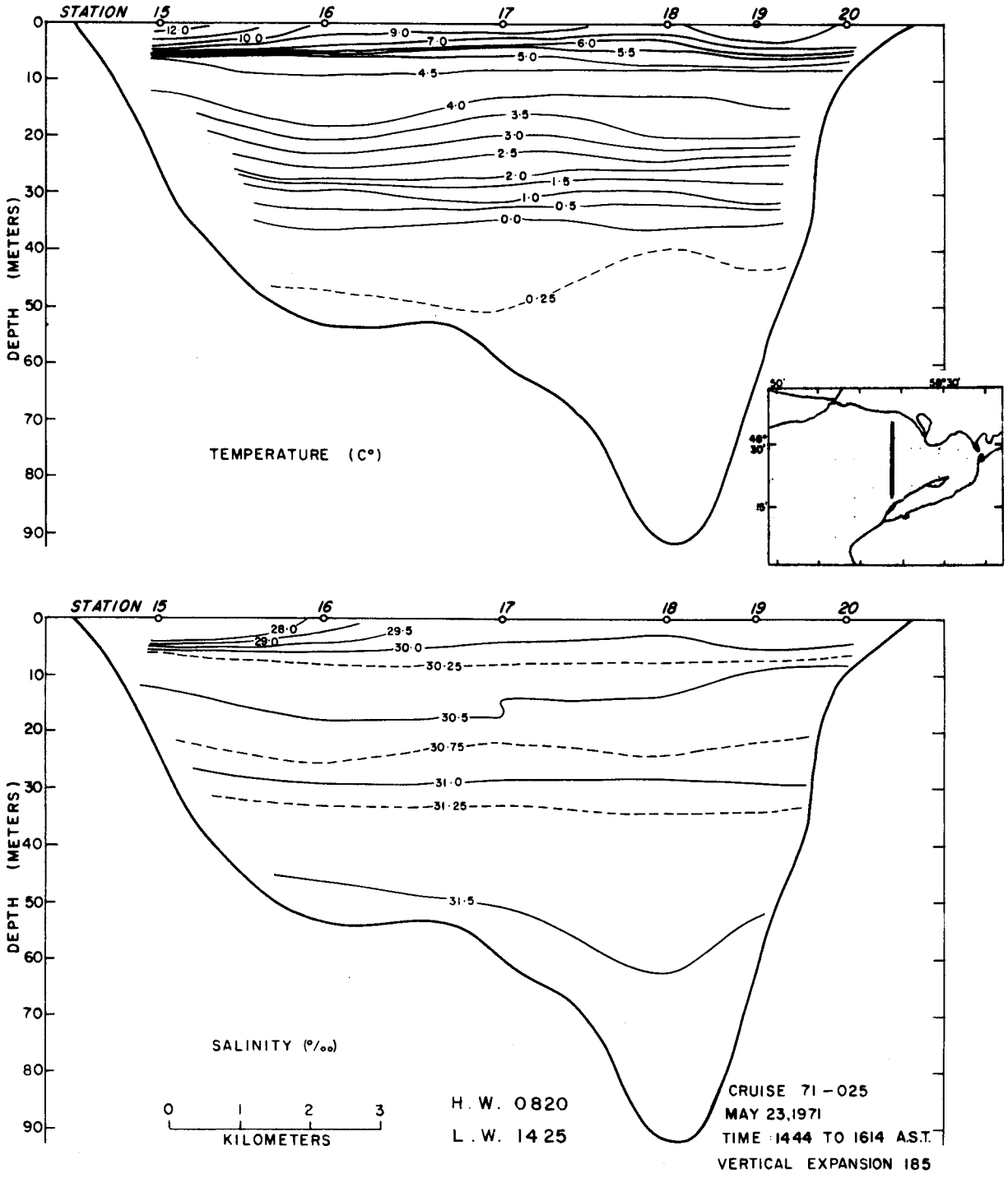

Fig. 27. Transverse temperature, salinity section (2) May 23, 1971.

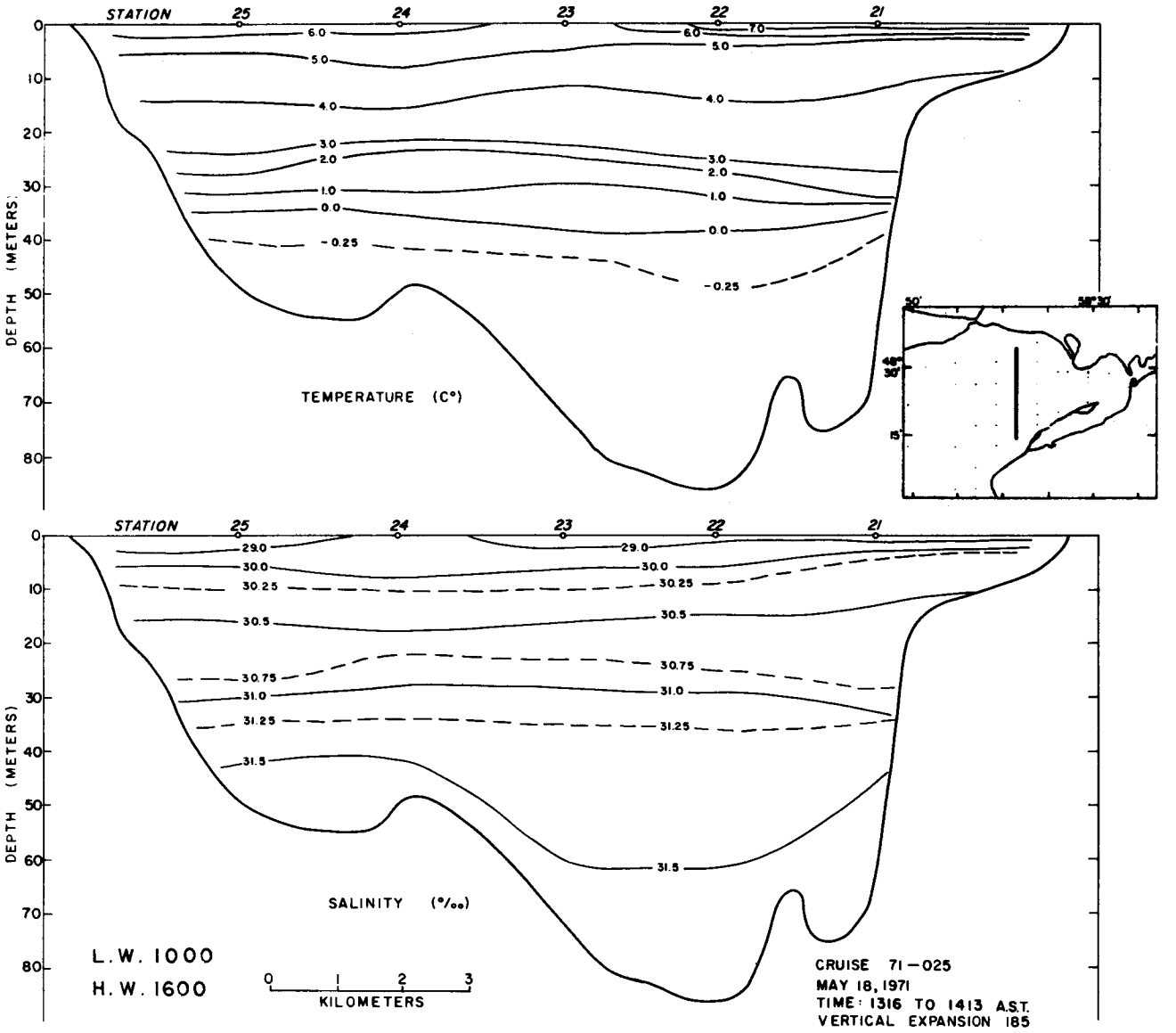

Fig. 28. Transverse temperature, salinity section (3) May 18, 1971.

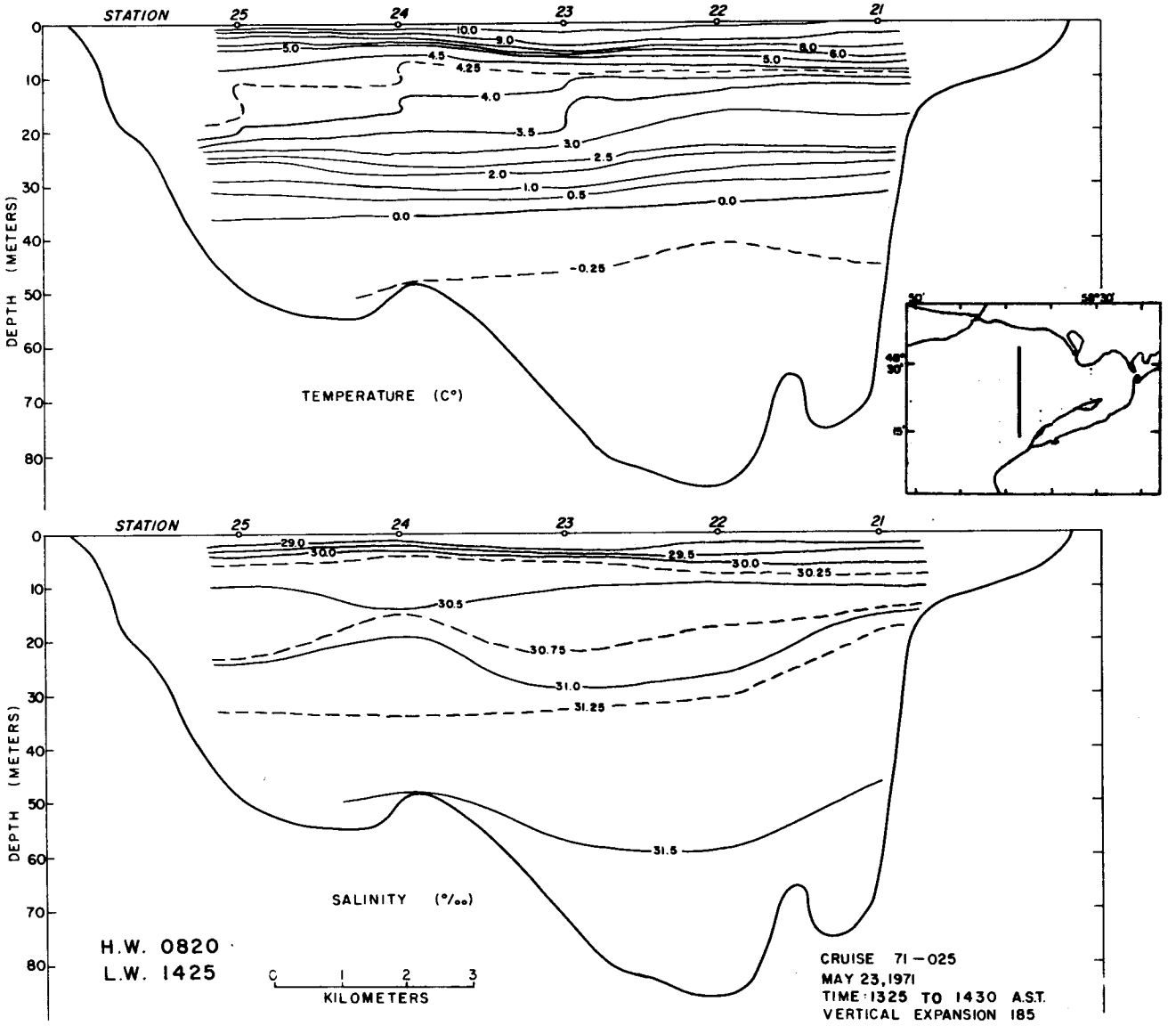

Fig. 29. Transverse temperature, salinity section (3) May 23, 1971.

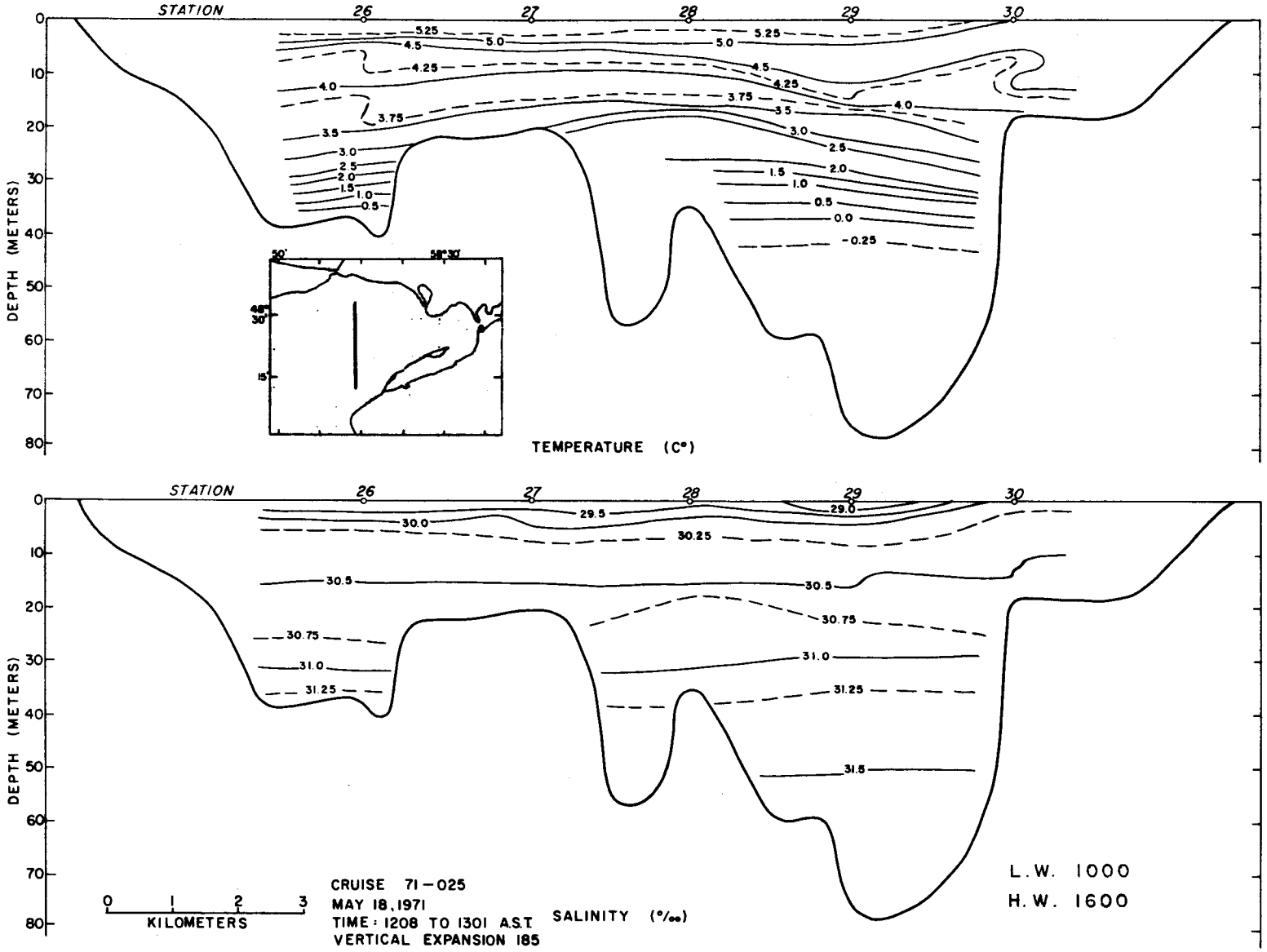

Fig. 30. Transverse temperature, salinity section (4) May 18, 1971

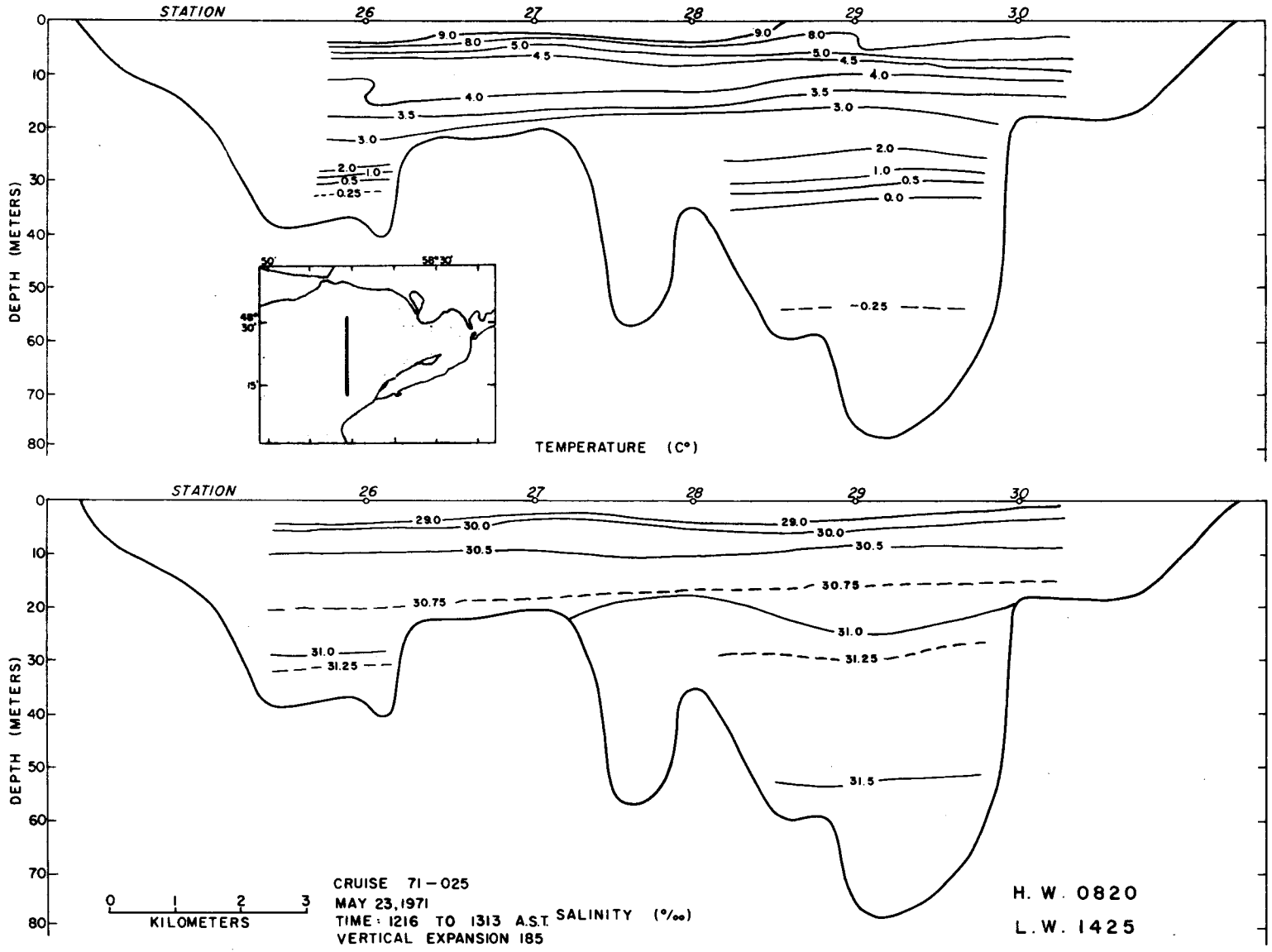

Fig. 31 Transverse temperature, salinity section (4) May 23, 1971

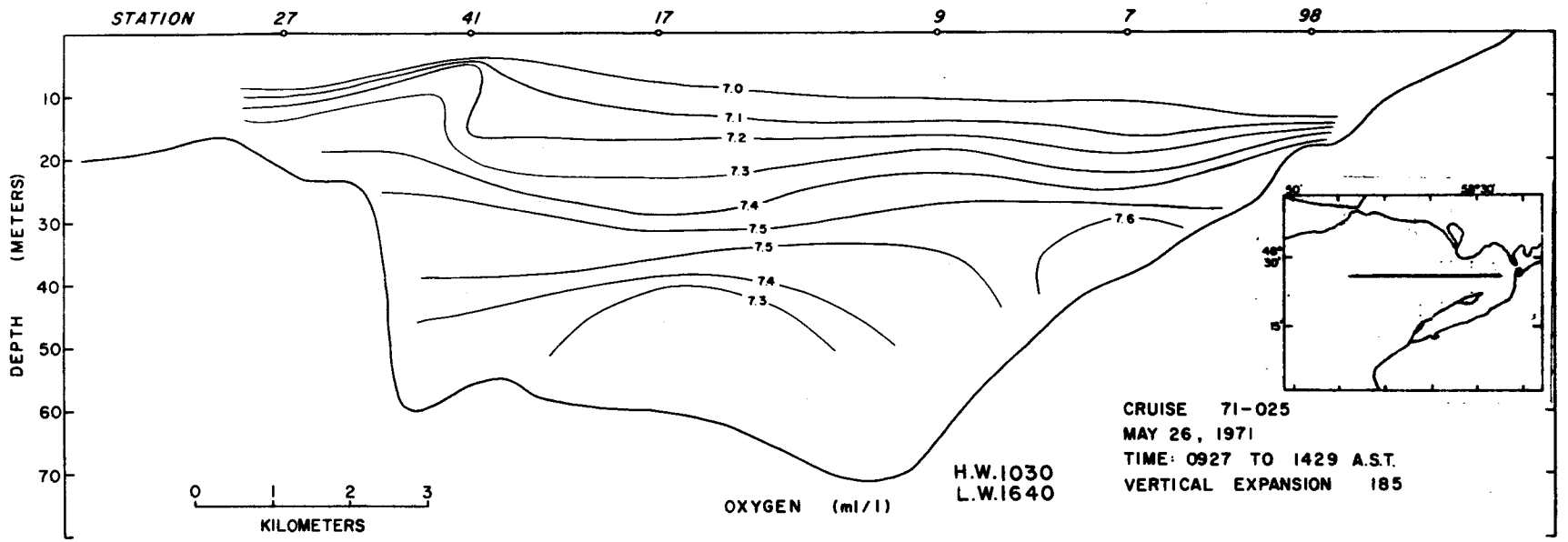

Fig. 32 Longitudinal oxygen distribution May 26, 1971

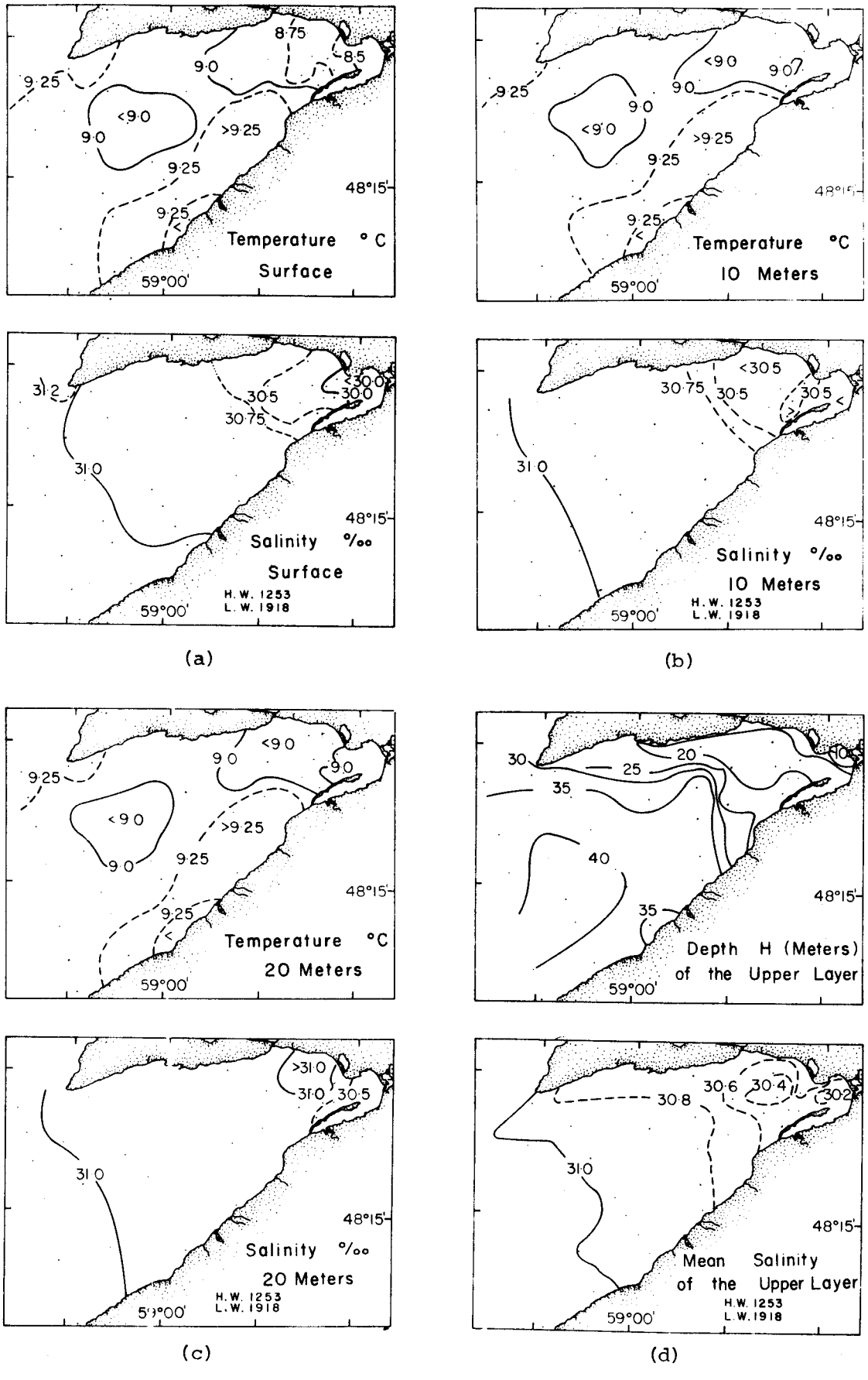

Fig. 33 Horizontal temperature and salinity distribution at the surface (a), 10(b) and 20(c) meters and the depth(i) and salinity(ii) of the upper layer(d) November 3 1970

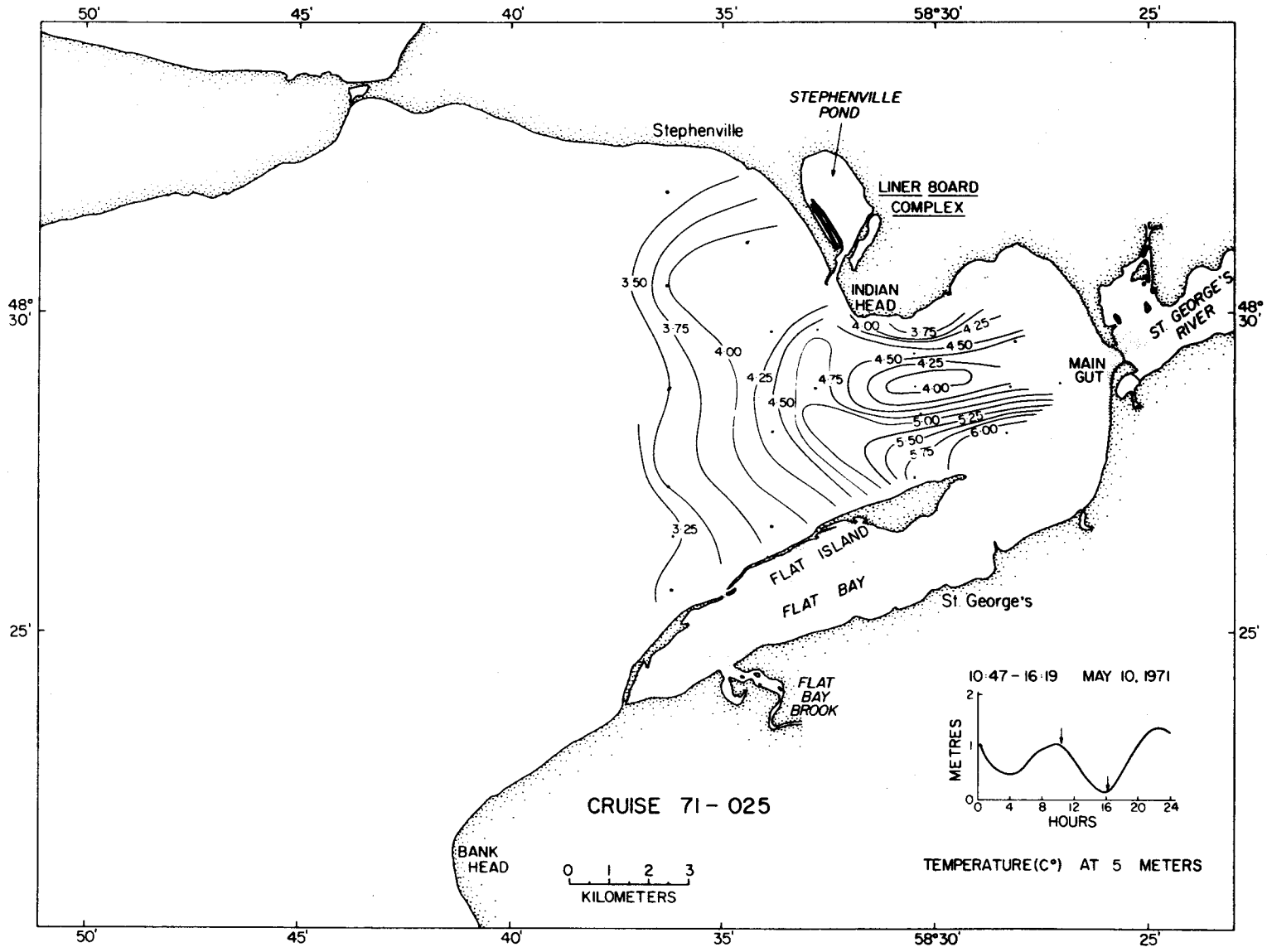

Fig. 34 Horizontal temperature distribution at 5 meters, May 10, 1971

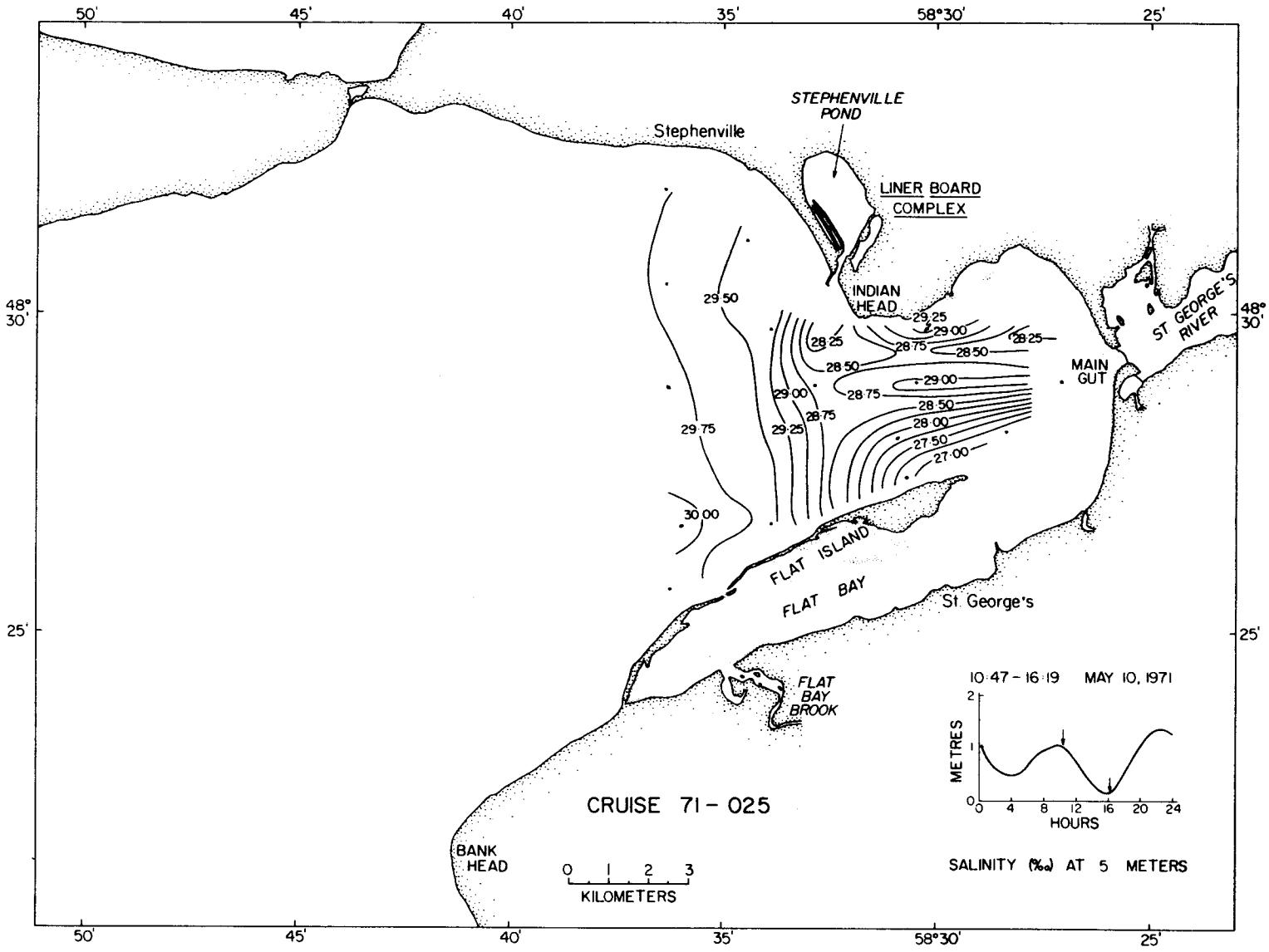

Fig. 35 Horizontal salinity distribution at 5 meters May 10, 1971

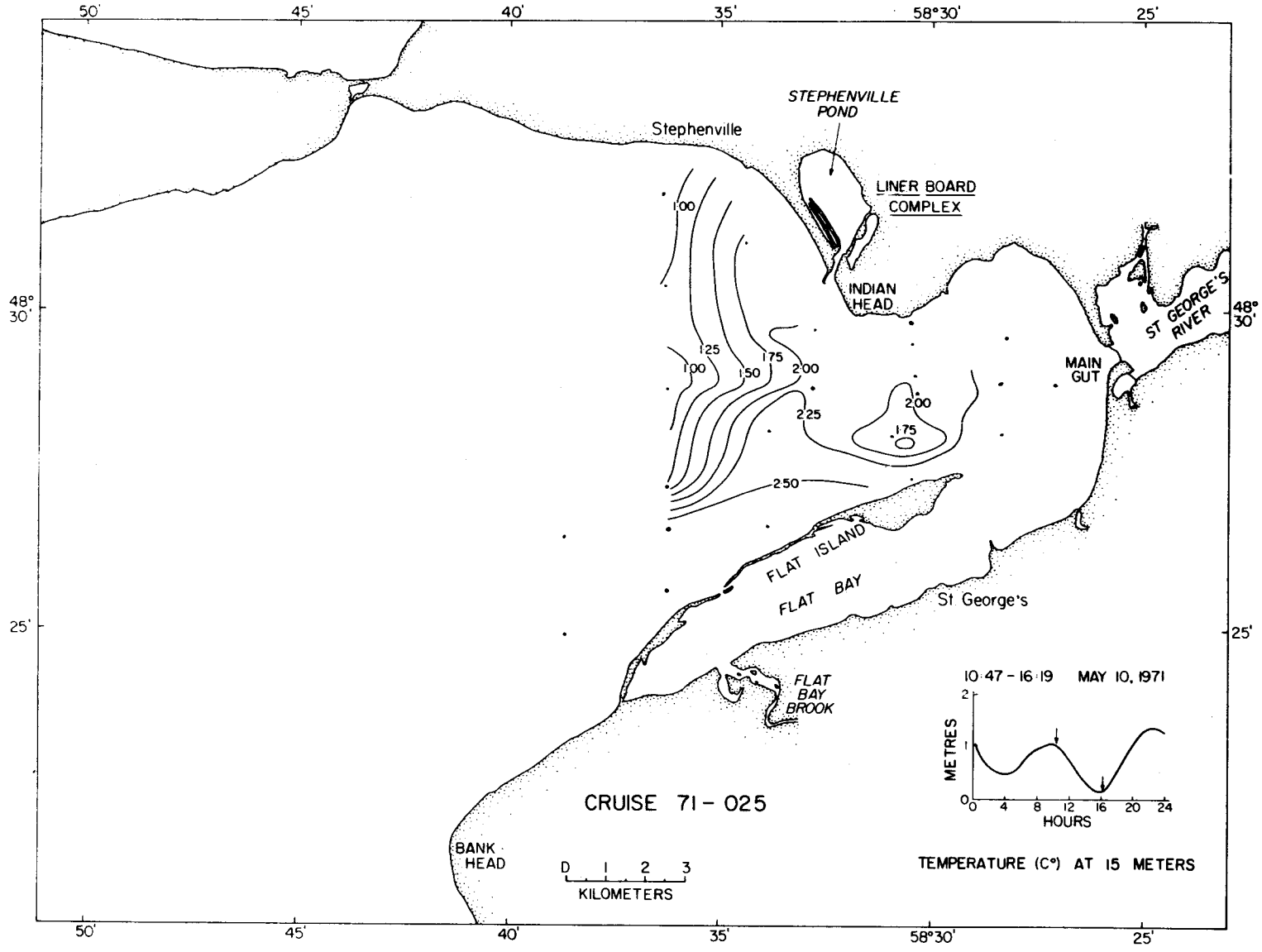

Fig. 36 Horizontal temperature distribution at 15 meters May 10, 1971

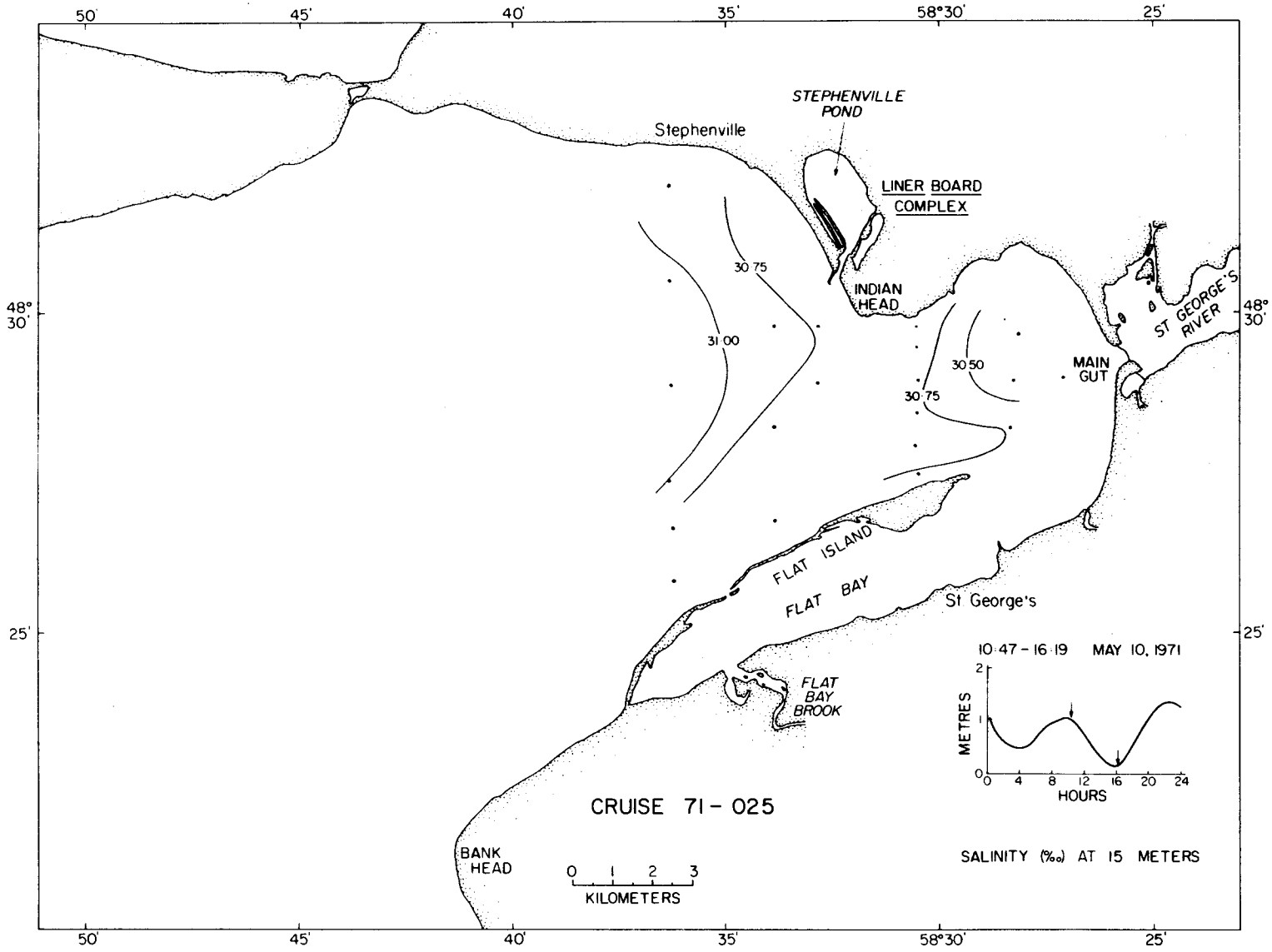

Fig. 37 Horizontal salinity distribution at 15 meters May 10, 1971

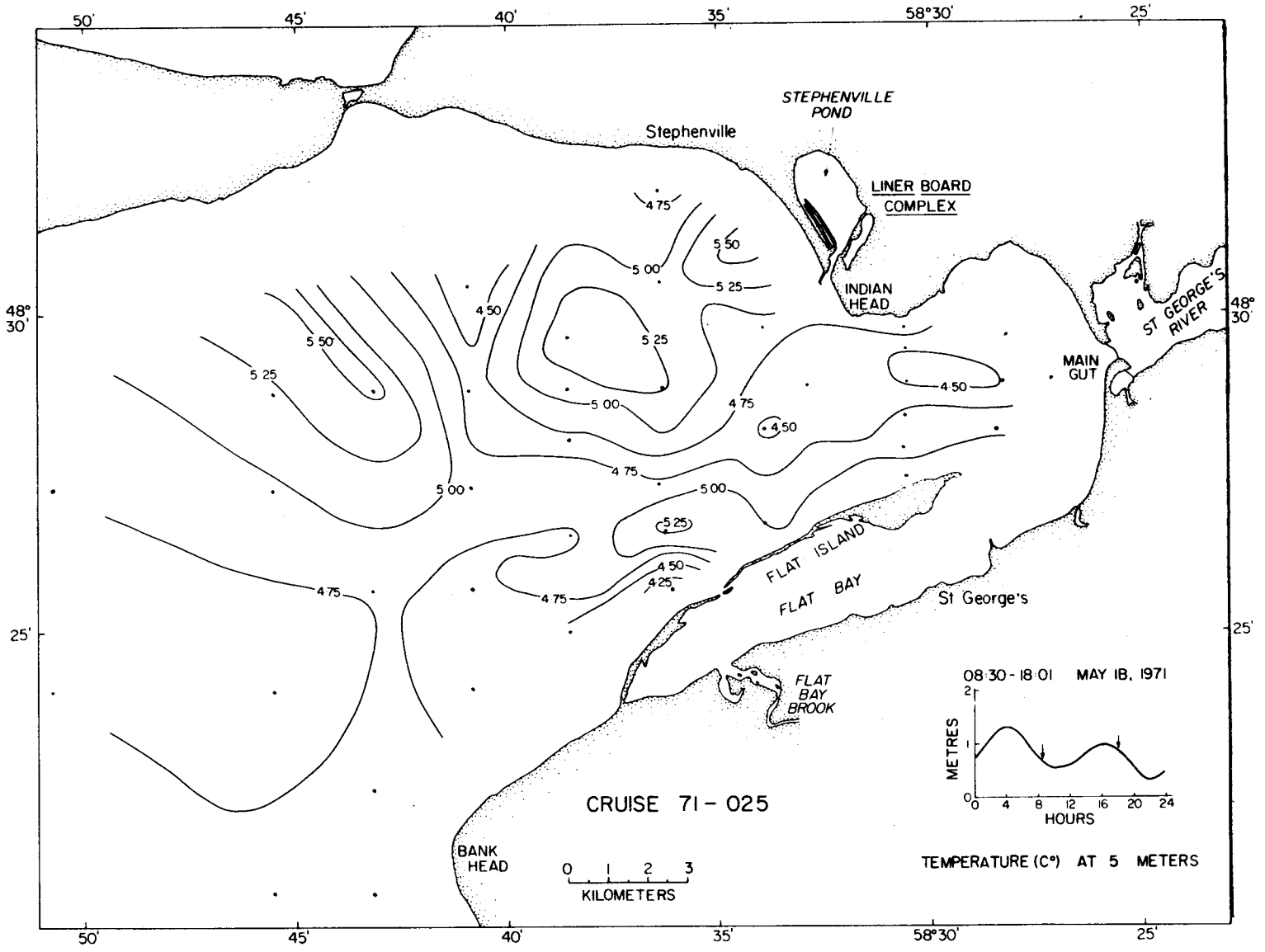

Fig. 38 Horizontal temperature distribution at 5 meters, May 18, 1971

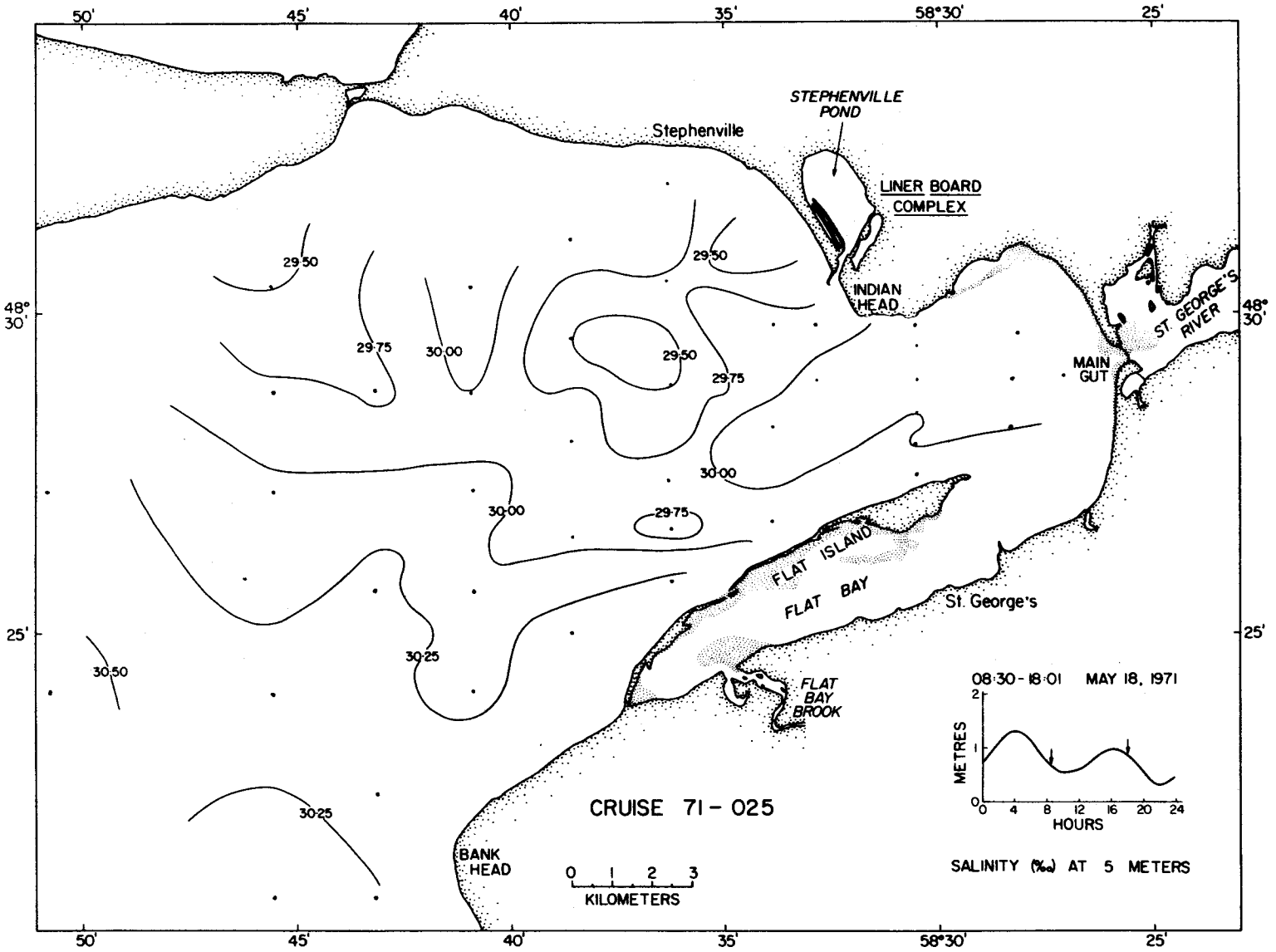

Fig. 39 Horizontal salinity distribution at 5 meters, May 18,1971

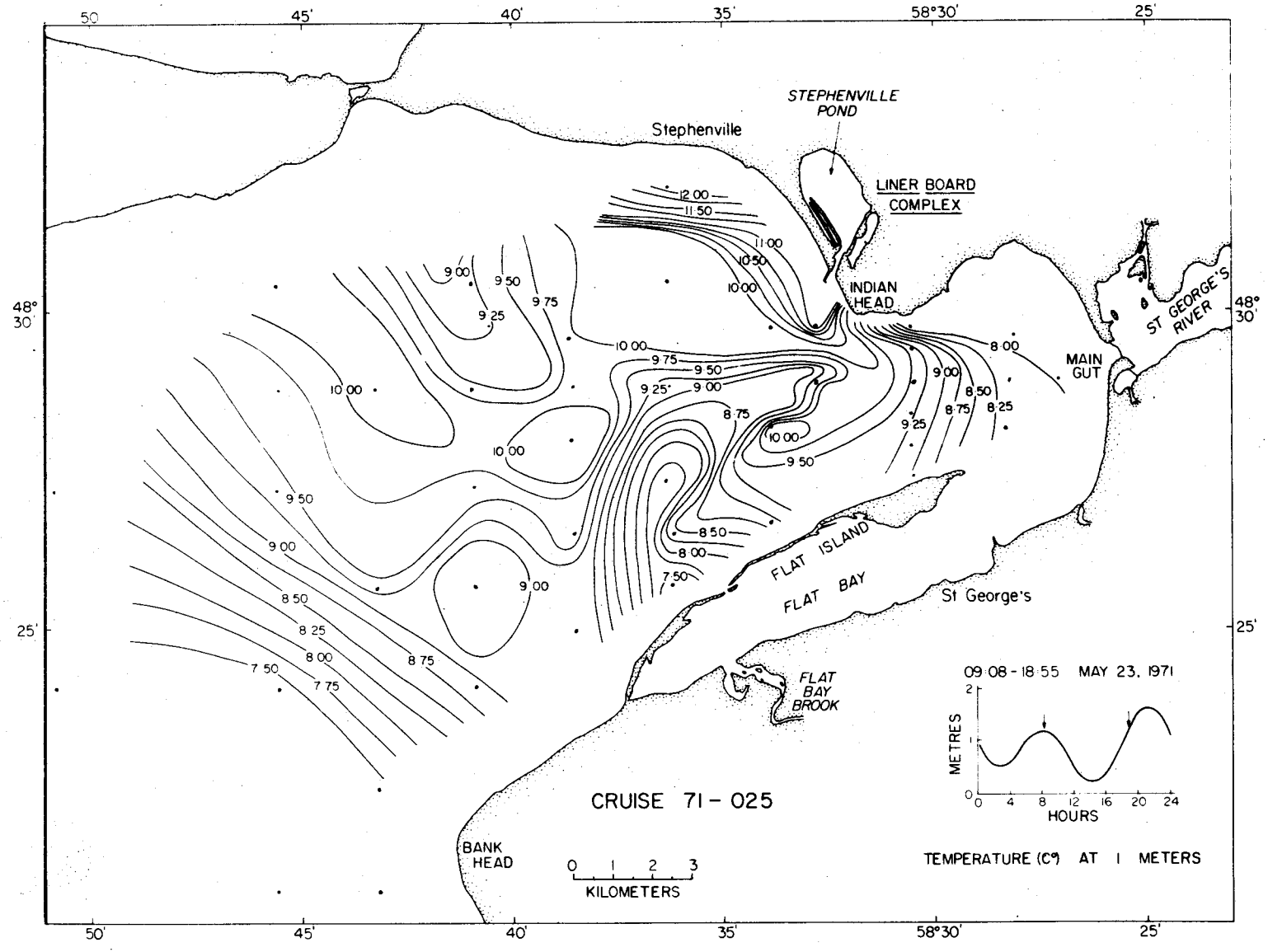

Fig. 40 Horizontal temperature distribution at 1 meter, May 23, 1971

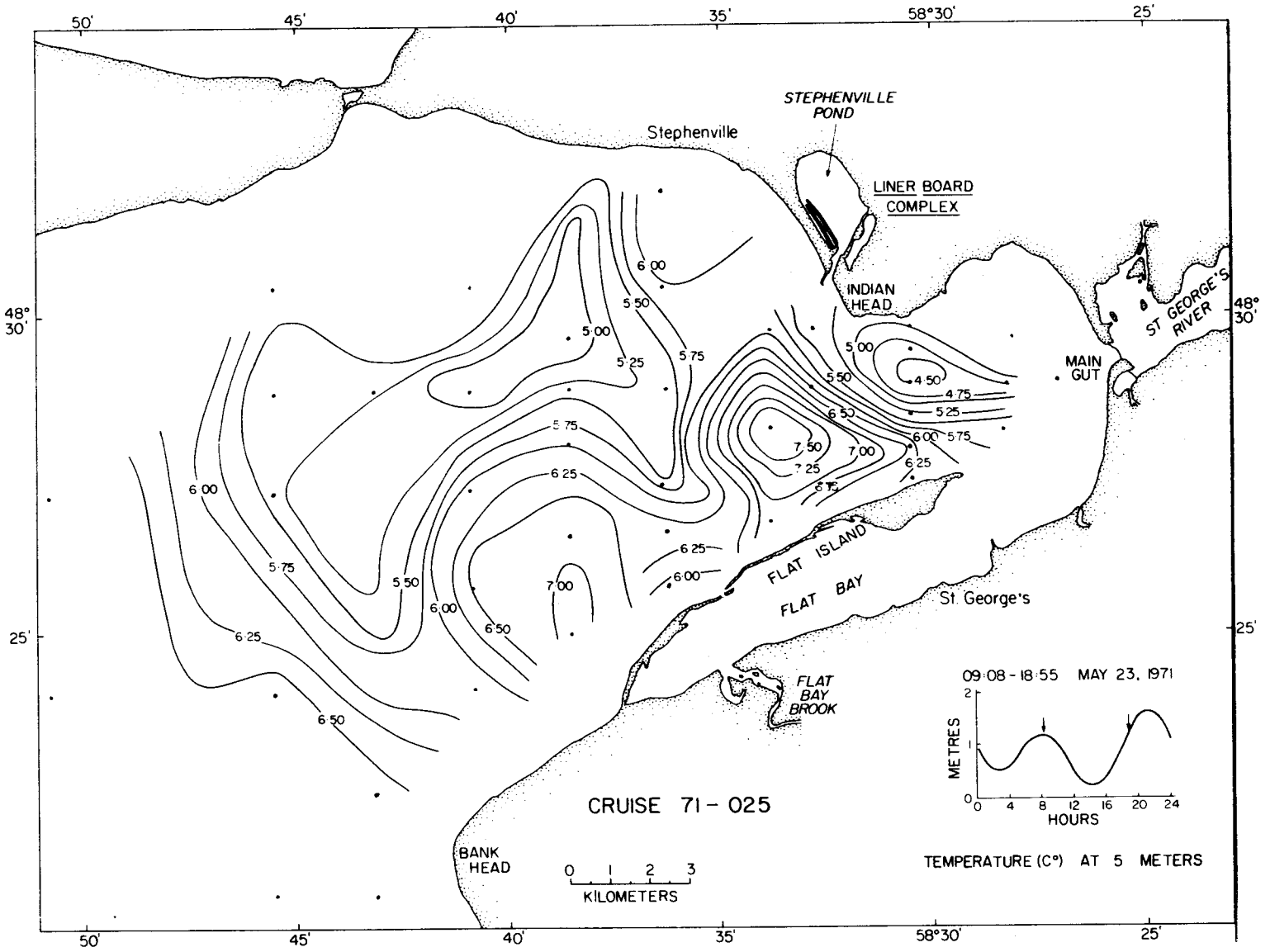

Fig. 41 Horizontal temperature distribution at 5 meters, May 23, 1971

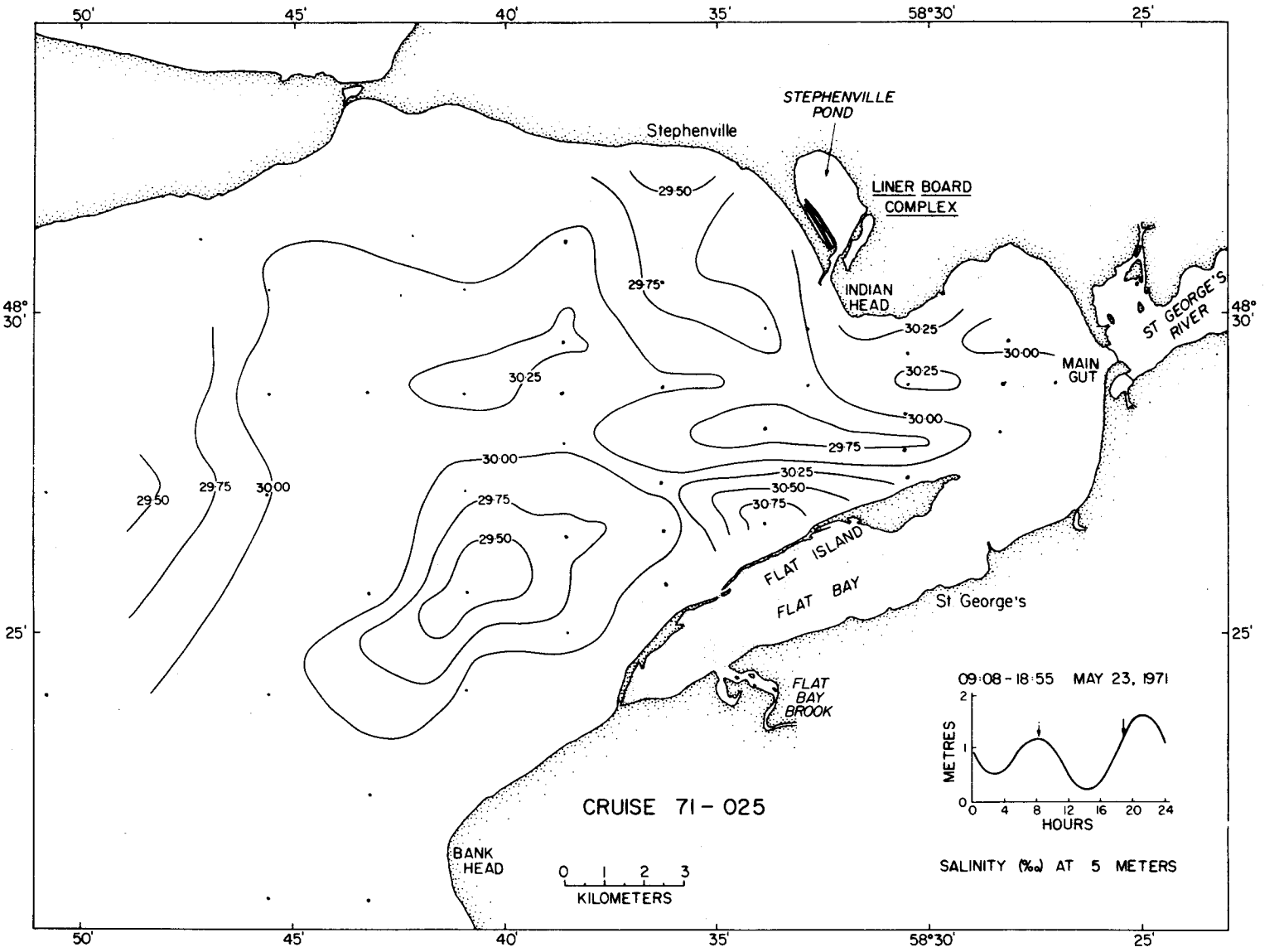

Fig. 42 Horizontal salinity distribution at 5 meters, May 23,1971

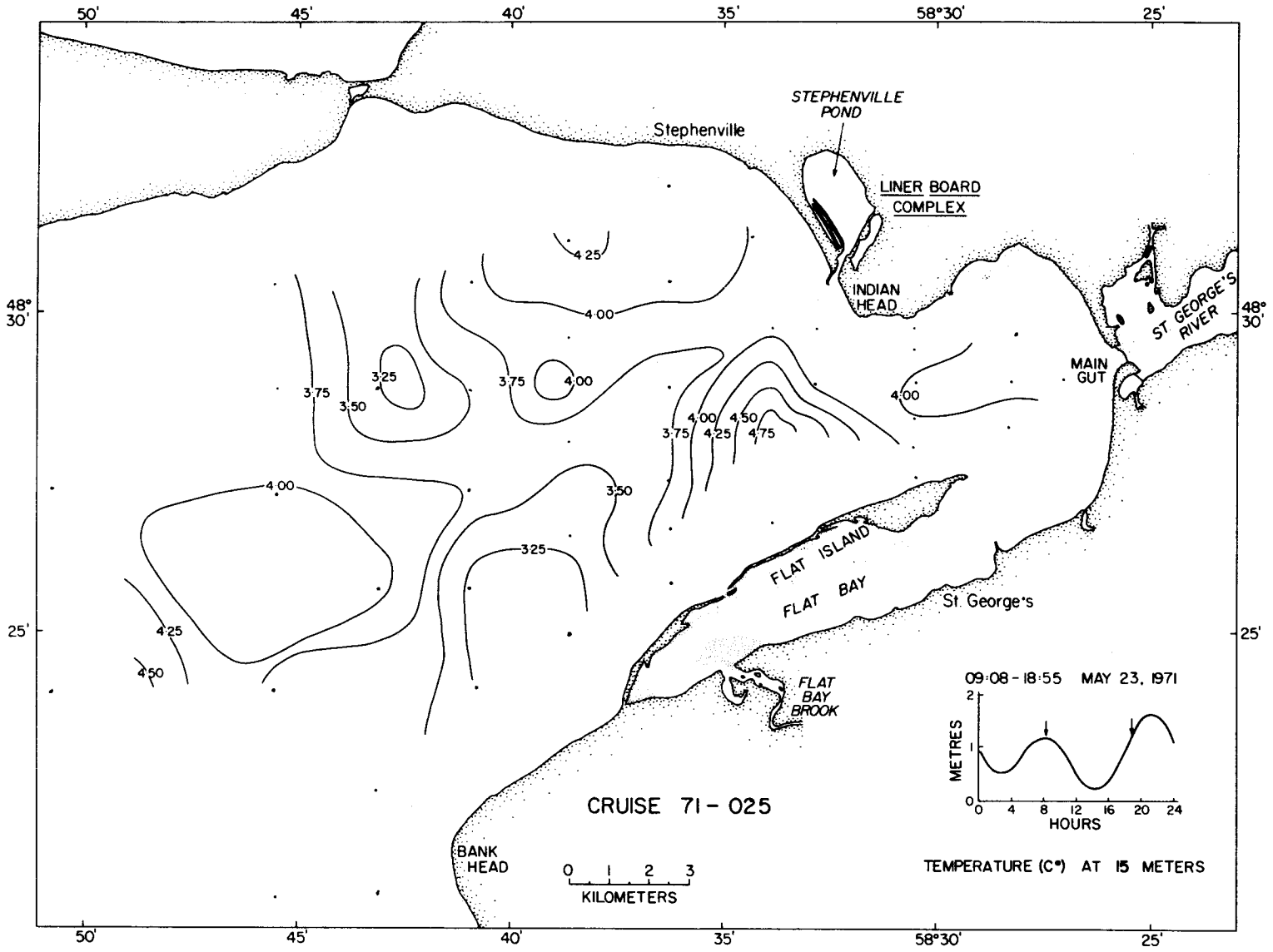

Fig. 43 Horizontal temperature distribution at 15 meters, May 23, 1971

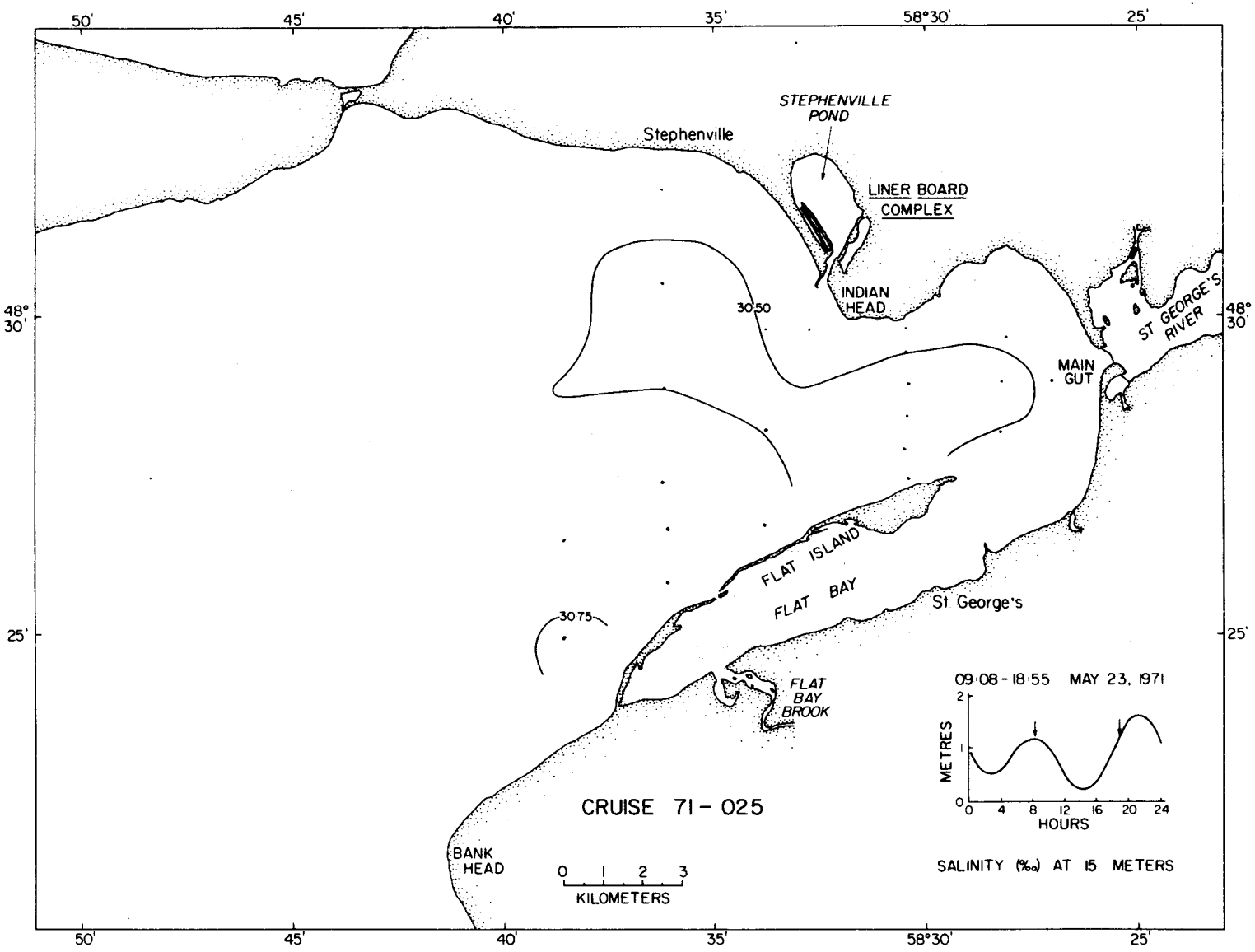

Fig. 44 Horizontal salinity distribution at 15 meters, May 23, 1971

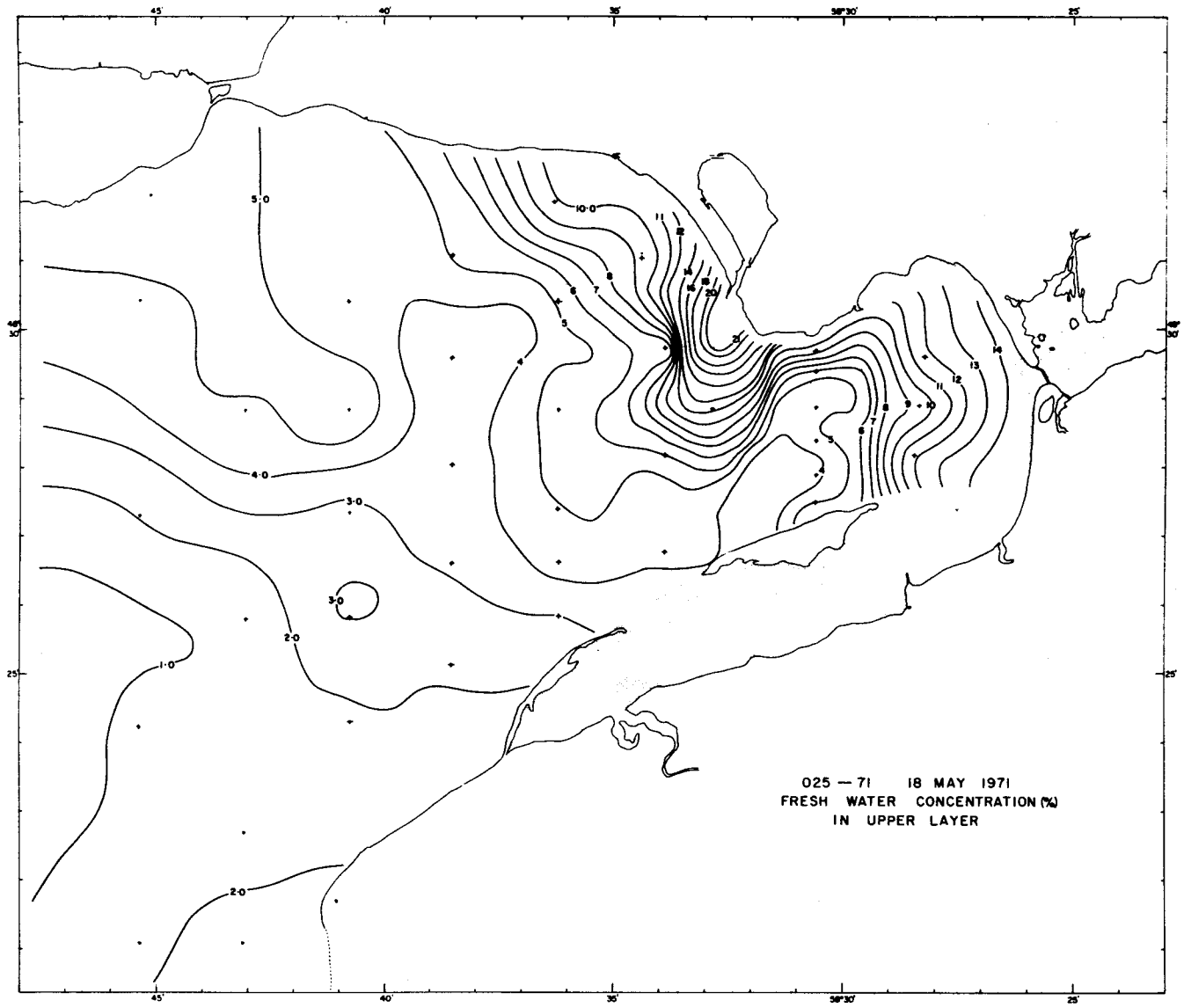

Fig. 45 Freshwater concentration (%) in the upper layer, May 18, 1971

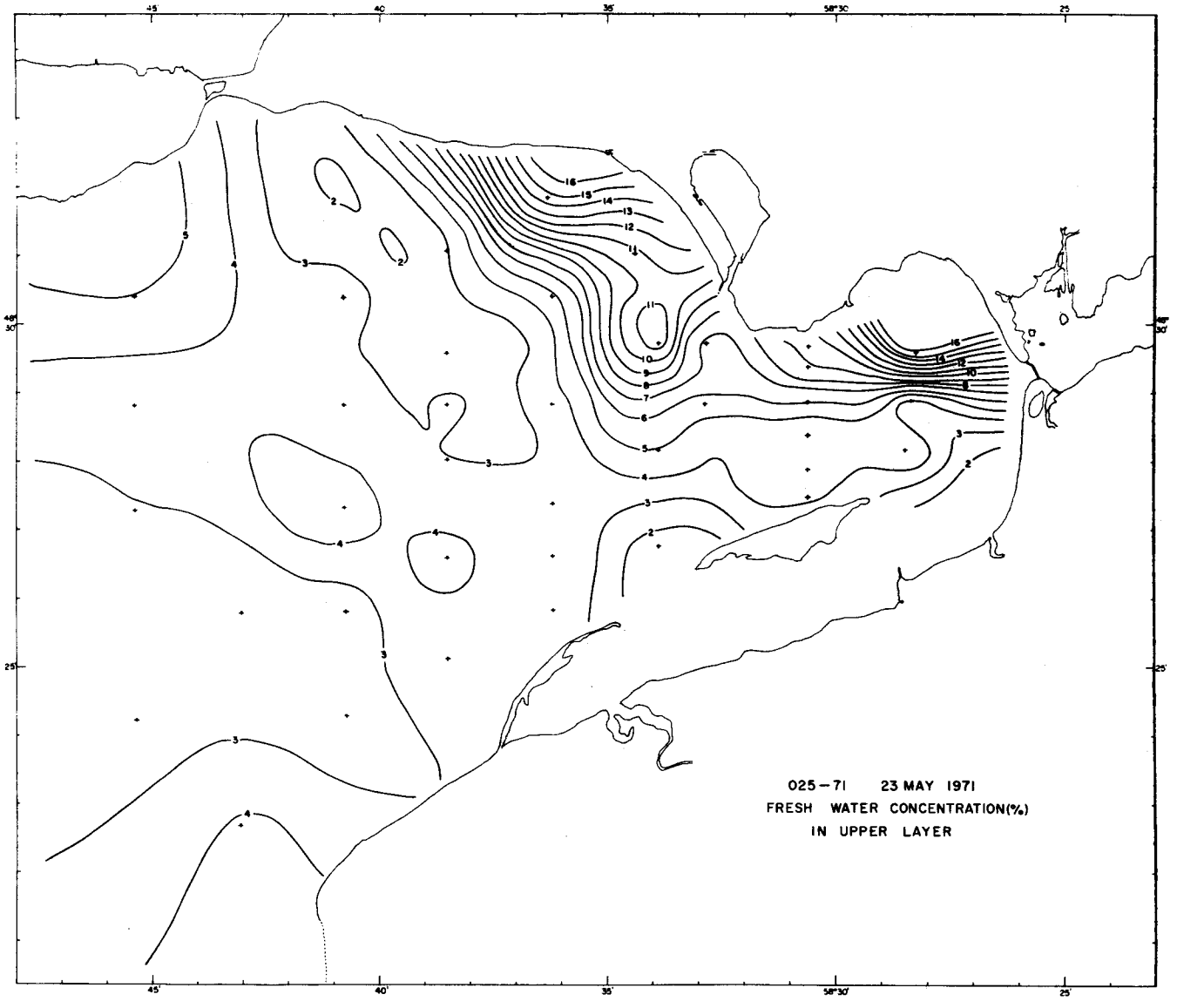

Fig. 46 Freshwater concentration (%) in the upper layer, May 23, 1971

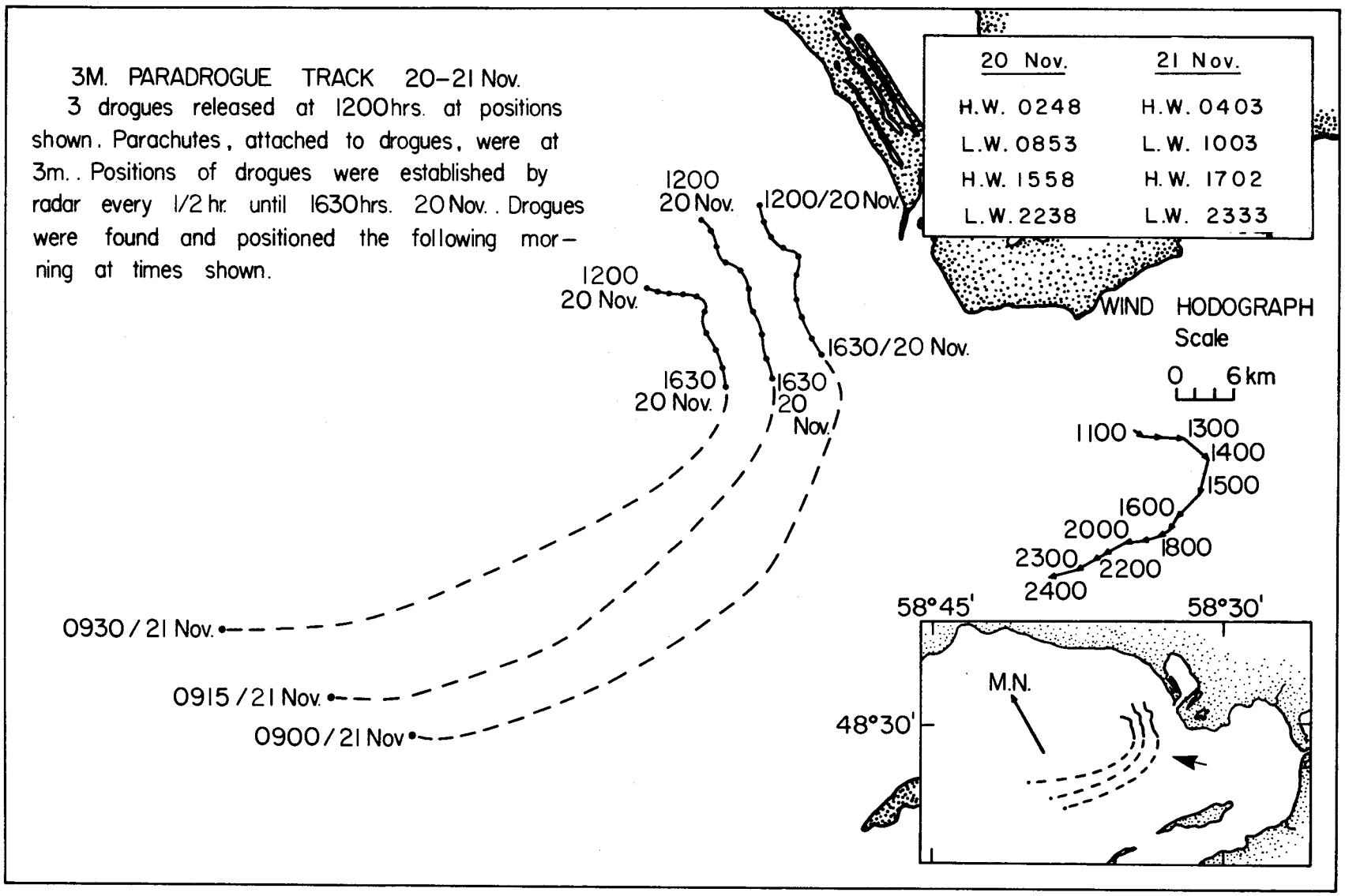

Fig. 47 Drogue trajectories at 3 m depth, November 20-21, 1970

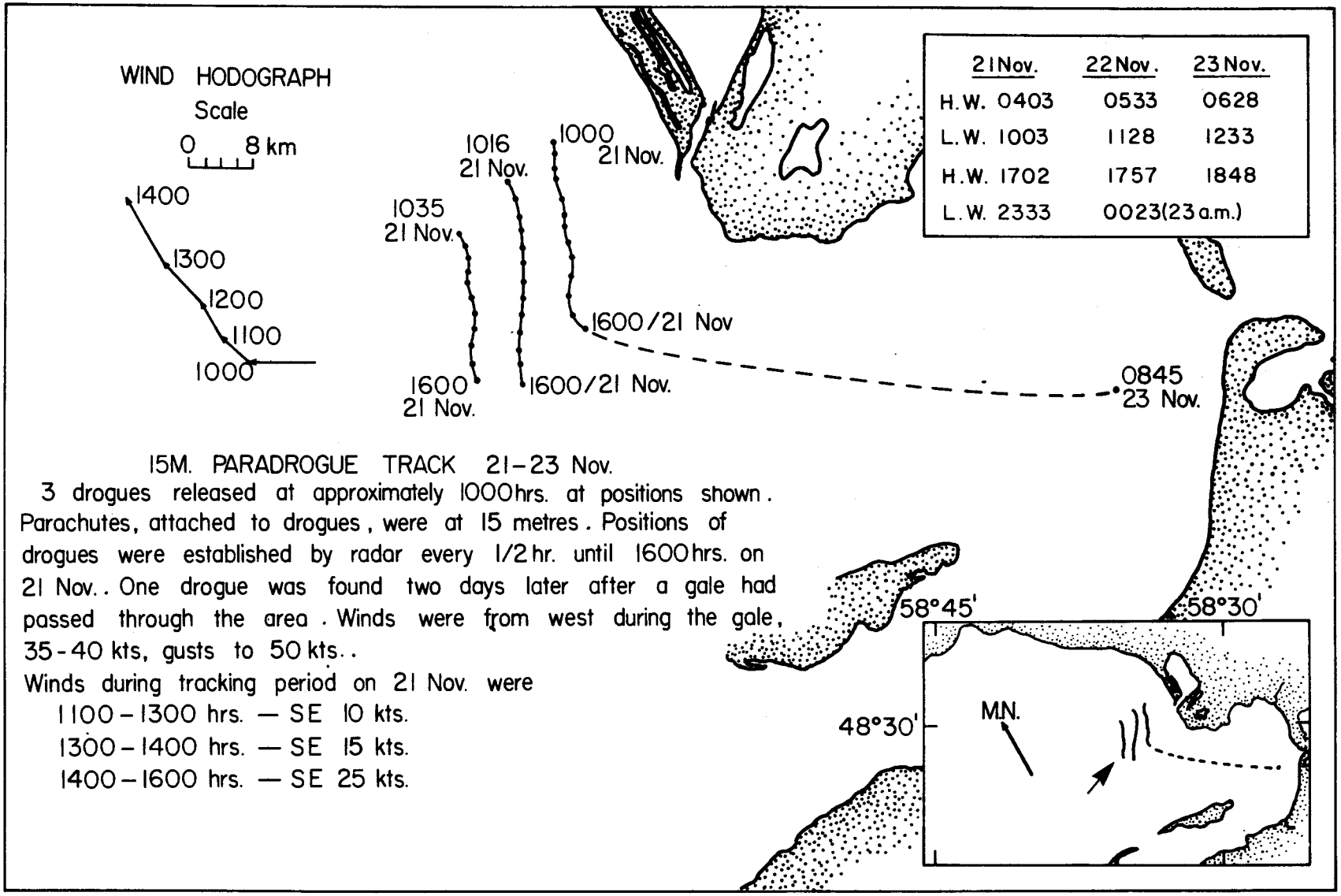

Fig. 48 Drogue trajectories at 15 m depth, November 21-23, 1970

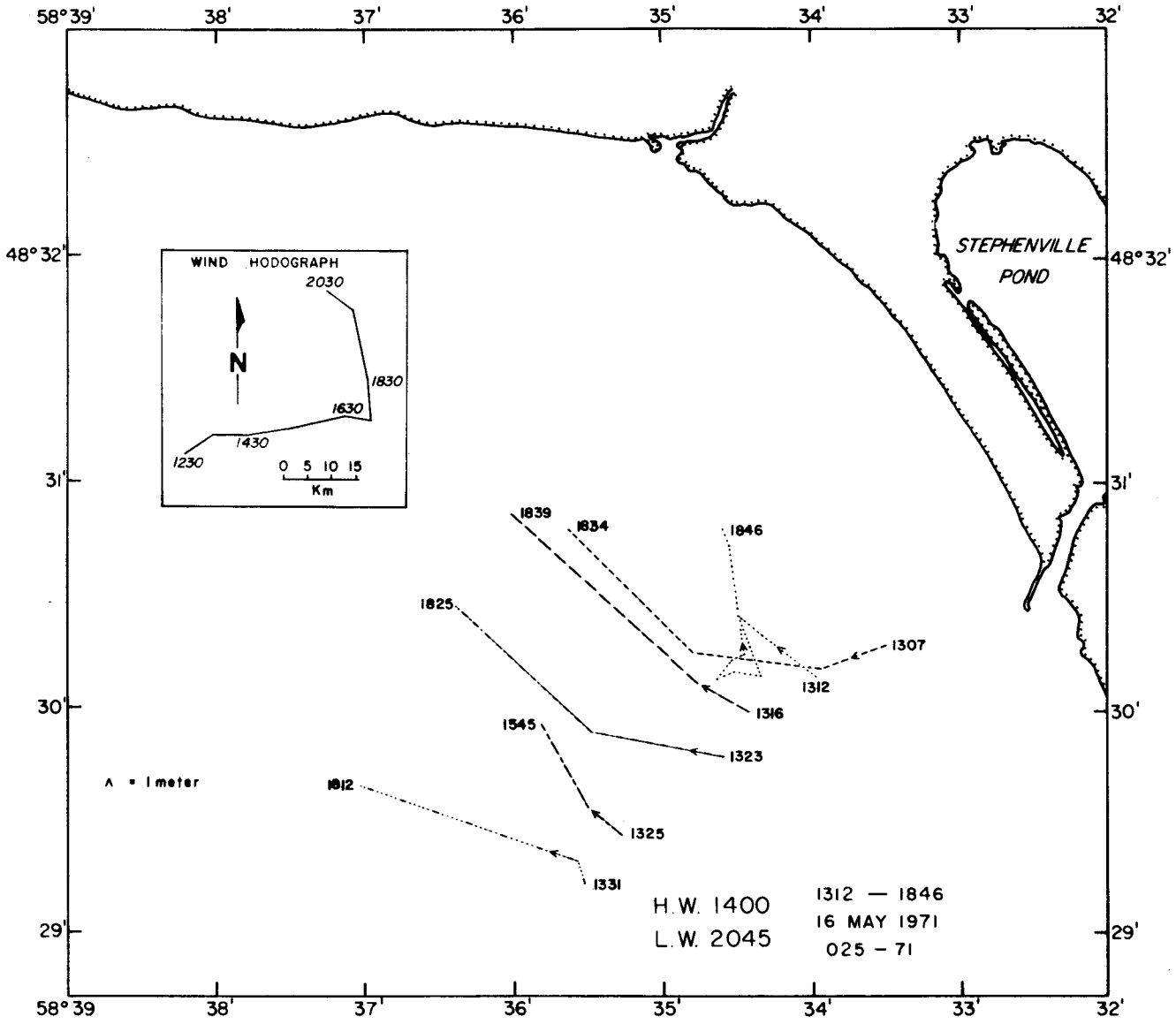

Fig. 49 Drogue trajectories at 1 meter, May 16, 1971

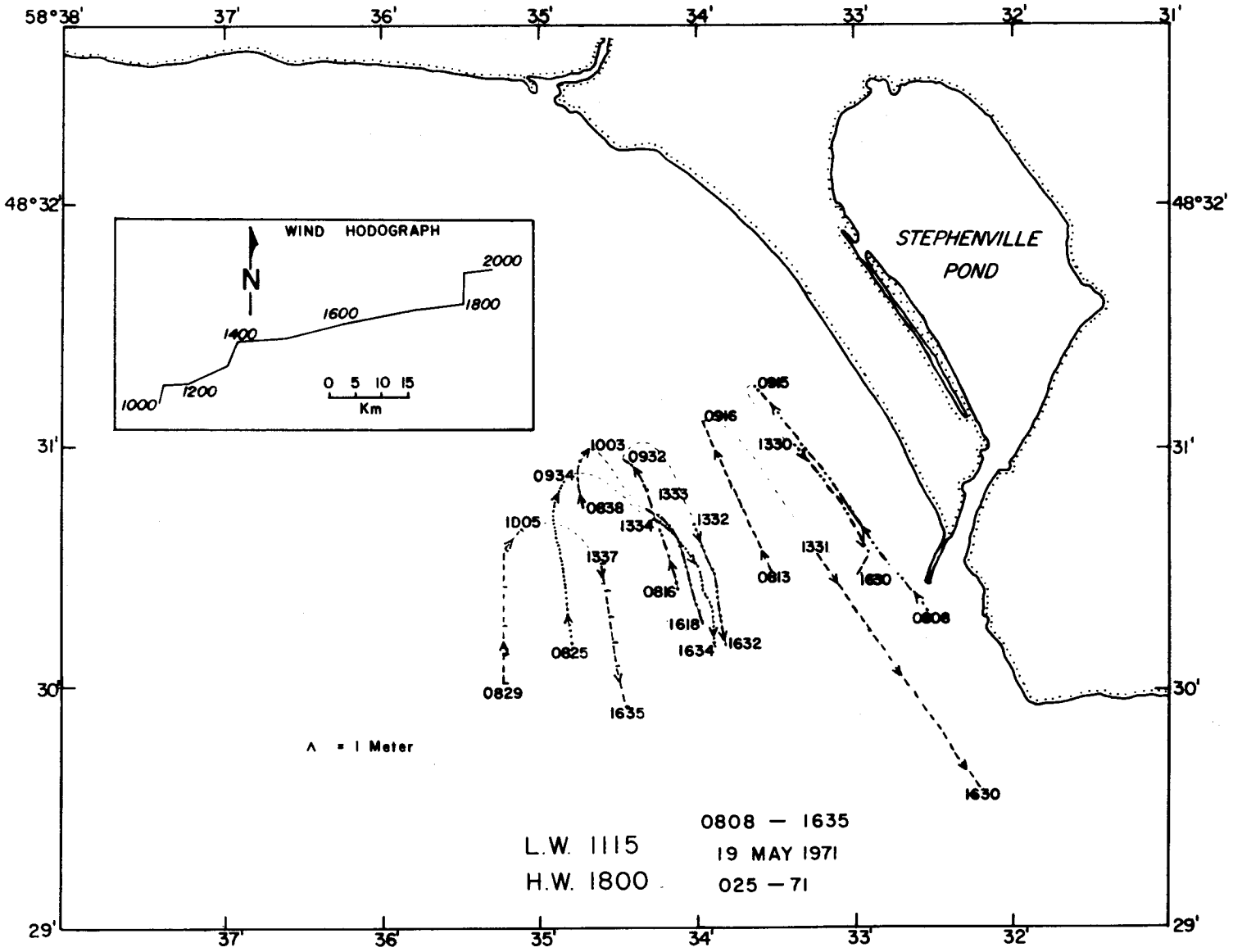

Fig. 50 Drogue trajectories at 1 meter, May 19, 1971

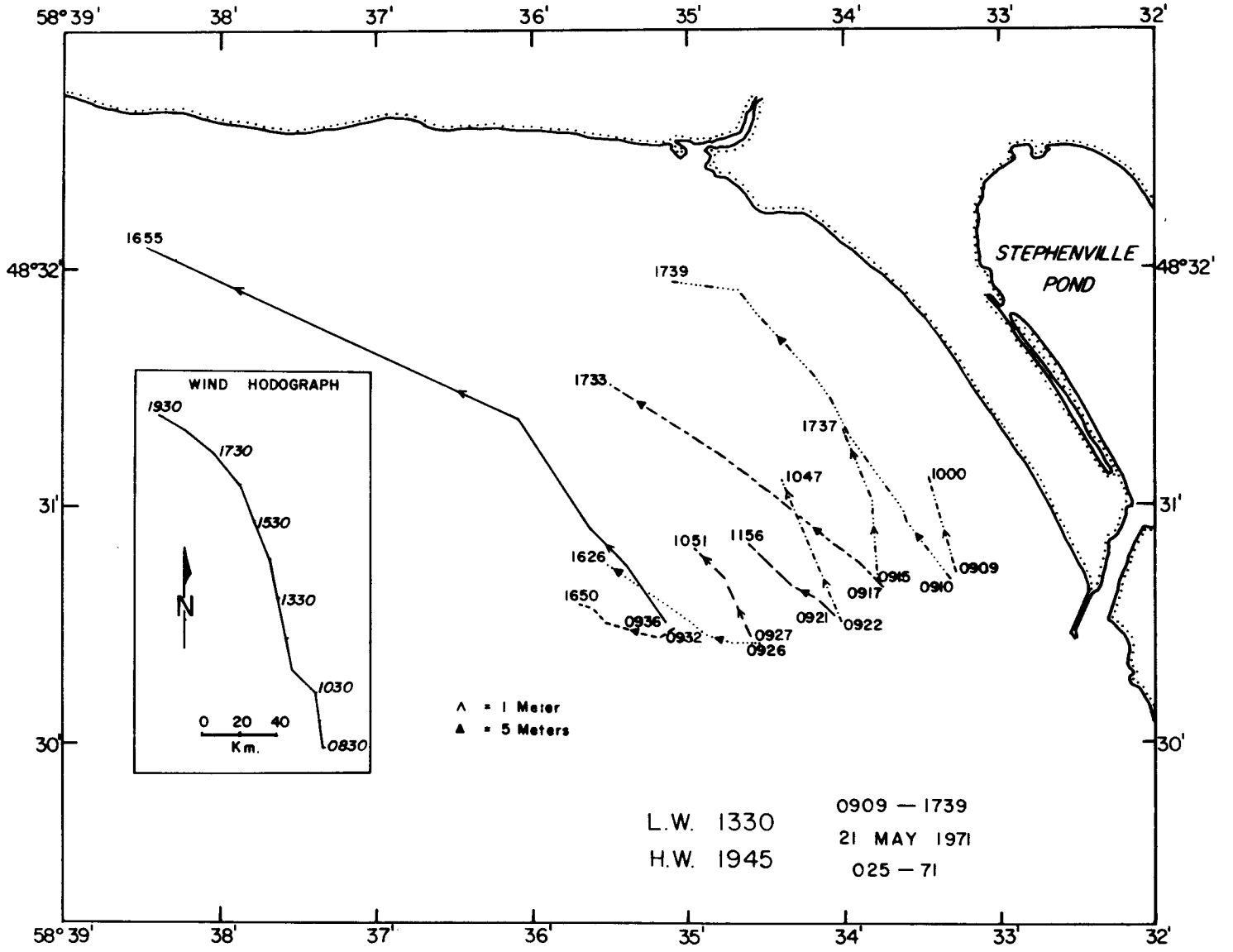

Fig. 51 Drogue trajectories at 1 and 5 meters, May 21, 1971

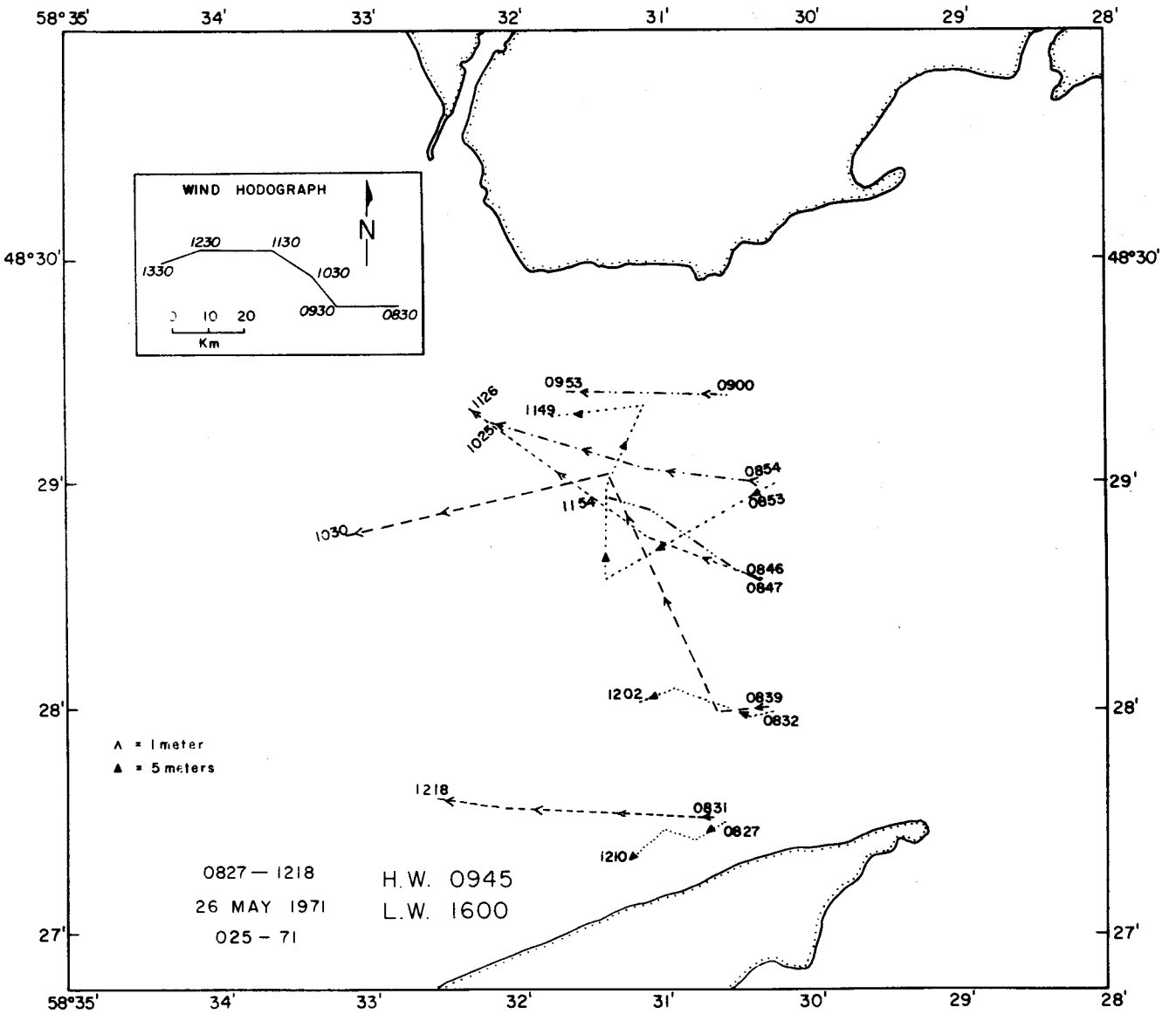

Fig. 52 Drogue trajectories at 1 and 5 meters, May 26, 1971

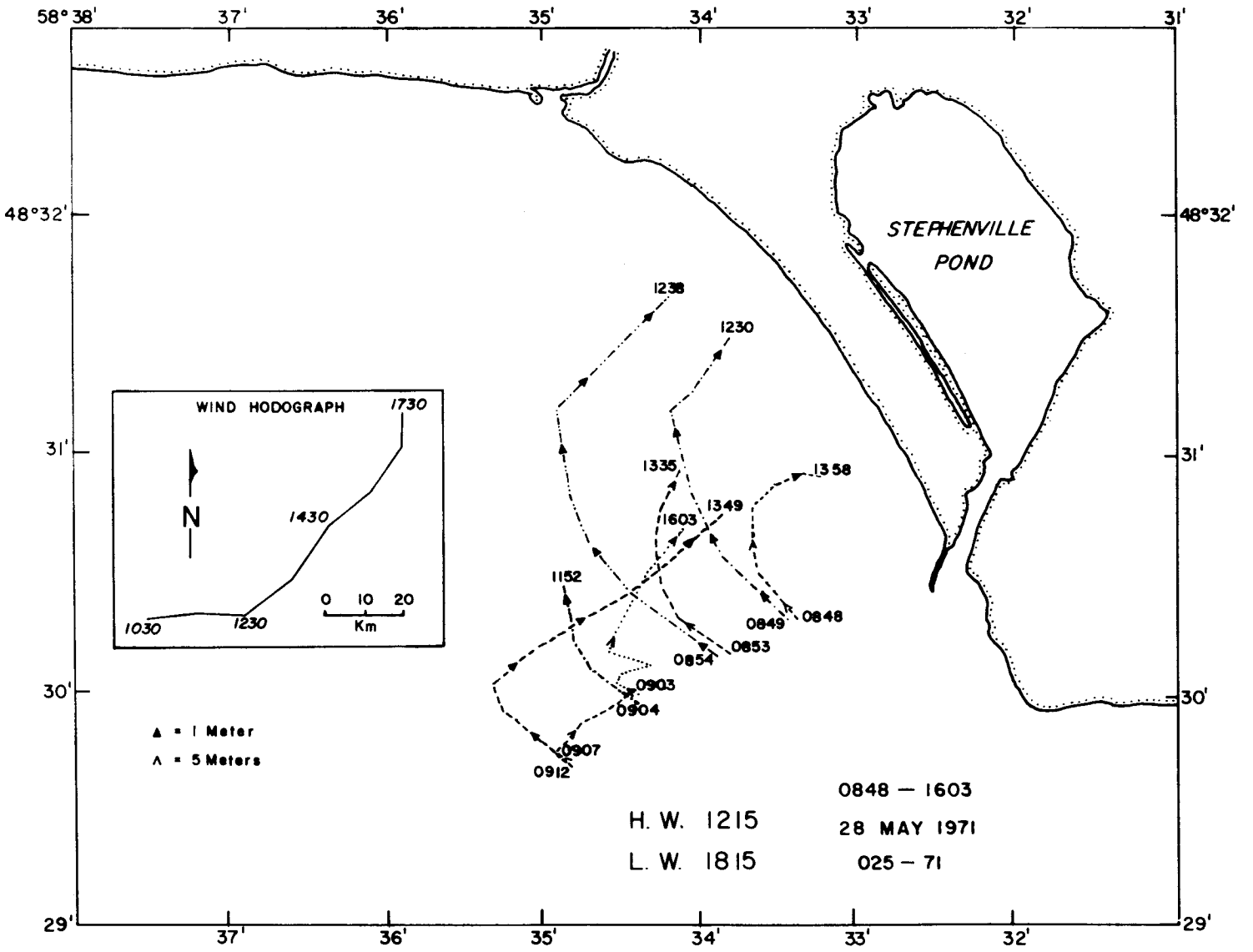

Fig. 53 Drogue trajectories at 1 and 5 meters, May 28, 1971

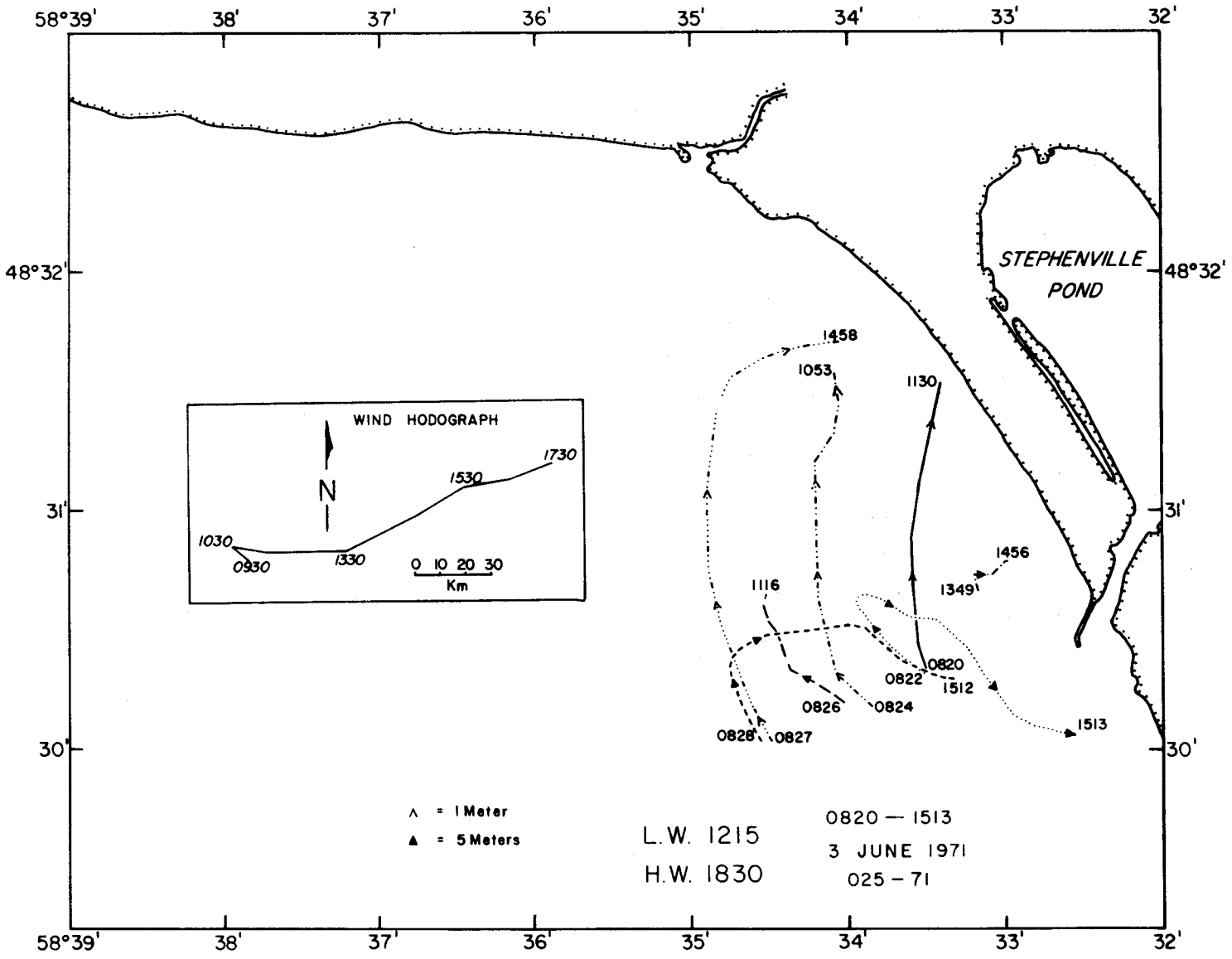

Fig. 54 Drogue trajectories at 1 and 5 meters, June 3, 1971

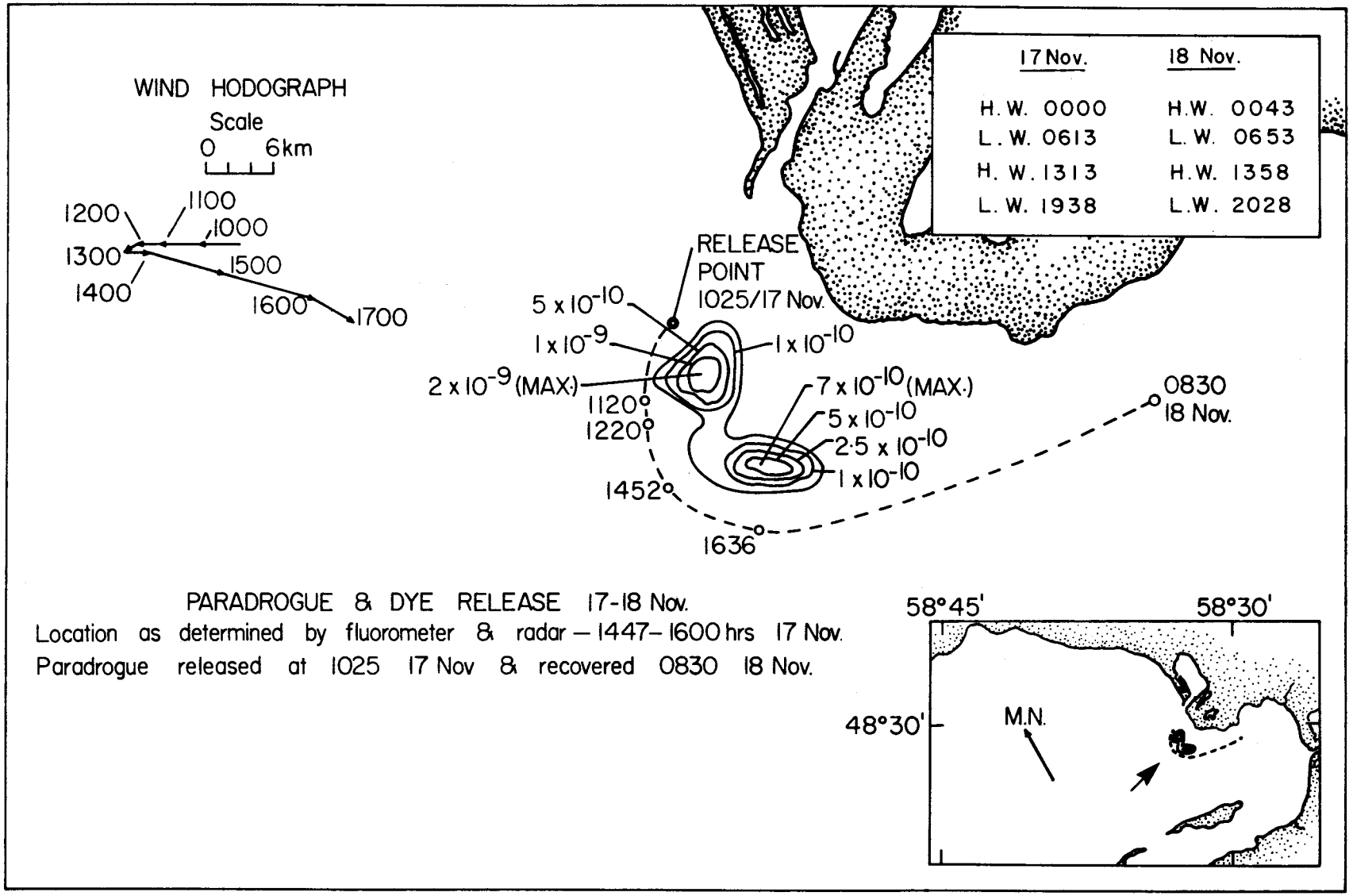

Fig. 55 Dye release No. 1, November 17-18, 1970

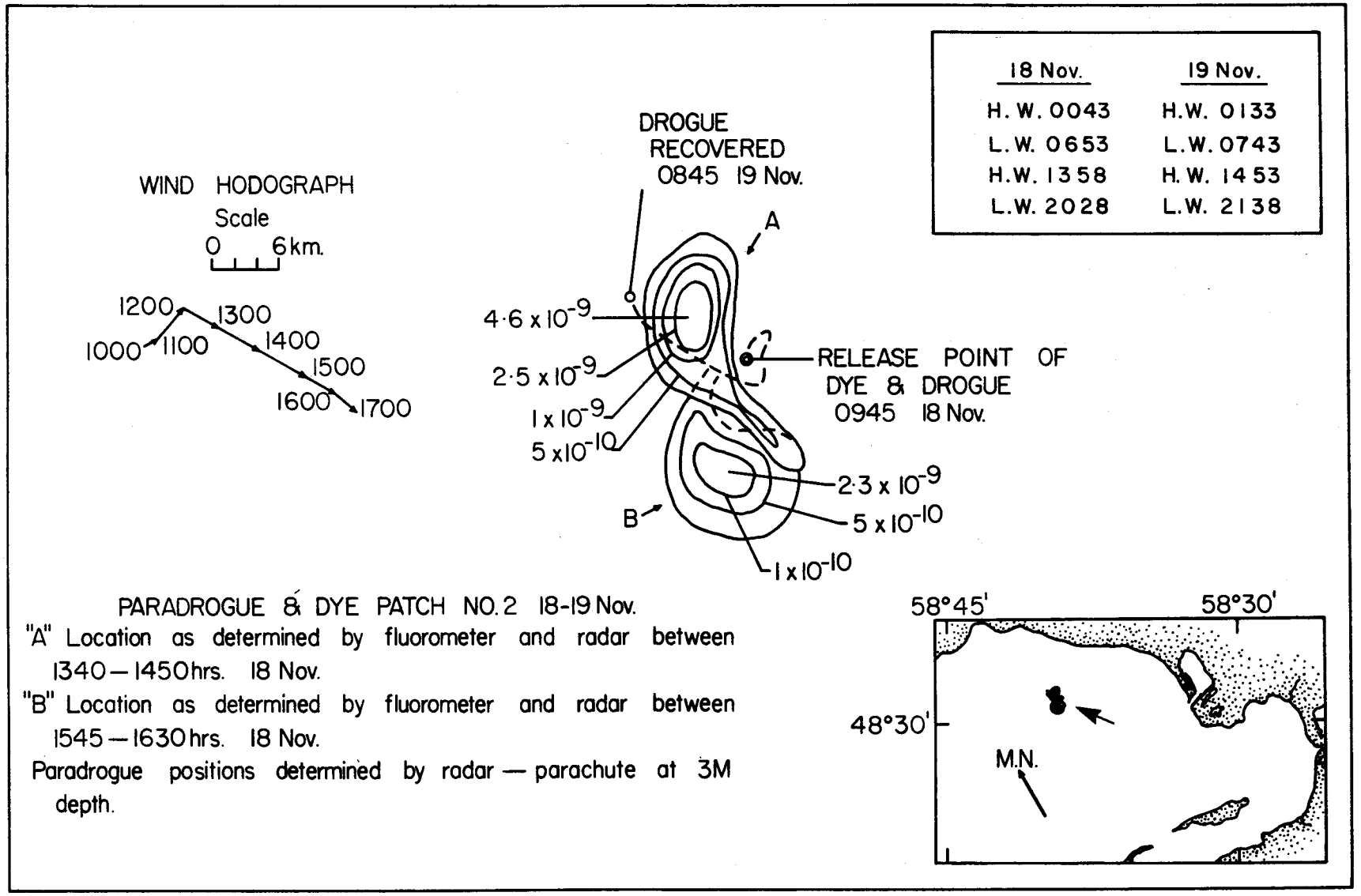

Fig. 56 Dye release No. 2, November 18-19, 1970

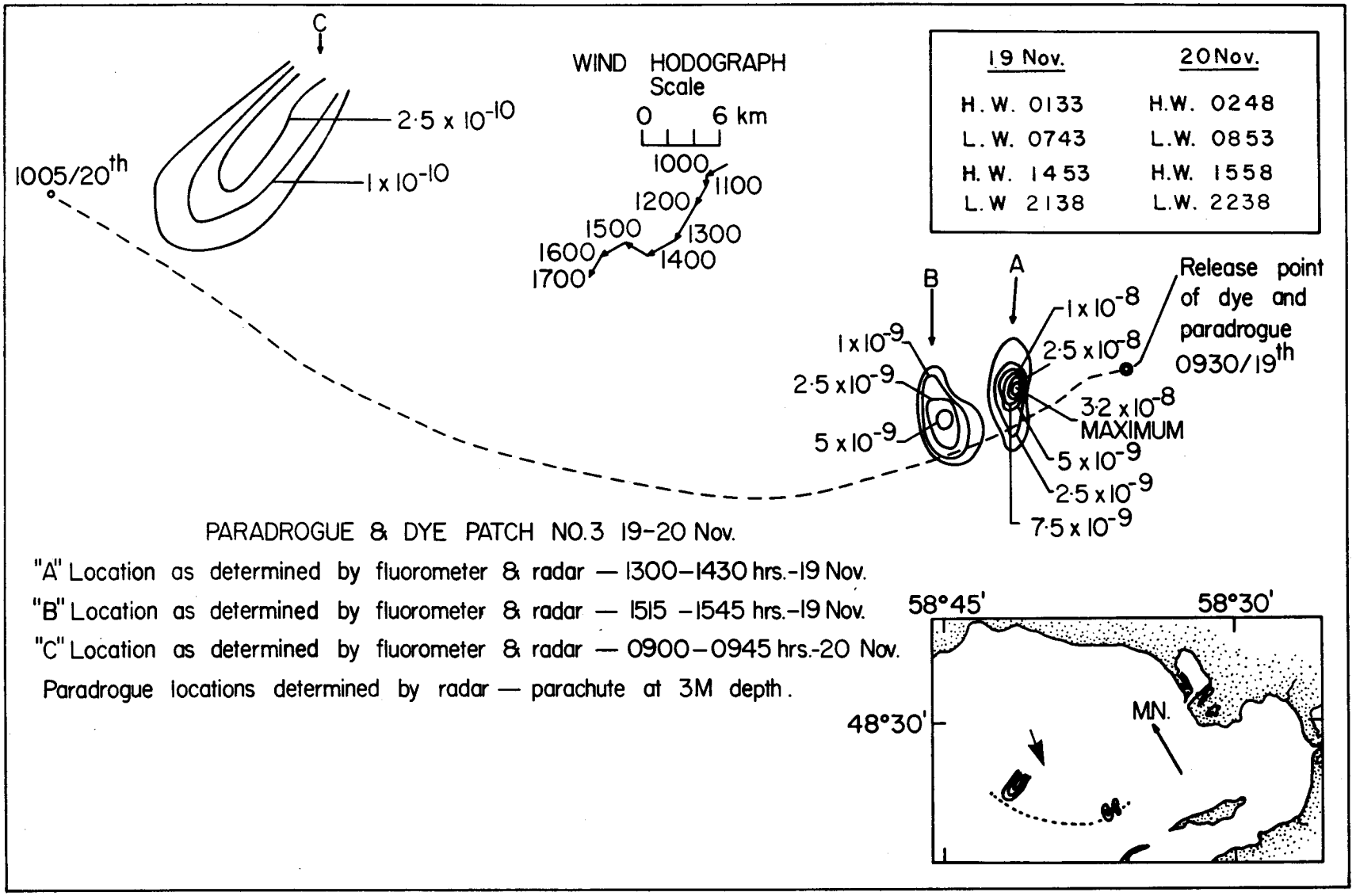

Fig. 57 Dye release No. 3, November 19-20, 1970

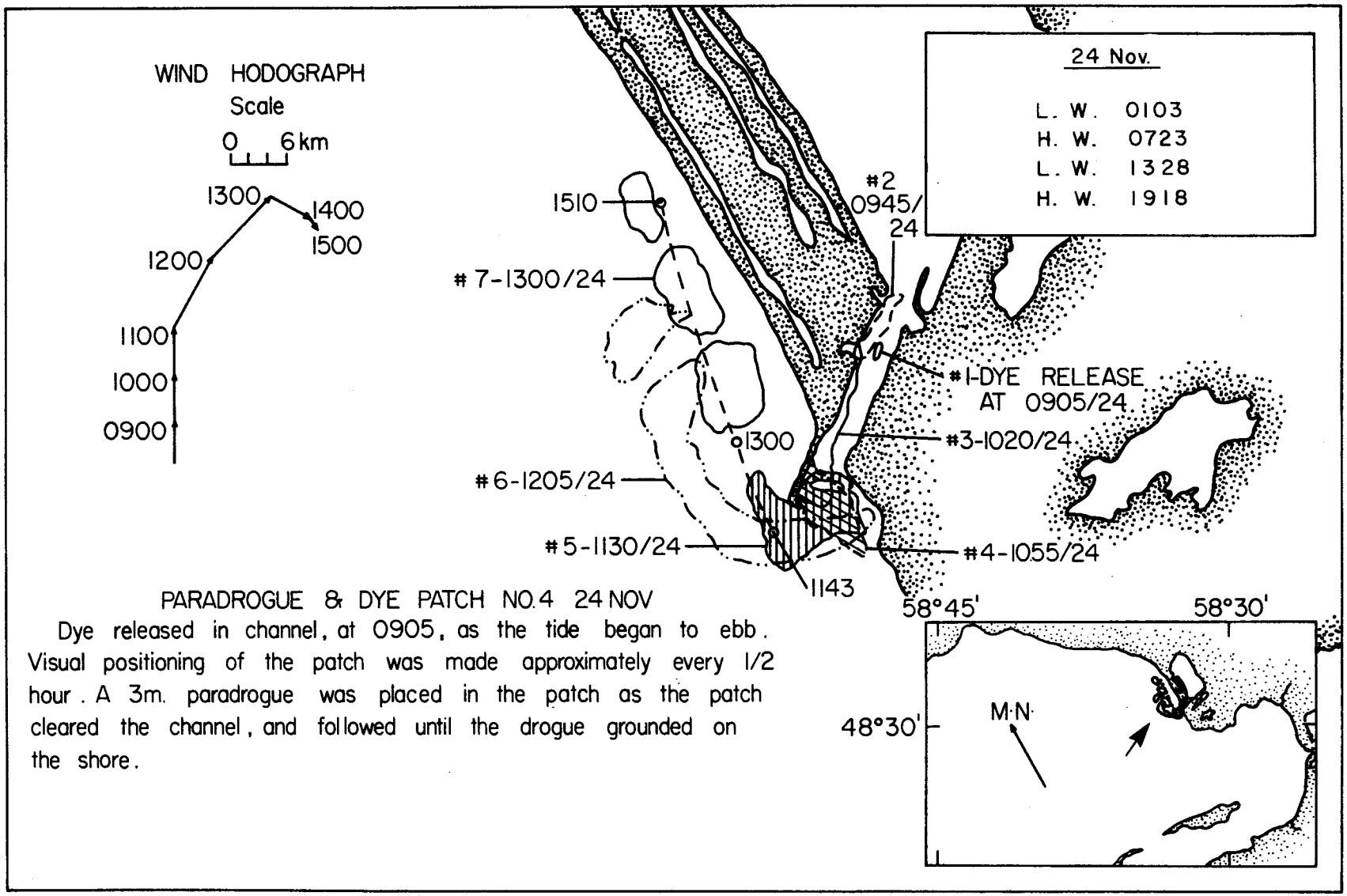

Fig. 58 Dye release No. 4, November 24, 1970

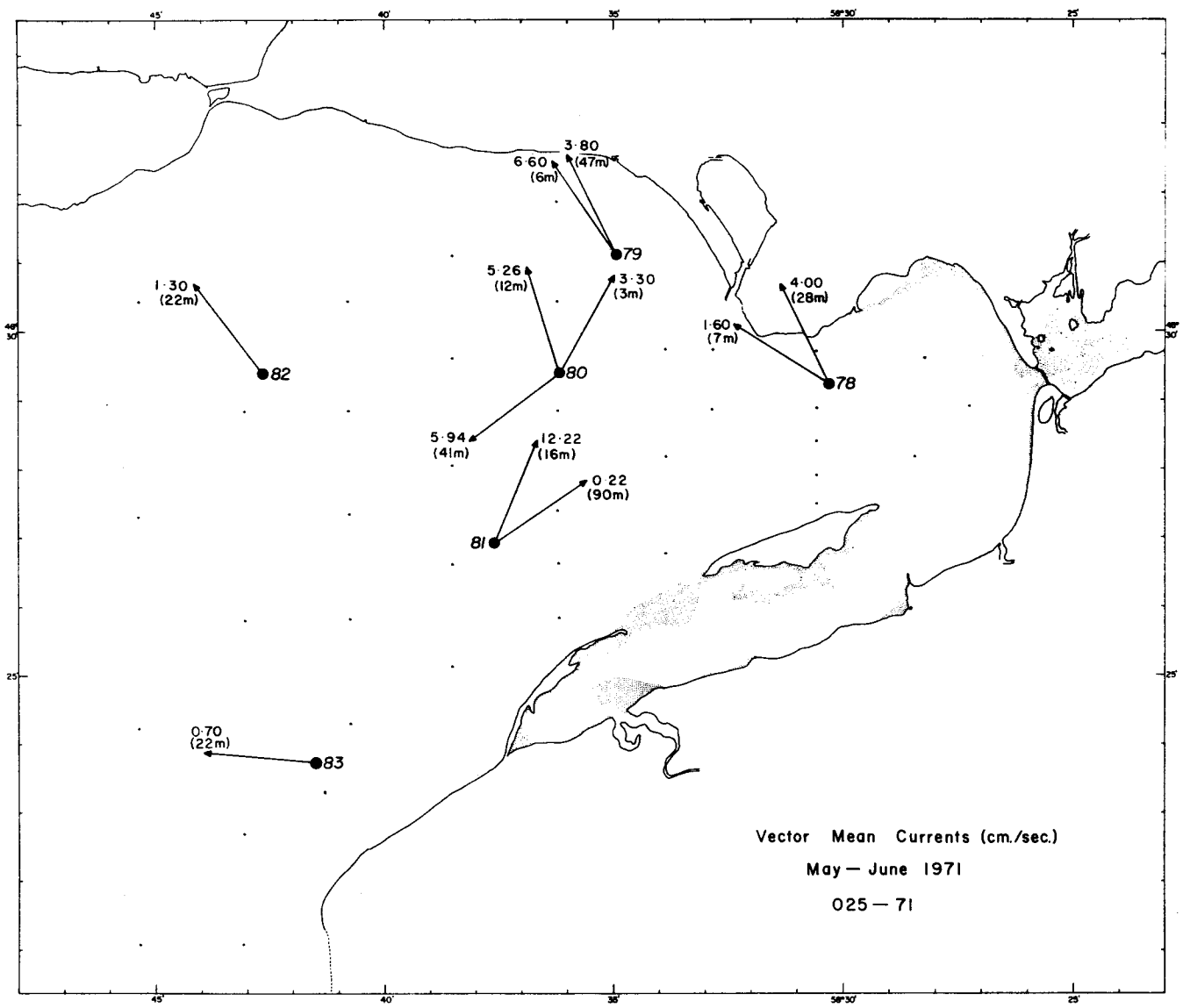

Fig. 59 Vector mean currents (cm/sec) May, 1971

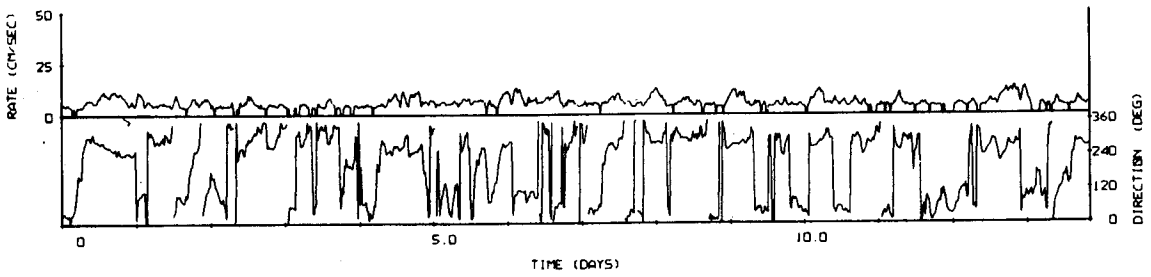

STATION NO. 78 DEPTH 7 M. METER NO. 137 BEGIN 0830Z 9/ 5/71

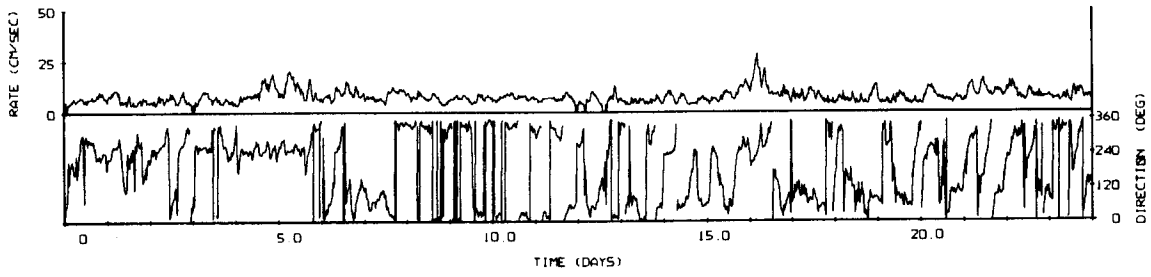

STATION NO. 78 DEPTH 28 M. METER NO. 147 BEGIN 0830Z 9/ 5/71

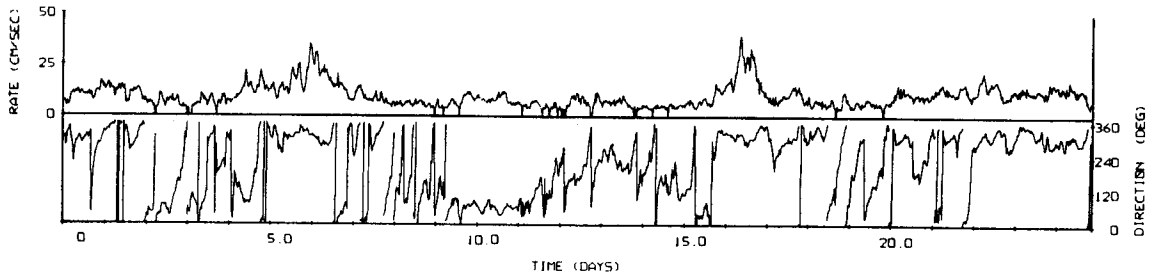

STATION NO. 79 DEPTH 6 M. METER NO. 200 BEGIN 1003Z 9/ 5/71

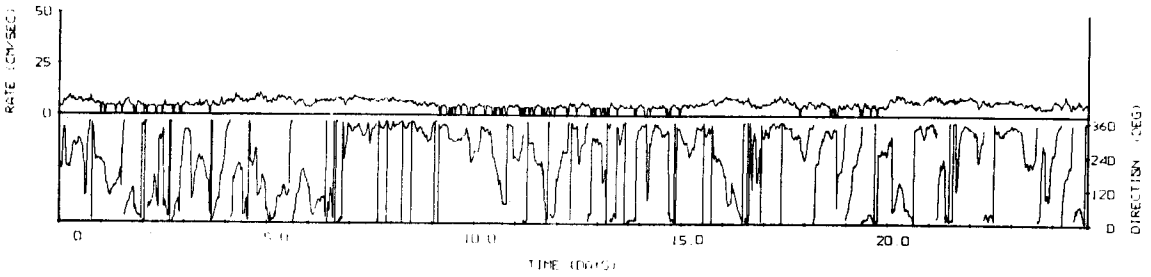

STATION NO. 79 DEPTH 42 M. METER NO. 196 BEGIN 1108Z 9/ 5/71

Fig. 60 Current rate and direction variations at Stn. 78 and 79

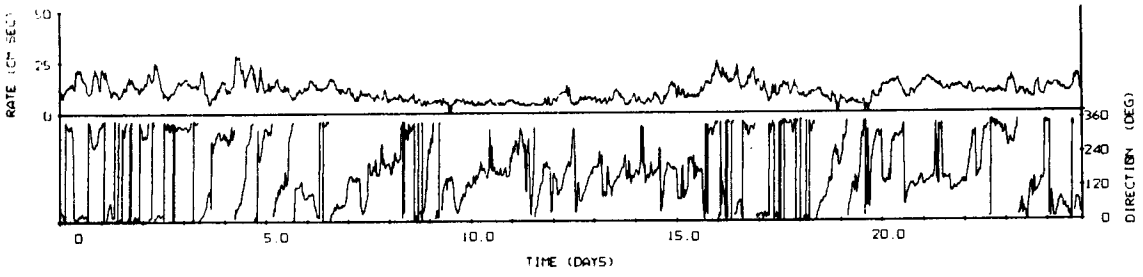

STATION NO. 80 DEPTH 3 M. METER NO. 149 BEGIN 1107 / 9/ 5/71

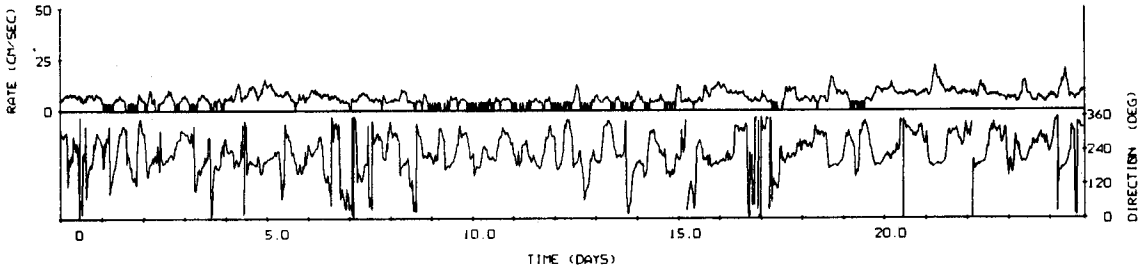

STATION NO. 80 DEPTH 41 M. METER NO. 140 BEGIN 1131 / 9/ 5/71

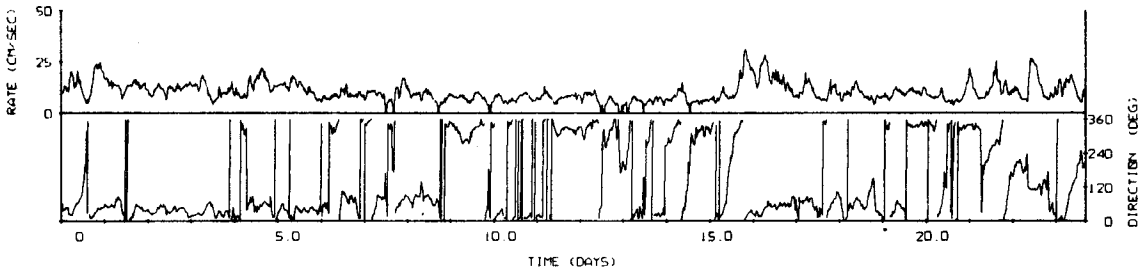

STATION NO. 81 DEPTH 16 M. METER NO. 138 BEGIN 1410 / 9/ 5/71

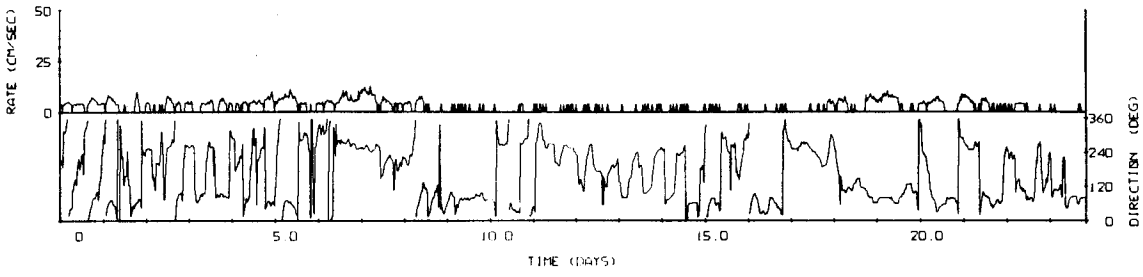

STATION NO. 81 DEPTH 90 M. METER NO. 087 BEGIN 1239 / 9/ 5/71

Fig. 61 Current rate and direction variations at Stn. 80 and 81

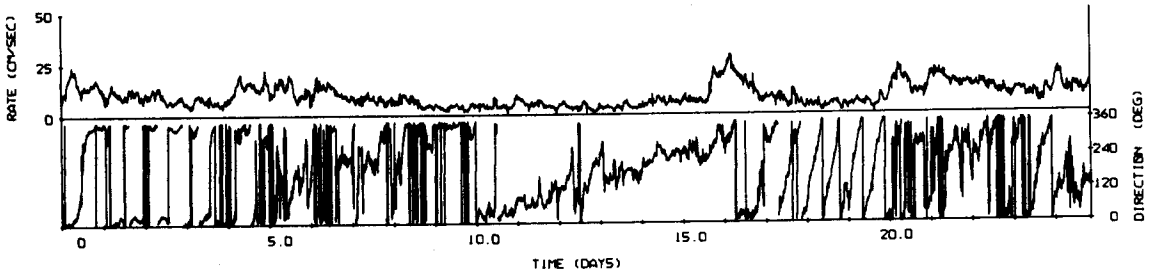

STATION NO. 80 DEPTH 12 M. METER NO. 307 BEGIN 1131 / 9/ 5/71

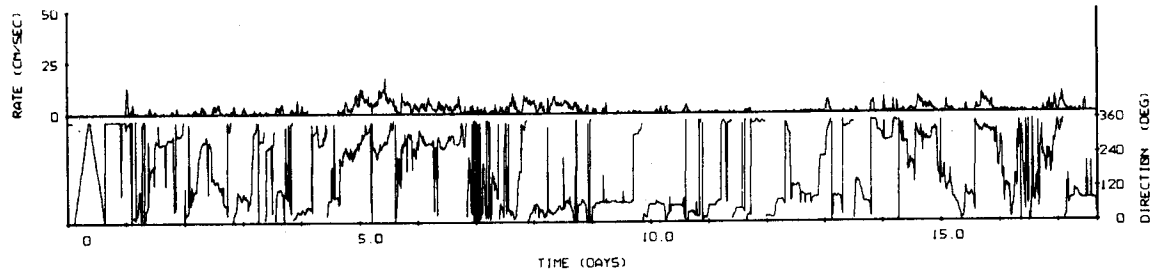

STATION NO. 82 DEPTH 22 M. METER NO. 325 BEGIN 1550/ 9/ 5/71

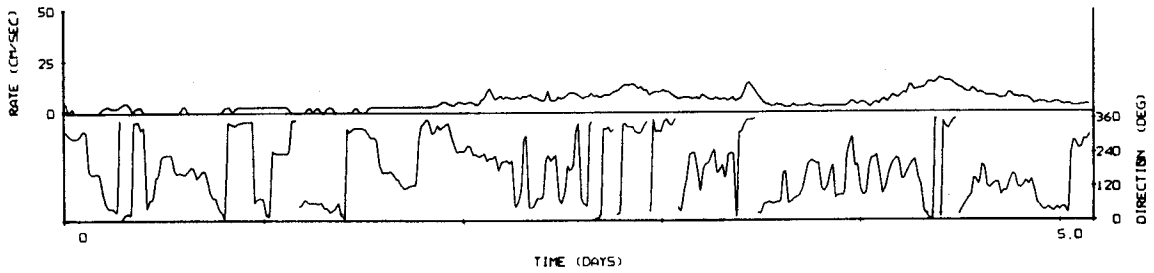

STATION NO. 83 DEPTH 22 M. METER NO. 134 BEGIN 1230/11/ 5/71

Fig. 62 Current rate and direction variations at Stn. 80, 82 and 83

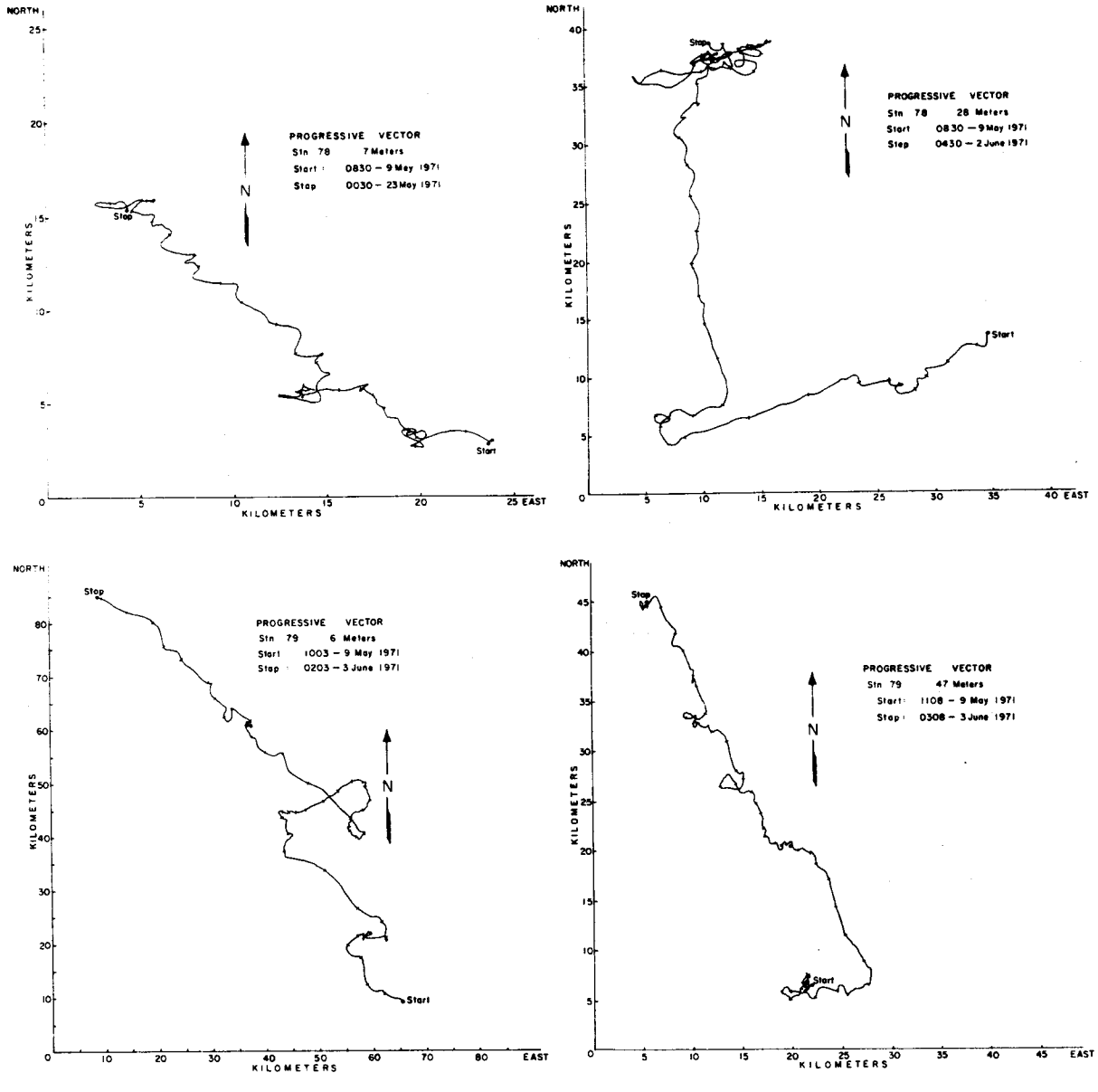

Fig. 63 Progressive vectors Stn. 78 and 79

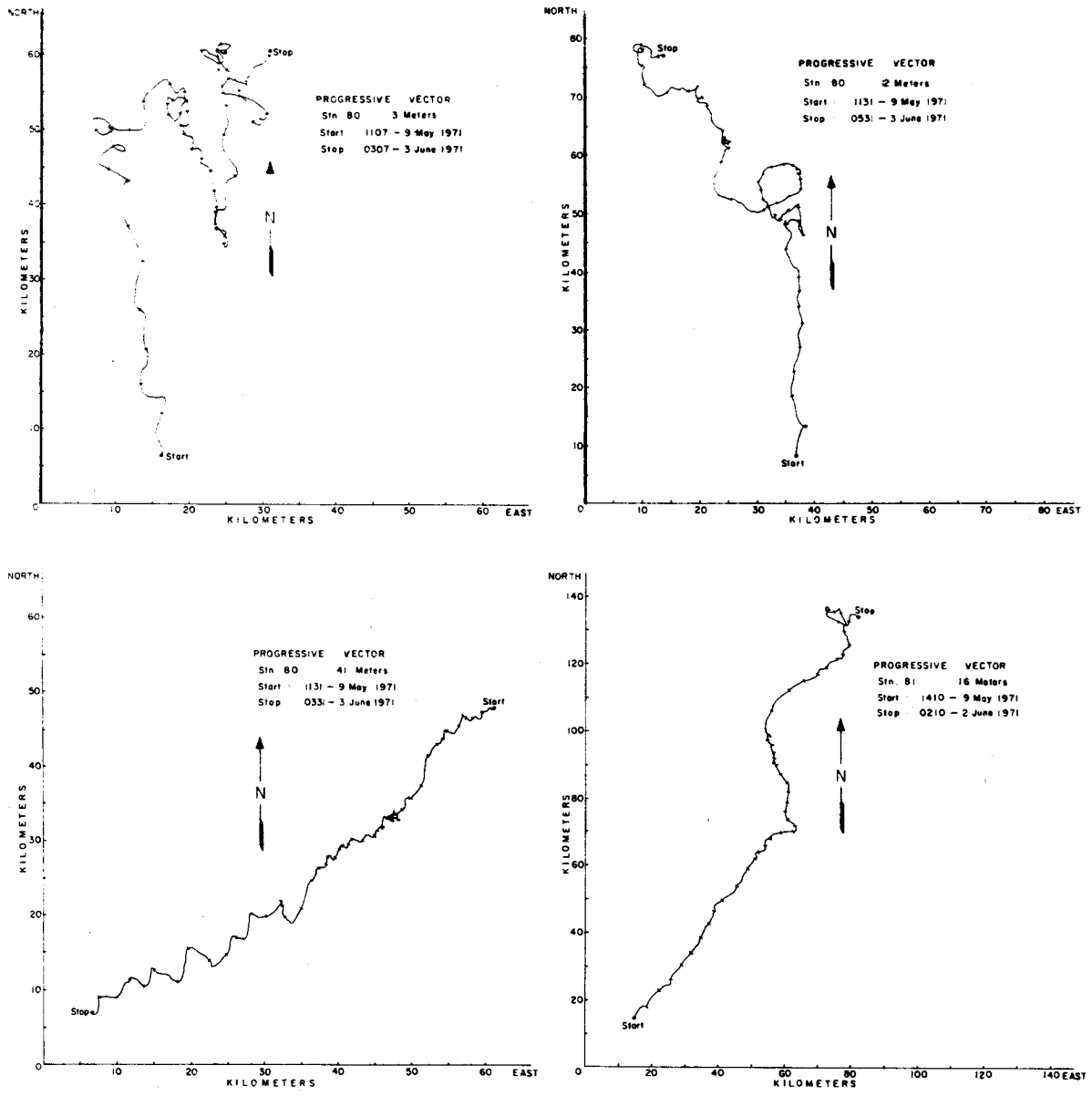

Fig. 64 Progressive vectors Stn. 80 and 81

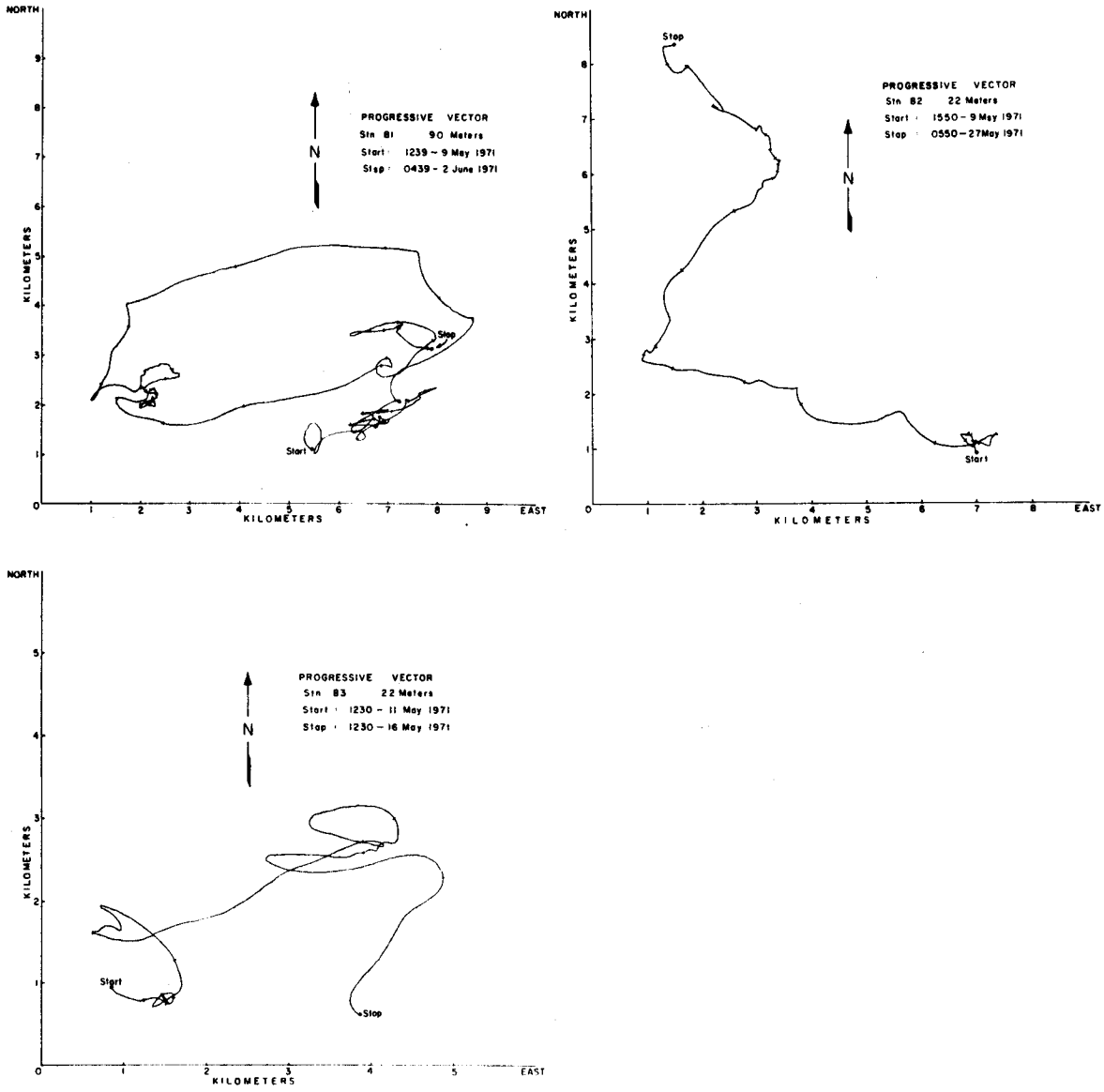

Fig. 65 Progressive vectors Stn. 81, 82 and 83

Environment
Canada

Department of Energy,
Mines and Resources

Environnement
Canada

Ministère de l'Énergie,
des Mines et des Ressources